WOODHEAD PUBLISHING IN MATERIALS

ADVANCED NANOCARBON POLYMER BIOCOMPOSITES

SUSTAINABILITY TOWARDS ZERO BIOWASTE

Edited by
MD REZAUR RAHMAN
MUHAMMAD KHUSAIRY BIN BAKRI

ELSEVIER

Advanced Nanocarbon Polymer Biocomposites

This page intentionally left blank

Woodhead Publishing in Materials

Advanced Nanocarbon Polymer Biocomposites

Sustainability Towards Zero Biowaste

Edited by

MD REZAUR RAHMAN

MUHAMMAD KHUSAIRY BIN BAKRI

ELSEVIER

WP
WOODHEAD PUBLISHING
An imprint of Elsevier

Woodhead Publishing is an imprint of Elsevier
50 Hampshire Street, 5th Floor, Cambridge, MA 02139, United States
125 London Wall, London EC2Y 5AS, United Kingdom

ISBN: 978-0-443-13981-9 (print)

ISBN: 978-0-443-13982-6 (online)

For information on all Woodhead Publishing publications
visit our website at https://www.elsevier.com/books-and-journals

Publisher: Matthew Deans
Acquisitions Editor: Gwen Jones
Editorial Project Manager: Tessa Kathryn
Production Project Manager: Maria Bernard
Cover Designer: Greg Harris

Typeset by MPS Limited, Chennai, India

Dedication

This work is dedicated to my amazing wife and daughters—Shirin Akther, Fahriah Rahman, and Faizah Rahman, who are very special to me and made it possible for me to complete this work.

—Ts. Dr. Md Rezaur Rahman

First, I would like to thank the Almighty God for the guidance, strength, power of mind, protection, and for giving us a healthy life. All of these we offer to you. Every difficult task needs self-effort as well as the guidance of elders, particularly those who are near to our hearts. I offer my humble dedications to my beautiful and loving father, mother, wife, and brothers, whose devotion, love, support, and nightly prayers have enabled me to work toward this significant achievement, along with all the dedicated, well-liked, and well-respected teachers and supervisors.

—Ts. Dr. Hj. Muhammad Khusairy Bin Bakri

This page intentionally left blank

Contents

Section 1 Nanocarbon from pine and aspen wood sawdust and its biocomposite applications

Section 2 Experimental and case study on pine and aspen wood

List of contributors

Mohammad Amran
Faculty of Science, Department of Chemistry, Bioorganic and Medicinal Chemistry Laboratory, University of Chittagong, Hathajari, Chittagong, Bangladesh

Sayeda Halima Begum
Faculty of Science, Department of Chemistry, Bioorganic and Medicinal Chemistry Laboratory, University of Chittagong, Hathajari, Chittagong, Bangladesh

Muhammad Khusairy Bin Bakri
Faculty of Engineering, Department of Chemical Engineering and Energy Sustainability, Universiti Malaysia Sarawak, Jalan Datuk Mohammad Musa, Kota Samarahan, Malaysia; Composite Materials and Engineering Center, Washington State University, Pullman, WA, United States

Khairul Anwar Bin Mohamad Said
UNIMAS Water Centre (UWC), Faculty of Engineering, Universiti Malaysia Sarawak (UNIMAS), Kota Samarahan, Sarawak, Malaysia; Faculty of Engineering, Department of Chemical Engineering and Energy Sustainability, Universiti Malaysia Sarawak, Jalan Datuk Mohammad Musa, Kota Samarahan, Malaysia

Andrey Burkov
Building Structures and Machines Department, Vyatka State University, Kirov, Russia

Faisal Islam Chowdhury
Faculty of Science, Department of Chemistry, University of Chittagong, Chittagong, Bangladesh

Bijoy Chandra Ghos
Department of Chemistry, Comilla University, Cumilla, Bangladesh

Syed Ragibul Haque
Department of Physics, Comilla University, Cumilla, Bangladesh

Mohin Hasnain
Faculty of Science, Department of Chemistry, Bioorganic and Medicinal Chemistry Laboratory, University of Chittagong, Hathajari, Chittagong, Bangladesh

Durul Huda
Department of Mechanical Engineering and Product Design Engineering, Swinburne University of Technology, Hawthorn, VIC, Australia

Md. Badrul Islam
Faculty of Science, Department of Chemistry, Bioorganic and Medicinal Chemistry Laboratory, University of Chittagong, Hathajari, Chittagong, Bangladesh

Anthonette Anak James
Faculty of Engineering, Department of Chemical Engineering and Energy Sustainability, Universiti Malaysia Sarawak, Jalan Datuk Mohammad Musa, Kota Samarahan, Malaysia

Perry Law Nyuk Khui
Faculty of Engineering, Department of Chemical Engineering and Energy Sustainability, Universiti Malaysia Sarawak, Jalan Datuk Mohammad Musa, Kota Samarahan, Malaysia

Kuok King Kuok
Faculty of Engineering, Computing and Science, Swinburne University of Technology, Sarawak Campus, Kuching, Sarawak, Malaysia

Mohammed Mahbubul Matin
Faculty of Science, Department of Chemistry, Bioorganic and Medicinal Chemistry Laboratory, University of Chittagong, Hathajari, Chittagong, Bangladesh

Murtala Namakka
Faculty of Engineering, Department of Chemical Engineering and Energy Sustainability, Universiti Malaysia Sarawak, Jalan Datuk Mohammad Musa, Kota Samarahan, Malaysia

Al-Khalid Othman
Faculty of Engineering, Department of Chemical Engineering and Energy Sustainability, Universiti Malaysia Sarawak, Jalan Datuk Mohammad Musa, Kota Samarahan, Malaysia

Md. Abdul Majed Patwary
Department of Chemistry, Comilla University, Cumilla, Bangladesh

Md Rezaur Rahman
UNIMAS Water Centre (UWC), Faculty of Engineering, Universiti Malaysia Sarawak (UNIMAS), Kota Samarahan, Sarawak, Malaysia; Faculty of Engineering, Department of Chemical Engineering and Energy Sustainability, Universiti Malaysia Sarawak, Jalan Datuk Mohammad Musa, Kota Samarahan, Malaysia

Mohammad Atiqur Rahman
Department of Chemistry, Comilla University, Cumilla, Bangladesh

Mohammed Muzibur Rahman
Faculty of Science, Department of Chemistry, Center of Excellence for Advanced Materials Research (CEAMR), King Abdulaziz University, Jeddah, Saudi Arabia

Ain Zaienah Sueraya
Faculty of Engineering, Department of Chemical Engineering and Energy Sustainability, Universiti Malaysia Sarawak, Jalan Datuk Mohammad Musa, Kota Samarahan, Malaysia

Jamal Uddin
Department of Natural Science, Coppin State University, Science and Technology Center, Baltimore, MD, United States

Yuriy Yurkin
Building Structures and Machines Department, Vyatka State University, Kirov, Russia

Md. Shahid Uz Zaman
Faculty of Electrical and Computer Engineering, Rajshahi University of Engineering & Technology, Rajshahi, Bangladesh

About the editors

Ts. Dr. Md Rezaur Rahman is an Associate Professor in the Department of Chemical Engineering and Energy Sustainability, Faculty of Engineering, Universiti Malaysia Sarawak (UNIMAS), Malaysia. He has also been a Visiting Research Fellow at the Faculty of Engineering, Tokushima University, Japan, since June 2012. Previously, he worked as a Teaching Assistant at the Faculty of Engineering, Bangladesh University of Engineering and Technology (BUET), and as a Research Project Leader supported by the Ministry of Higher Education, Malaysia. He was appointed an External Supervisor for the Faculty of Engineering, Swinburne University of Technology, Melbourne, Australia, in 2015. He received his PhD from the Universiti Malaysia Sarawak, Malaysia. He has more than 15 years of experience in teaching, research, and working with industry. His areas of research include carbon, conducting polymers, silica/clay dispersed elastomeric polymer nanocomposites, hybrid filled loaded polymer composites, advanced materials: graphene/nanoclay/fire retardants, nanocellulose (cellulose nanocrystals and nano-fibrillar) cellulose reinforced/filled polymer composites, chemical modification, and treatment of lignocellulosic fibers, including jute, coir, sisal, kenaf, hemp and solid wood, nanocomposites and nanocellulose fibers, and polymer blends. He has more than 300 publications, listed among the Top 2% Scientists Worldwide 2023 by Stanford University.

Ts. Dr. Hj. Muhammad Khusairy Bin Capt. Hj. Bakri obtained his doctor of philosophy, PhD (2018), master of engineering (by research), MEng (2016), and bachelor of engineering (mechanical engineer), BEng (2014) from Swinburne University of Technology, Australia (SUT). Currently, he is working with Washington State University (WSU) as a Postdoctoral Research Associate in Composite Materials and Engineering Center (CMEC), focusing on materials science, wood composites, polymer composites, biomaterials, and biocarbons. Previously, he was a Research Fellow at Universiti Malaysia Sarawak (UNIMAS) from 2019 to 2021, prioritizing materials science, membrane, concrete, polymer composites, biomaterials, and education. He was also a Higher Degree Researcher/Teaching Assistant from 2014 to 2018 in Swinburne University of Technology Sarawak Campus (SUTS). During that time, he taught subjects such as computer-aided design (CAD), materials and processes, materials and manufacturing, and thermodynamics. He has published over 200 local and international publications (journals, book chapters, conference papers, newspapers, bulletin, etc.). He is a finalist of the Alumni Impact Awards 2022 under the Innovative Planet Impact Award recognized by Swinburne University of Technology, Australia. He is also listed in the Fifth Edition of *Successful People in Malaysia* of Britishpaedia, published by British Publishing House Ltd.

Preface

Integrating nanotechnology and polymer composites has emerged as a transformative paradigm in the rapidly evolving landscape of materials science and engineering, offering unprecedented opportunities to develop advanced materials with tailored properties and multifunctional applications. This book, *Advanced Nanocarbon Polymer Biocomposites*, represents a comprehensive exploration of the synergistic possibilities of the fusion of nanocarbons, polymers, and biocompatible elements.

Nanocarbon materials extracted from wood (pine and aspen) biomass (natural fiber, etc.) exhibit exceptional mechanical, thermal, and electrical properties. Harnessing the unique characteristics of these nanoscale entities and combining them with polymers, which provide flexibility, processability, and a wide range of functionalities, opens new frontiers in material design. Moreover, incorporating biocompatible components facilitates the development of materials that excel in mechanical, morphological, and chemical performance and demonstrate compatibility with living systems, paving the way for applications in biomedicine, construction and building, packaging, and sustainable technologies.

This book is crafted to provide a comprehensive overview of the fundamental and state-of-the-art research and developments in nanocarbon polymer biocomposites. Each chapter is meticulously crafted by experts in the respective areas, covering fundamental principles, synthesis methods, characterization techniques, and diverse applications. The chapters are organized to guide readers through the intricate landscape of nanocarbon polymer biocomposites, from theoretical foundations to practical applications, fostering a holistic understanding of this burgeoning field.

The multidisciplinary nature of this book makes it an invaluable resource for researchers, academics, and practitioners working at the intersection of nanotechnology, polymer science, and biocompatible materials. Whether delving into the fundamental science behind nanocarbon interactions with polymers or seeking insights into the practical applications of these advanced materials, this book serves as a roadmap to navigate the complexities and potentials of nanocarbon polymer biocomposites.

As editors, we would like to express our gratitude to the contributing authors for their scholarly contributions and dedication to advancing the knowledge in this field. We believe this compilation will inspire further exploration, foster collaboration, and contribute to the evolution of nano-carbon polymer biocomposites as a transformative technology.

Md Rezaur Rahman
Muhammad Khusairy Bin Bakri

CHAPTER EIGHT

Montmorillonite-activated nanocarbon from pine wood sawdust and its biocomposites

Md Rezaur Rahman[1], Durul Huda[2], Al-Khalid Othman[1], Md. Shahid Uz Zaman[3], Jamal Uddin[4], Khairul Anwar Bin Mohamad Said[1], Yuriy Yurkin[5], Andrey Burkov[5], Muhammad Khusairy Bin Bakri[1] and Kuok King Kuok[6]

[1]Faculty of Engineering, Department of Chemical Engineering and Energy Sustainability, Universiti Malaysia Sarawak, Jalan Datuk Mohammad Musa, Kota Samarahan, Malaysia
[2]Department of Mechanical Engineering and Product Design Engineering, Swinburne University of Technology, Hawthorn, VIC, Australia
[3]Faculty of Electrical and Computer Engineering, Rajshahi University of Engineering & Technology, Rajshahi, Bangladesh
[4]Department of Natural Science, Coppin State University, Science and Technology Center, Baltimore, MD, United States
[5]Building Structures and Machines Department, Vyatka State University, Kirov, Russia
[6]Faculty of Engineering, Computing and Science, Swinburne University of Technology, Sarawak Campus, Kuching, Sarawak, Malaysia

8.1 Introduction

Due to plastic's promising qualities, including corrosion resistance, low density, and user-friendly design, their manufacturing, and use have significantly risen over the last 60 years. The growth of the plastics industry has resulted in the development of various plastic products with broad applications using various plastics, such as the introduction of natural polymers, modified natural polymers, synthetic plastics, biodegradable plastics, thermoplastics, and thermosetting plastics. Fig. 8.1 depicts the global plastic demand broken down by polymer type (What Is Hot - Multi-client study, 2023). According to the information provided by Pardos Marketing (What Is Hot - Multi-client study, 2023), polypropylene (PP), accounts for 31% of high-demand plastic, low-density polyethylene (LDPE), and linear low-density polyethylene (LLDPE), accounts for 18% of high-demand plastic, and polyvinyl chloride (PVC), accounts for 14% of high-demand plastic (PVC). Whereas the low-demand plastic is followed by 3% of acrylonitrile

Advanced Nanocarbon Polymer Biocomposites.
DOI: https://doi.org/10.1016/B978-0-443-13981-9.00008-9

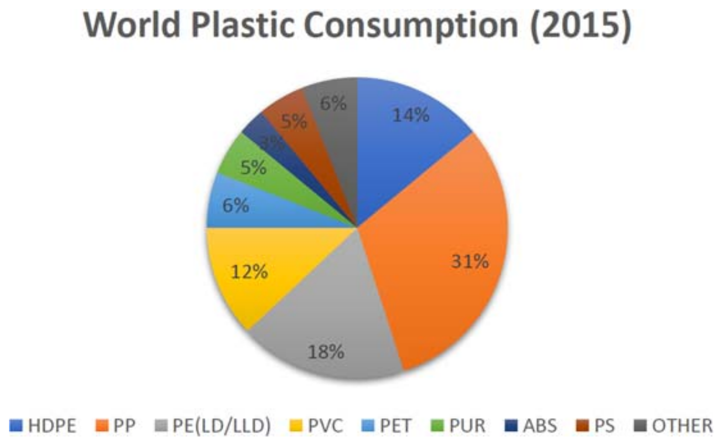

Figure 8.1 Shows the amount of plastic consumed in 2015, broken down by polymer type. *From What Is Hot - Multi-client study, World plastics supply 2005–2015. (n.d.). Retrieved July 17, 2023, from http://www.pardos-marketing.com/hot01.htm.*

butadiene styrene (ABS), 5% of polyurethane (PUR), 5% of polystyrene (PS), and 6% of all other types of plastic. According to the statistics, acetate butadiene styrene is the least popular plastic, whereas polypropylene is the most popular (ABS). Yet, since these polymers cannot be decomposed, plastic trash is continuously rising in the landfill.

Nowadays, biopolymer is used owing to environmental concerns and the depletion of natural resources (Jayamani et al., 2017; Rahman et al., 2021b; Yun et al., 2022b). When biopolymer degrades, it releases organic by-products like water and carbon dioxide that less influence the environment (Samir et al., 2022). Today's use of novel composites employ nanotechnology has ushered in a new age of material science and engineering research (Jayamani et al., 2019; Nyuk Khui et al., 2019; Rahman & Bakri, 2021). Thus the need to produce materials that are reliable, affordable, and sustainable on an environmental level must be addressed (Bakri & Rahman, 2021; Khui et al., 2021). Therefore, a growing interest in the pursuit of inexpensive reinforced composites, composed completely of biodegradable elements is gradually rising.

Additives are substances that often are combined with a polymer matrix. Additives make polymeric materials more colorful, stiffer, and more durable, giving them biodegradable/degradable-resistance qualities (Islam et al., n.d.; Jaafar, 2017; Rahman et al., 2011). Colorants, antioxidants, plasticizers, fillers, reinforcement, and blowing agents are examples of existent additives, each of which has a different purpose. Several types of reinforcement and filler sources are shown in Fig. 8.2 (Jaafar, 2017; Rahman et al., 2011; Rahman et al., 2013). The additives are divided into three primary groups: active, inactive, and reinforcement. These groups are determined by the aspect ratio (L/D) and the compatibility factor of nanoparticles. Long continuous fibers are often referred to as reinforcement. It is often utilized for thermosetting plastic with various fiber arrangements (uni-dimensional, 2D, and 1D). The mechanical characteristics of a polymer are improved by the fiber's occupancy of 60−70 vol%. Active filler is defined as filler that aims to improve the mixed material's qualities. In contrast, an inactive filler is a filler that is intended to lower the cost of the compound. The arrangement of fillers is determined in the fabrication process. These fillers are typically utilized in short, discontinuous fiber, flake, and particle geometries in randomly oriented arrangements, producing isotropic characteristics. These fillers make up between 30 and 40 vol% of polymer composites (Jaafar, 2017).

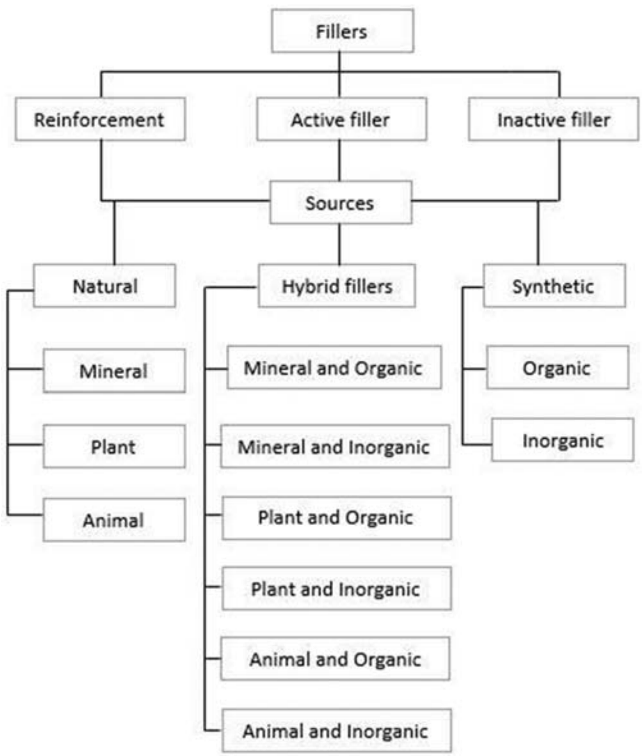

Figure 8.2 ***Several sources for infill and reinforcement.*** Fillers tree description.

There are two types of fillers: natural fillers and synthetic fillers. Natural fillers come from different sources including minerals, vegetation, and wildlife. There are two types of synthetic fillers: organic fillers and inorganic fillers (Adamu et al., 2019, 2020; Hamdan et al., n.d.; Jaafar, 2017). Diamond, graphene, and carbon nanotubes (CNTs) are examples of inorganic synthetic fillers (CNTs). The flammability and chemical resistance of the mixture may also be affected by organic additives. Researchers have recently been more interested in using hybrid filler to create nanocomposite materials by combining them with various reinforcing sources. There is plenty of research outlining the advantages of employing hybrid filler. Ali Mohsin (Ali Mohsin et al., 2014) created a mixed filler system by adding montmorillonite (MMT) to a CNT/HDPE nanocomposite and researched the nanocomposite's thermal and mechanical characteristics. It was discovered to exhibit better tensile and flexural strength and thermal stability. Combining nanoscale boron nitrides and graphene nanoplatelets in epoxy has also improved heat conductivity (Shtein et al., 2015). The tensile modulus and yield stresses of the hybrid PP composite and the composite's thermal stability were improved by the synergy effect of utilizing inorganic filler $CaCO_3$ and clays as hybrid filler. Few researchers (Aguilar et al., 2014; Gill et al., 2019) used a hybrid mix of nickel and carbon black as a conducting and reinforcing filler for polypropylene polymers. It has been discovered that filler loading improves both mechanical and electrical characteristics. While developing the polymer composite, choosing the right filler may enhance the economics and polymer characteristics, such as mechanical behavior. In addition to its other advantages, the filler has helped the goods to be more rigid and stable in their dimensions.

Over 200 million tons of synthetic polymers are produced worldwide (Sam et al., 2015). The inadequate biodegradability of synthetic polymers has led to the rise of worldwide disposal of solid waste (Khui et al., 2023; Yun et al., 2022a, 2022b, 2022c, 2022d). Researchers are thus advised to create a novel kind of environmentally friendly polymer matrix that is sustainable, biodegradable, and environmentally benign. There are predictions for the increase of nanocomposite materials in the market. For example, the US Freedonia Group estimated that by 2020, the demand for innovative polymer/nanoclay composite materials might reach 3.2 million tons, costing US$15 billion annually (Gul et al., 2015). To create a polymer/nanoclay combination that offers good performance, the scientists recommend paying more attention to theory and modeling.

Recently, nanocarbon and nano clay have drawn more interest due to their potential use as natural nanofiller materials in various sectors

(Bakri & Rahman, 2021; James et al., 2022; Khairulzaim et al., 2021; Rahman et al., 2023, 2021a). However, using current nanotubes or graphene is not economically viable. Costs for research-grade nanotubes vary from \$5/g for MWCNT to \$75/g for SWCNT, while graphene oxide costs around \$100/g (Bhattacharya, 2016). There has not been much research done in the past on making nanocarbon filler from the pyrolysis output.

Prior studies have addressed the pyrolysis type and the creation of biomass bio-oil, charcoal, and syngas. Also, there is little research on creating bio-nanocomposites employing green filler derived from biomass and biodegradable polymers. Moreover, there is not enough research on hybrid fillers or numerous fillers in nanocomposite materials. The current work aims to create a unique bio-nanocomposite by combining nanoclay (green filler) obtained from pyrolysis with biochar using a ball milling technique, confirming the research gap. This study's primary objective is to create a hybrid filler bio-composite using solution casting to combine MMT nanoclay and acetic acid-activated nanocarbon in polylactic synthetic, synthetic biopolymer (PLA).

Several goals have been established to accomplish the objective, including (i) creating nanocarbon from pine sawdust and activating it with acetic acid; (ii) examining the characteristics of activated nanocarbon (AC) and contrasting them with nonactivated nanocarbon; and (iii) examining the characterization of an AC/MMT/PLA bio-composite with various AC filler loadings. The research aims are to create bio-nanocomposites utilizing a hybrid filler called MMT that combines nanocarbon and nanoclay as reinforcement in a PLA biopolymer. Pine sawdust from the Russian Federation is the biomass used to make nanocarbon. Carbonization was carried out in an LT furnace with little oxygen available to produce nanoscale nanocarbon. A part was isolated and used with acetic acid to create activated carbon. Using particle size distribution (PSD), Brunauer–Emmett–Teller (BET), and energy dispersive X-ray (EDX) analyses, nonactivated and activated carbon were compared and characterized. The bio-nanocomposite was then created using the solution casting process, and the performance of the newly generated matrix was examined utilizing FTIR, SEM, and EDX characterization tests. The morphological characteristics, elemental composition, and physical and chemical interactions within the bio-composite are among the characteristics that have been analyzed. The performance of the newly produced composite is then evaluated in light of earlier investigations. The general chemistry and analytical labs at Chemical

Engineering and Energy Sustainability are used to do the experimental work. Ball milling is done at the University of Malaysia Sarawak's Mechanical Engineering Department and Civil Engineering Department (UNIMAS).

The work focuses on creating ecologically friendly nanocomposite materials using biomass as a nanofiller. The importance of newly created nanocomposite materials with enhanced capabilities and characteristics may be used to reduce the use of synthetic polymers finally led to a decrease in the amount of solid waste produced on earth. The work focuses on creating nanocarbon filler from the byproduct of pyrolysis and utilizing it to create bio-nanocomposite materials, which prior researchers seldom investigate. This discovery is crucial because it offers researchers a fresh perspective to work on the characteristics of nanocomposite materials made using biomass filler. It also gives them a leg up in their quest to develop better nanocomposite materials for the good of human civilization. Through various applications in the fields of health and biomedicine, food safety and packaging, and generating environmentally conscious materials (biodegradable), water adsorbent, and fire-retardant materials, this research study will help society.

8.2 Polymer and biopolymer

A material of repeating units of big molecules, or macromolecules, is called a polymer. Polymers may be broadly divided into two types: natural polymers and synthetic polymers. Wool, silk, rubber, hemp, shellac, and cellulose, all naturally occurring polymeric materials harvested from plants or animals, are examples of natural polymers (Shrivastava, 2018). Natural polymers such as cellulose, chitosan, starch, and agar are generated from carbohydrates and protein (Shankar & Rhim, 2018). Polyethylene (PE), PP, PVC, PS, thermoplastic polyurethane (TPU), Teflon, and nylon are examples of synthetic polymers.

Biopolymers are long-chain molecules comprising monomeric components connected to create polymers. The source of the biopolymer is a living creature, and it is biodegradable. As a biopolymer breaks down, it releases organic byproducts with a reduced environmental effect, such as water and carbon dioxide. Synthetic biopolymer is a new form of polymer produced, thanks to technology. It is a kind of synthetic biopolymer created via abiotic chemical processes (Vert et al., 2012). Shankar and Rhim divided biopolymers into four classes: natural biopolymers, synthetic biopolymers made by chemical synthesis, and synthetic biopolymers made from petroleum products (Shankar & Rhim, 2018). Biomass materials such as wood, straws, chitosan, gelatin, and gluten make natural biopolymers. The two sources of synthetic biopolymers are chemical synthesis from biomass or microbial generation. PLA, polyglycolide, polycaprolactone (PCL), polybutylene succinate, and polyvinyl alcohol are examples of chemically synthesized biopolymers. Microbiological biopolymers include polyhydroxyalkanoates (PHA), polyhydroxybutyrate (PHB), and polyhydroxybutyrate-cohydroxyvalerate (PHBV). The most often investigated biopolymer is PLA, made from lactic acid produced by the fermentation of carbohydrates found in plant resources like sugar beet and maize (Sorrentino et al., 2007). Further advantages of PLA, besides its biodegradability, are its flexibility in terms of shelf life (Shankar & Rhim, 2018).

According to Ray et al., microorganisms might quickly biodegrade PLA and its nanocomposites made with modified MMT containing trimethyl octadecyl ammonium (C^3C_{18}-MMT) (Ray et al., 2002). The test was conducted at 58°C, and the compost was made using food waste. Fig. 8.3 depicts a plot of the percentage for Residual molecular weight (Rw) compared to the initial weight (Mw) of the test sample (neat PLA and PLACN4 (C^3C_{18}-MMT = 4 wt.%)) from the compost with time.

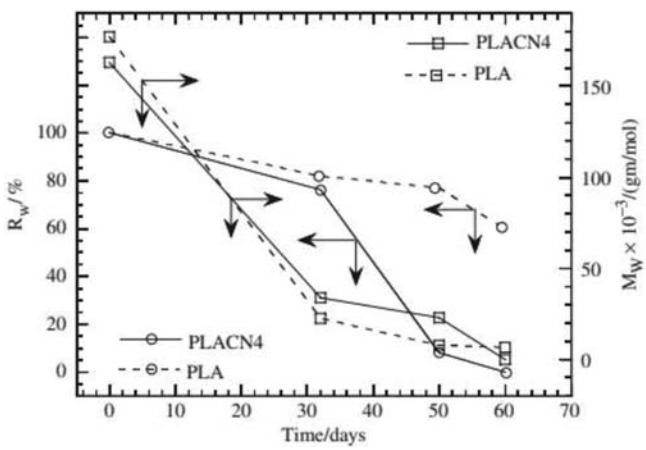

Figure 8.3 ***Time-dependent residual weight (Rw) of polylactic acid (PLA) and PLACN4 during composting at 58°C.*** Graph of PLA and PLACN4 at 58°C. *From Ray, S. S., Yamada, K., Okamoto, M. & Ueda, K. (2002). Polylactide-layered silicate nanocomposite: A novel biodegradable material.* Nano Letters, *2(10), 1093–1096. https://doi.org/10.1021/nl0202152.*

With weight loss starting after one month and total decomposition occurring after two months, PLACN4 underwent a major alteration.

Another form of biopolymer with biodegradable characteristics is PHA. PHA loses mass and starts to dissolve in the early phases of biodegradation when disorder chains are generated, and sample deterioration in crystalline is as follows (Avella et al., 2000). PHA is flexible because of its amorphous area, and crystallinity is predicted to rise as it deteriorates. According to Muniyasamy et al., features of soil biodegradation might be seen after 30 days (Muniyasamy et al., 2016), but those of marine biodegradation took roughly 60 days (Deroiné et al., 2015). After 30 or 200 days, it was anticipated that up to 60% less crystallinity would have been lost in the soil's biodegradation in a controlled composting setting environment (Muniyasamy et al., 2016).

The use of petroleum-based polymers might be reduced in favor of bio-based polymers. It will be a possible solution to create low carbon emissions and meet energy production needs. Fig. 8.4 contrasts commercial petroleum-based polymers with biodegradable materials, demonstrating the latter reduced environmental effect (Gironi & Piemonte, 2011;

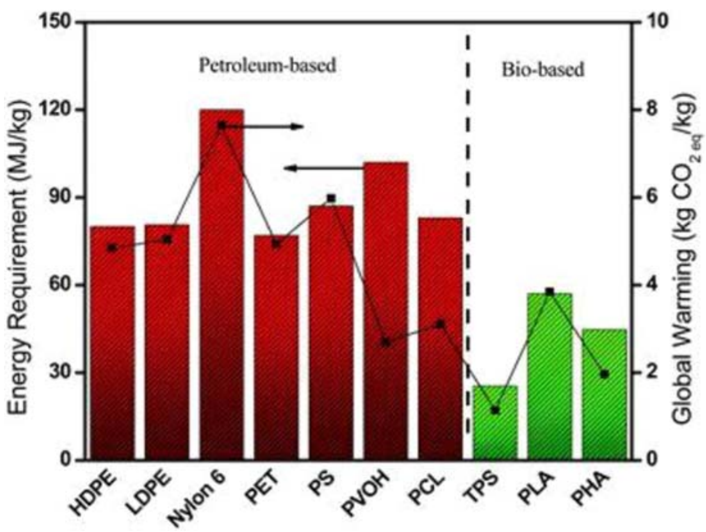

Figure 8.4 ***The energy usage and CO_2*** emission of petroleum-based and bio-based polymers. *From Harding, K., Dennis, J., Vonblottnitz, H. & Harrison, S. (2007). Environmental analysis of plastic production processes: Comparing petroleum-based polypropylene and polyethylene with biologically-based poly-β-hydroxybutyric acid using life cycle analysis.* Journal of Biotechnology, 130*(1), 57–66.* *https://doi.org/10.1016/j.jbiotec.2007.02.012*.

HARDING et al., 2007). Most plastics are disposed of either in the landfills, burned, or recycled after their useful life and emit carbon dioxide or methane over time. Nondegradable polymers may also release contaminants or additives into the soil and run into the water sources, further harming the digestive systems of animals (Gallo et al., 2018). Contrarily, bio-based polymers may still assist the environment after their useful lives are gone through.

8.3 Nanocomposites

Nanocomposites are artificially created or naturally occurring solid materials having several parts that have nanoscale shapes with a single phase. These are multiphasic compounds with sizes between 10 and 100 nm, each with distinct physical and chemical characteristics. Lamellar nanostructures or nanotubes are two examples of them (Sen, 2020). Conceptually, the nanocomposite may be divided into polymer-based composite and nonpolymer-based composite depending on whether polymeric material is included, as indicated in Table 8.1.

The polymer dispersed with nanofiller in the polymer matrix is known as poly-nanocomposite (PNC) (polymer-based nanocomposite). Fischer (2003) classifies PNC as a multiphase system, which includes composites, foams, and blends that may absorb up to 95% of the plastic produced (Fischer, 2003). The term "nanofiller" refers to nanoscale particles having a size between 1 and 1000 nm, where the upper limit is 100 nm. Examples include synthetic silica, carbon black, and precipitated calcium carbonate (Drobny, 2014).

Recently, CNTs, nanoclay such as smectite and MMT, and needle-shaped nanowhiskers have been commercially available. Previous studies have shown that adding nanofiller might enhance the characteristics of a polymer matrix. It has been discovered that it may improve the polymer's durability, stiffness, flexibility, barrier quality, heat resistance, and electrical conductivity and also boosts the propagation of light transmission inside the polymer (Bakri et al., 2018; Gulrez et al., 2013a, 2013b; Liew et al., 2018, 2020; Moniruzzaman & Winey, 2006; Thostenson et al., 2001). Nevertheless, an earlier study noted that attaining homogenous nanofiller dispersion inside the polymer matrix and ensuring chemical compatibility between the polymer, the matrix, and the nanofiller are two major

Table 8.1 Nanocomposite classification.

Nanocomposite	Type	Description
Polymer-based	Polymer/ceramic	• Composites consist of ceramic fillers and a matrix of organic polymers. • Example: polysiloxanes.
	Hybrid inorganic/ organic polymer	• Addition of organic side groups to an inorganic backbone chain. • Important in biomedical applications. • Example: coating of an implanted glucose sensor, chitosan-epoxy silane film.
	Polymer/layered silicate	• Polymer filled with low amounts of layered silicate. • As fire retardant materials.
Nonpolymer based	Metal nanocomposite	• Comprise of nanosized material of ductile metal or alloy matrix as reinforcement. • Improved mechanical properties: strength, modulus, ductility, and toughness.
	Ceramic nanocomposite	• Composites of ceramic are multiple solid phases with more than one nanoscale range dimension. • Have improved chemical, mechanical, magnetic, and optical properties. • Examples: Silicon nitride/silicon carbide, Hydroxyapatite/Titania nanocomposites, Baron Carbide/Titanium diboride nanocomposites.
	Ceramic-ceramic nanocomposite	• Use to mitigate fracture failure in artificial joint implants. • Example: zirconia-toughened alumina nanocomposite, calcium sulfate-biomimetic apatite

hurdles in producing polymer/nanoclay composite (Guo et al., 2018). The scientists also recommended focusing on theory and modeling to create a polymer/nanoclay combination that performs well and which is also mentioned earlier.

According to Schmidt et al. (2002), PNCs have been developed into various hybrid and innovative materials, such as nanoclay/conductive polymer (PPy, PANI, PT, PEDOT), bio-nanocomposite and organoclay hybrid films that have better qualities than composite materials (Schmidt et al., 2002). PNCs' distinctive properties have led to various industrial uses, including building, medicine, aerospace, food packaging, and textiles.

Future research in science and technology is anticipated to result in the synthesis of novel polymers and nanomaterials inspired by biological systems.

8.4 Nanofiller

Nanoparticles are tiny particles with sizes between 1 and 100 nm on the nanoscale. The usage of nanofillers in composite biopolymers should be graded by dimension, including 1D nanofiller, 2D nanofiller, and 3D nanofiller (Akpan et al., 2019). Fillers having one dimension under 100 nm are known as 1D nanofiller. They are branched-like structures, nanowalls, nanodisks, nanoplates, nanosheets, and nanoprisms. Due to its promising features, 1D nanofiller is often employed in biosensors, biomedical, microelectronics, and coating applications (Li et al., 2013; Vengatesan, 2016). MMT clay and graphene plats are the most prevalent examples of 1D nanofiller. At the same time, 2D nanofillers have two dimensions that are smaller than 100 nm. It comes in the form of filaments, tubes, or fibers. Examples of 2D nanofillers include cellulose fibers, CNTs, clay nanotubes, and boron nitride tubes. It often appears in energy, catalysis, sensors, electronics, nanoreactors, optoelectronics, and nanocontainers (Akpan et al., 2019). As 0D or iso-dimensional materials, 3D nanofillers essentially have identical dimensions in all directions at the nanoscale. Examples of 3D nanofillers include nano-silica, silver carbide, nanotitanium oxide, nanoalumina, and semiconductor nanoclusters. They have a high refractive index, are harmless, and inexpensive (Vengatesan, 2016). It is generally used in biomedicine, coating, and processes for purification and separation (Zhao et al., 2015).

There are several varieties of nanofiller in use today. It is classified into metal, ceramic, and carbon nanofiller. Carbon nanofiller is the most widely used kind of nanofiller. According to earlier research (Bitinis et al., 2011; Müller et al., 2017), incorporating nanofiller in low content within a polymer matrix is capable of enhancing its mechanical, thermal, barrier property, and flammability properties without compromising its processability. The addition of various nanofillers often improves the performance of biopolymers. According to Table 8.2, fillers with nanoscaled sizes may be either organic or inorganic, such as metal, metal oxide, clay, natural biopolymers, and substances that naturally fight microbes. These are some examples of nanofiller that may be used to create nanocomposite films.

Table 8.2 Nanofiller classification.

Organic/ Inorganic	Type of Nanofiller	Example	References
Organic	Nanofiber/whisker	Cellulose, starch, chitin, chitosan	Shankar and Rhim (2018)
	Natural antimicrobial agents	Nisin	Imran et al. (2010)
Inorganic	Nanoclay	Montmorillonite, kaolinite, hectorite, bentonite, saponite, organically modified clay	Shankar and Rhim (2018)
	Metallic nanoparticles	Silica, gold, silver, zinc oxide, titanium oxide, copper, copper oxide	Shankar and Rhim (2018)
	Carbon nanofiller	Carbon nanotubes, graphene, graphite, flurrenes, carbon fibers	Saba et al. (2019)

8.4.1 Carbonaceous nanofiller

Research on carbonaceous nanofiller such as CNTs, fullerene, diamond, and graphite have been more popular for many years. The CNTs have exceptional physical characteristics, including a high young modulus of 1TPa, a specific area of around 1315 m^2/g, a high thermal conductivity of 3500 W/m.K, and an electrical conductivity of 10,000 cm^2/Vs. Moreover, it can support a current density of up to 109 A/cm^2 because of its low electrical resistance, great strength, and high thermal conductivity (Annu et al., 2017; Kordás et al., 2007; Liu et al., 2018). Single-walled carbon nanotubes (SWCNTs), double-walled carbon nanotubes (DWCNTs), and multiwalled carbon nanotubes (MWCNTs) are the three different types of CNTs. SWCNTs have a diameter of less than 1 nm, whereas MWCNTs have a diameter of more than 100 nm. According to Zhang and Li (2009), rolling graphene sheets produce SWCNTs, which are seamless cylindrical materials (Zhang & Li, 2009). When additional graphene sheets are rolled up, DWCNTs and MWCNTs are created. Chemical vapor deposition, laser ablation, arc discharge, and premixed flame techniques generally synthesize SWCNTs and MWCNTs. SWCNTs exhibit exceptional performance in terms of mechanical and chemical characteristics, such as physical toughness, thermal stability, and electrical conductivity. MWCNTs and MWCNTs have excellent metallic characteristics, making them an excellent choice for electrochemical processes. Moreover, the favorable optical characteristics of CNTs are often used to transfer biomolecules into cells, including plasmid DNA.

In a hexagonal lattice structure with six carbon atoms at 0.142 nm molecular bonding, graphene comprises 2D sp^2-bonded carbon atoms with a single atomic layer (Foo & Gopinath, 2017). It is a crucial structural component of graphite, created by arranging graphene differently. With its high specific area of roughly 2630 m^2/g, the large elastic modulus of 1 TPa, the excellent thermal conductivity of between 3000 and 5000 W/mK at room temperature, the electrical conductivity of 15,000/cm^2 (VS), superior catalytic properties, and surface properties, graphene is used in a variety of applications (Saba et al., 2019). Several processes may be used, including thermal expansion, chemical reduction of graphene oxide, and micromechanical exfoliation of graphite to create graphene (Dantas de Oliveira & Augusto Gonçalves Beatrice, 2019). The development of exfoliated graphene in a sheet due to mechanical, chemical, and mechanical vapor exfoliation is one of them (Dantas de Oliveira & Augusto Gonçalves Beatrice, 2019). Before using mechanical or reduction exfoliation procedures, oxidation chemistry, the most widely used process, is used to make graphite oxides (GOs). Graphene offers many potential applications in energy storage devices, semiconductor materials, solar cells, and fuel cells.

A porous carbonaceous substance called biochar is created during the oxygen-limited pyrolysis process from various feedstocks (Lehmann et al., 2006). Biomass includes wood, plant seeds, fruit and nut shells, and agricultural waste. Pyrolysis, or the heat degradation of raw biomass under an oxygen gas supply that is either nonexistent or restricted, is used to create biochar (Lehmann & Joseph, 2012). Pyrolysis results in biochar, bio-oil, and biogas. According to Antal and Grønli (2003), the end product of pyrolysis may be impacted by the kind of biomass used as feedstock and the pyrolysis conditions (Antal & Grønli, 2003). Depending on the pyrolytic situation, the pyrolysis process is divided into different states and forms, including gasification, slow pyrolysis (also known as carbonization), and rapid pyrolysis. Table 8.3 displays the pyrolysis product with working conditions. The data shows that slow pyrolysis, yielding 35% of the dry biomass weight, is the most effective method for producing biochar. Whereas gasification and rapid pyrolysis are the most efficient ways to produce biogas and bio-oil, they are often utilized to produce heat and energy (Cheah et al., 2016). Fast pyrolysis produces the most bio-oil when the heating rate is high, and the residence duration is short. In

Table 8.3 Condition of the pyrolysis product in operation (Tomczyk et al., 2020).

Process	Temperature	Pressure	Residence time	The proportion of products in the pyrolysis process (%)		
				Bio-oil	**Biogas**	**Biochar**
Pyrolysis	400°C–600°C	Vacuum-atmospheric	Seconds	75.10	13.0	12.0
Biocarbonization (slow pyrolysis)	350°C–800°C	Atmospheric	Seconds-hours	30.0	35.0	35.0
Gasification	700°C–1500°C	Atmospheric-elevated	Second-minutes	5.0	85.0	10.0

Source: From Tomczyk, A., Sokołowska, Z. & Boguta, P. (2020). Biochar physicochemical properties: pyrolysis temperature and feedstock kind effects. Reviews in Environmental Science and Biotechnology, 19(1), 191–215. https://doi.org/10.1007/s11157-020-09523-3.

comparison, slower heating rates and a longer slow pyrolysis residence period will create more biochar (Daful & Chandraratne, 2018)

According to Sakhiya et al. (2020), biochar is widely used as a water adsorbent due to its large surface area to adsorb aromatic compounds and heavy metal ions and hence removes the pollutants from wastewater (Sakhiya et al., 2020). Singh et al. (2019) also stated that biochar could boost soil fertility and hold water longer (Singh et al., 2019). Biochar also used in other applications such as air purification (Creamer et al., 2014), as a catalyst (Shen, 2015), fuel alternative (Balat, 2007), as a building material (Gupta & Kua, 2017), etc.

8.4.2 Nanoclay

Lately, nanoclay has been explored and produced in several domains of applications because of the fast expansion of nanotechnology. Their advantages include accessibility, affordability, and environmental friendliness. Stacks of mineral silicates with layered structural units make up nanoclays, a complicated clay crystalline nanoparticle. Both octahedral and tetrahedral sheets made up those layers. In general, nanoclay materials are divided into three clay layers with sheet arrangements of 1:1, 2:1, and 2:1:1. Table 8.4 categorizes the clay layer, clay group, and clay species. It may be utilized in various applications depending on how they are arranged and what minerals are in them.

The well-known kind of clay utilized as a nanofiller in polymer structures to create composites of polymer and nanoclay is MMT 2:1 nanoclay. Alumina's octahedral sheet, which is joined to two silica tetrahedral sheets in a 2:1 sheet configuration, is around 1 nm thick. Guo et al. (2018) claim that MMT nanoclay (2:1) has a significant

Table 8.4 Clay minerals.

Types of layers	Group	Species
1:1	Chysotile, hallosite, kaolinite, rectorite	Berthierine, brindleyite, cronstedtite, dickite, fraipontite, kellyite, lizardite,
2:1	Mica, pyrophylite talc, smectite, vermiculite,	Bentonite, bityite, clintonite, hectorite, laponite, montmorillonite, muscovite, sepiolite, vermiculite
2:1:1	Chlorite	Amesite, cookeite

Source: From Guo, F., Aryana, S., Han, Y. & Jiao, Y. (2018). A review of the synthesis and applications of polymer–nanoclay composites. *Applied Sciences, 8*(9), 1696. https://doi.org/10.3390/app8091696.

Table 8.5 Montmorillonite physical properties.

Type	Properties
Density	2–3 g/cm^3
Hardness	1–2 on the Mohs scale, fine-grained
Crystal system	Monoclinic
General formula	(Ca, Na, H) $(Al, Mg, Fe, Zn)_2$ $(Si, Al)_4$ $O_{10}(OH)_2$. nH_2O
Fracture	Irregular/uneven
Lustre	Earthy and dull
Color	White, yellow, buff, usually pale pink to red (pink-red coloration due to the presence of Manganese (Mn))
Transparency	Translucent

surface area, a high cation capacity, and swelling behavior (Guo et al., 2018). Due to their distinct structural characteristics, clays are selected as the appropriate substance to modify the polymeric membrane. It has been discovered that clay alteration may enhance the physicochemical function of membranes. Additives are often applied to incorporate functional groups that may affect the interaction activity between soluble species and membranes on the surface of the MMT layer. MMT's physical characteristics are listed in Table 8.5.

According to past studies, acid-modified clay would cause the clay to disassemble, elute mineral impurities, and lose its outer layer. Aluminum and magnesium ions would replace hydrogen ions, H^+, due to the acid activation clay, increasing surface area and pore size. Additionally, clay surfaces with more broken bonds due to acid activation, typically have more surface area and are more reactive.

There was no discernible change in the mineral structure of the clay throughout the acid treatment of MMT. However, activity and surface area have been increased, and the Al3 + ion was separated during leaching (Jeon & Nam, 2019). Heavy metals, including Ni (II), Cu (II), and Pb, have been removed using hydroxyl groups introduced to the surface of activated clay (II) (Al-Essa, 2018). According to Ndé et al. (2019), the most often employed acids in the acid activation process are hydrochloric acid (HCl) and sulfuric acid (H_2SO_4) (Ndé et al., 2019). They investigated the formation of bleaching agents and the activation of acids in the smectite clay.

Regarding palm oil bleaching effectiveness and cost, it was discovered that H_2SO_4 was more effective than HCl acid. At the same time, Amari et al. (2018) investigated the relationship between the chemical activation characteristics of green clay minerals and their structural makeup (Amari et al., 2018). A larger degree of acid activation caused the treated mineral's silica structure to transition from crystalline to amorphous. When the amount of acid treatment is raised, it also increase the total pore volume and surface area. According to Zhang et al. (2019), activated clays may be adsorbents to remove dyes (Zhang et al., 2019). The polymer/nanoclay composites may also be used as thickening and gelling agents, flame-resistant materials, gas permeability modifiers, wastewater treatment processes, and mechanical strength enhancers, according to numerous works of literature (Choudalakis & Gotsis, 2009; Giannelis, 1996; Irshidat & Al-Saleh, 2018; Yusoh et al., 2018).

The cation exchange capacity of clay and organic materials Is one of their key characteristics. Al^{3+}, Ca^{2+}, Mg^{2+}, Mn^{2+}, Zn^{2+}, Cu^{2+}, Fe^{2+}, Na^{+}, K^{+}, and H^{+} may all be held by clay, thanks to the negatively charged surfaces of the clay minerals (Agronomy Fact Sheet Series Fact Sheet 22, 2008). A tiny particle with a diameter between 0.002 and 0.001 mm will have a much bigger surface area and can adsorb many more cations. The high degree of conductivity in clay is often reflected in the adsorbing cations (FHWA, 2003). Because of its superior heat resistance, MMT is often used as an ingredient in various compounds. Nanoclay may be added to polymer composites to increase thermal stability and flame retardancy. Typically, a polymer's thermal expansion coefficient falls between 20 and 100 ppm/°C. Adding MMT, a filler with excellent thermal stability to polymers causes lower thermal expansion. Nonetheless, a high aspect ratio of above 100 is beneficial for enhancing thermal stability.

8.5 Nanocomposite properties

8.5.1 Reinforcement

It is generally known that adding nanofiller improves the mechanical characteristics of composite materials. With the use of a nanofiller, the possibility of strain or break is reduced. Like the nanotubes, the greater loading percentage will raise the graphene-filled nanocomposite's modulus. Elastomeric matrices exhibit observable modulus increases due to their smaller inherent moduli. Research has also shown that graphene performs better as a mechanical reinforcement in composites than carbon black or SWCNTs (Kim et al., 2010). Increases in graphene content have often enhanced tensile strength; however, this is not the case sometimes (Yasmin et al., 2006). In contrast, elongation either declines or remains constant. Similar mechanical characteristics of nanoclay are shown in composite materials made of nanotubes or graphene polymers. Further addition enhances modulus and tensile strength while decreasing elongation at break. Nevertheless, clay reinforcing for a given volume percent of filler in the composite is substantially lower than graphene or CNTs composites. The fabrication of nanocomposite from pure or organically modified clay has strengthened the mechanical characteristics of polymeric materials in terms of tensile modulus. According to Manias et al. (2001), as the clay percentage rises, so does the modulus in a PP-clay composite (Manias et al., 2001). Nevertheless, when clay concentration rises over 3 wt.%, modulus only slightly improves.

8.5.2 Electrical conductivity

Due to the exceptional conductivity of CNTs and graphene, a conventional insulating polymer matrix may be converted into a conductive material. According to Bhattacharya (2016), the dielectric matrix is created as filler when percolation is below a certain threshold (critical loading) (Bhattacharya, 2016). This is due to its inability to establish a continuous network for electron flow. Meanwhile, conductivity increases when loading increases over the percolation threshold. As filler loading rises, the filler becomes close to one another. A conduction channel was predicted to develop in the dielectric matrix near the percolation threshold, increasing conductivity. Conductivity would not alter beyond a particular filler concentration in the polymeric matrix. Research shows that the electrical percolation threshold of CNTs is greater than that of graphene (Steurer et al., 2009). Generally, SWNT typically has lower conductivity than MWCNT owing to the higher contact resistance in SWCNT caused by the shorter diameter. The same technique may be used to study the conductivity of graphene PS films is much lower than that of CNTS films (Qi et al., 2011).

8.5.3 Thermal conductivity

Comparatively, a normal polymer has a thermal conductivity of between 0.3 and 0.4 W/mK, whereas CNTs have an estimated range of

650−1000 W/mK (Bhattacharya, 2016). The heat conductivity of the composite improves with the amount of filler used, and a 20-fold increase was made by using a nanofiller to fill the composite (Monica Veca et al., 2009). Thermal conductivity is predicted to increase also in nanotube-based composite materials; however, it will likely remain relatively low (less than 1 W/m.K.). According to (Xie et al., 2007), functionalized nanotubes have an extraordinarily high thermal conductivity compared to unfunctionalized nanotubes because of their increased dispersion, which helps with conductivity.

8.5.4 Thermal stability

Polymers have a high thermal expansion coefficient compared to metals. By limiting the degree of mobility of the polymer chain owing to its interaction with the filler, the insertion of nanofiller such as clay or graphene nanotubes in polymer reduces its thermal expansion. Adding GO and SWNTs to resins has been discovered to result in less thermal expansion (Wang et al., 2009). As a result, GO, and SWNTs have greater thermal stability due to their low thermal expansion coefficient values.

8.5.5 Barrier properties

Excellent gas barriers are present in the nanocomposite. Broad aspect ratio filler has the potential to block the direction of diffusion of penetrating molecules. A well-distributed filler creates a path for permeants to flow. Clay-reinforced composites' gas permeability falls regardless of the kind of gas (Kojima et al., 1993). When clay (1 wt.%) is added to PET, the oxygen permeability is reduced twice. Clay nanocomposite of PCL has less water vapor permeability than PCL (Messersmith & Giannelis, 1995). The amount of water vapor that moves across PU urea sheets has significantly decreased (Xu et al., 2001). Moreover, the layered silicate/PI nanocomposite exhibits excellent barrier characteristics against the vapors of ethylacetate, CO_2, HE, and N_2 (Fu & Qutubuddin, 2000).

8.5.6 Flammable resistance

It has been discovered that adding nanofiller to polymer has significantly reduced heat release, compared to plain polymer, even if the overall heat release has remained constant (Bhattacharya, 2016; Morgan, 2006). Moreover, the aspect ratio of the distributed silicate layers and the manufacturing method might affect their fire-retardant qualities (Bartholmal & Schartel, 2004;

Schütz et al., 2011). Both clays and nanotubes have been reported to have flame-retardant characteristics, although nanotubes are more successful than clay in containing flames (Costache et al., 2007; Kashiwagi et al., 2005). The filler should only be included in polymers with proper quantity. Yet, ignition occurs more quickly because of the localization of heat caused by high thermal conductivity and low specific heat, and the inclusion of nanotubes. Low concentration and poorly distributed filler will create a discontinuous network, lowering flame resistance (Kashiwagi et al., 2005).

8.5.7 Glass transition temperature

Introduction to Plastics and Elastomers, 2012refers to the temperature at which a polymer changes from hard and brittle to soft and malleable. Research showed that nanofiller might affect the glass transition temperature and its transition width (Ding et al., 1993; Sasaki et al., 2003). The interaction of the filler determines how much T_g changes (Keddie et al., 1994; Tate et al., 2001). The surface's intimate interactions with the polymer increase T_g compared to the bulk. Most literary examples reflect a small decrease in T_g value (10%) (Paul & Robeson, 2008).

8.6 Preparation of activated carbon

Preparing AC involves two steps: the carbonization of the raw material and the activation procedure. Odetoye et al. (2019) defined carbonization as creating biochar by high-temperature pyrolysis or gasification in an oxygen-restricted atmosphere (Odetoye et al., 2019). The fixed carbon content was increased throughout this procedure by eliminating volatile, noncarbon components like N_2, O_2, and H_2 by thermal deterioration in a furnace with continuous N_2 purging (Radenahmad et al., 2020). At this stage, narrow pore structures begin to develop, and as the temperature increases, tarry materials are deposited (Alhinai et al., 2018). There are instances exist when some compounds will collide with the walls of the pores, leading to hydrocracking and carbon deposition (Odetoye et al., 2018). Process variables, including temperature, heating rate, N_2 gas flow rate, and residence duration, are crucial since they impact the product's ultimate quality. Fig. 8.5 displays the four primary carbonization steps in order of their temperature (Chowdhury et al., 2013).

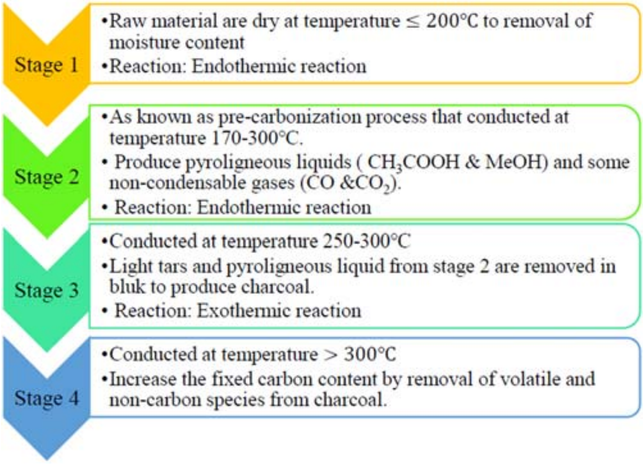

Figure 8.5 ***Process of carbonization in four stages.*** Stages of carbonization. *From Chowdhury, Z. Z., Hamid, S. B. A., Das, R., Hasan, M. R., Zain, S. M., Khalid, K. & Uddin, M. N. (2013). Preparation of carbonaceous adsorbents from lignocellulosic biomass and their use in removal of contaminants from aqueous solution.* BioResources, 8*(4), 6523–6555. https://doi.org/10.15376/biores.8.4.6523-6555*.

Biochar, bio-oil, and biogas are the three primary products of the thermal breakdown of biomass. The most significant element that might impact the creation of the finished product is temperature. Slow pyrolysis produces 35% biochar, 30% bio-oil, and 35% biogas. Fast pyrolysis, which occurs at a higher temperature, produces less bio-oil, 70% biochar, and 20% biogas. Gasification, which occurs at a temperature higher than fast pyrolysis, tends to produce more biogas, which is 85%, 10% biochar, and 5% bio-oil (Mohan et al., 2014). Fig. 8.6 illustrates the many activation strategies that may activate biomass, including physical, chemical, physio-chemical, and microwave-assisted activation (Reza et al., 2020). Physical activation happens in two steps. After carbonization, charcoal is activated at a high temperature using an activator such as carbon dioxide, ammonia, steam, air, oxygen gas, or their combination (Chowdhury et al., 2013). Physical activation, which includes carbonization and is more energy-intensive followed by pyrolysis at 800°C–1000°C (Wang et al., 2009). In chemical activation, raw materials are impregnated for dehydration purposes with a predetermined ratio of chemical activation agents. H_3PO_4, K_2CO_3, $ZnCl_2$, NaOH, LiOH, and KOH are a few examples of oxidants utilized for activation. Then, pyrolysis of activated biomass was placed at 500°C, substantially lower than the temperature required for physical

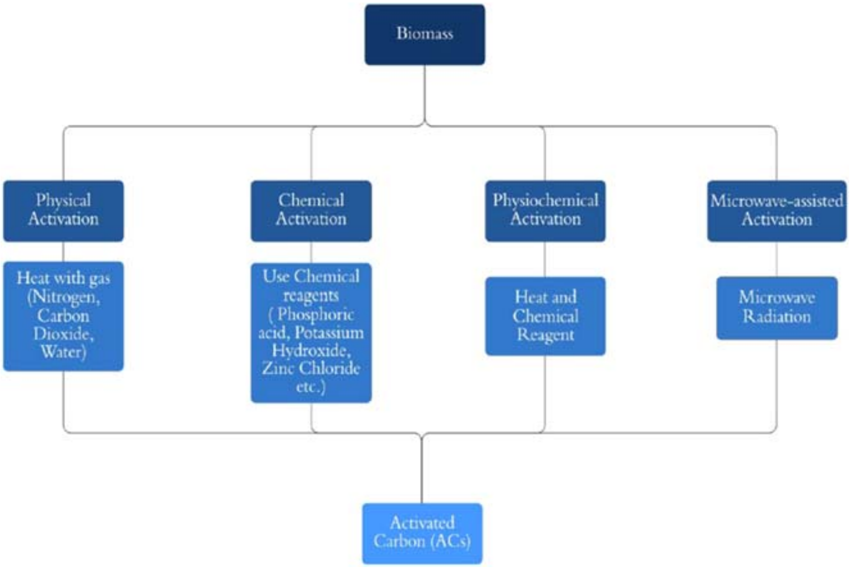

Figure 8.6 ***Different activation mechanisms.*** Chart of activation.

activation (Wang et al., 2019). Physiochemical activation combines physical and chemical activation (Chowdhury et al., 2013). It may be done in two different ways: chemically before carbonization and chemically after carbonization (Rashidi & Yusup, 2017). The biomass is chemically treated before being heated and physically activated (Mohd Din et al., 2009). The second process involves carbonizing biomass and then impregnating biochar with chemicals. Biochar is then heated in the presence of an oxidizing gas or carbonized at a high temperature between 600°C and 850°C. The order of the chemical activation in this process, according to Lee et al. (2014), will not have an impact on the quality and textural characteristics of ACs.

Microwave-assisted activation consists of two methods: one-step and two-step processes. In a one-step process, physical and chemical activation is accomplished simultaneously to produce higher quality using microwave radiation (Deng et al., 2010), and in a two-step process, carbonization is followed by activation separately (Abbas & Ahmed, 2016). According to Ao et al. (2018), the configuration procedure of the microwave, the strength of radiation, the period of activation, raw material properties, and the interaction between microwave and chemical substances are significant limitations of the activation process. Table 8.6 shows the preparation of biochar from different types of sawdust.

Table 8.6 Making biochar from several kinds of sawdust.

Raw material	Preparation method	References
Pine wood sawdust	Scots pine (*Pinus sylvestris L.*) was pyrolyzed using a fixed-bed reactor at a temperature of 500°C and heating rate of 5°C/min at a residence time of 1 h in nitrogen atmosphere (30 mL/min).	Özbay et al. (2015)
	Pine wood sawdust (PWS) was pyrolyzed in the microwave with 10wt.% of AC for 20 min processing time and power varying from 100 to 800 W.	Khelfa et al. (2020)
sawdust	Aspen (*Populus tremuloides*) wood chips were placed in the 3 vertical stacked zones in the vertical quartz reactor and heated in N2 to a temperature of 420°C −650°C at a heating rate of 4°C/min for 1−4 h.	Veksha et al. (2014)
Rubberwood sawdust (RWSD)	RWSD was pyrolyzed in a tube furnace at a temperature ranging from 300°C to 700°C with a continuous heating rate at 5°C/min for 3 h and continuous N_2 gas purging at 30 mL/min.	Shaaban et al. (2013)
Durian wood sawdust (*Durio zibethinus*)	Durian wood sawdust was produced through slow pyrolysis by a fixed bed reactor from room temperature to desired temperature 350°C−550°C at a heating rate of 10°C/min for 3 h of residence time with nitrogen purging at 30 mL/min.	Chowdhury et al. (2016)

8.7 Preparation of nanocomposite films

Synthesis techniques include melt intercalation, solution exfoliation, and in-situ polymerization (Shankar & Rhim, 2018). Either a mechanical or chemical procedure may be used to create it. The process is chosen depending on the required qualities of the final product, the polymeric matrix, and the nanofiller (Mallakpour & Naghdi, 2018). Using a catalyst or heat radiation, in situ, polymerization involves adding a monomer to layered clays and polymerizing. To guarantee that the polymer is created between the nanoparticles, the nanofiller is dissolved in a monomer solution before the commencement of the polymerization process. This method can create fillers with a high loading capacity and polymer-grafted nanoparticles that are dispersed well (Naz et al., 2015).

This method was the most effective for spreading the carbon nanofiller in the polymer matrix to produce a strong contact between them (Lyu et al., 2019). This method is also appropriate for creating nanocomposite materials employing insoluble and thermally unstable polymers (Shin et al., 2003). Solution exfoliation is another technique used to create the nanocomposite film in addition to polymerization. This process uses a solvent to dissolve the multilayer clays into thin, individual platelets, then mixed with clay suspension to allow the polymer to adhere to the platelets. In the melt intercalation process, layered clays and polymer matrices are combined and heated to a particular temperature to produce a molten state material, according to Zeng et al. (2005). An extruder can carry it out after that (Zeng et al., 2005).

Since nanocomposites' many components interact with one another and have varying characteristics and compositions, various variables may impact how well nanofiller performs its role as reinforcement in the polymer matrix. Regarding tensile strength and Young modulus, Bhattacharya (2016) mentioned that filler should have outstanding mechanical properties (Bhattacharya, 2016). The filler should also be able to distribute effectively without forming clumps, and it should have a greater aspect ratio (L/D) and surface area for interacting with the polymer. In particular, the physical and mechanical characteristics of the nanocomposite biopolymer may be impacted by the nanofiller's degree of dispersion (Liu et al., 2005). According to Dantas de Oliveira and Augusto Gonçalves Beatrice (2019), conventional composites, intercalated, and exfoliated nanocomposites are three different types of nanocomposite morphology (Dantas de Oliveira & Augusto Gonçalves Beatrice, 2019). A typical composite develops when there is no intercalation between the polymer and silicate layers, resulting in various composite phases. Intercalated nanocomposites are created when intercalation contact exists between the polymer and silicate layer. Several layers with well-organized morphology make up this kind of nanocomposite. Exfoliated structure, meantime, is produced by uniformly and thoroughly dispersing silicate layers in the polymer matrix. Previous researchers often acquired the intercalated and exfoliated structure. A more even distribution of stress is made possible by more dispersion, which enables a good load transmission to the network of nanofiller., The differences between nanofiller and polymer characteristics are addressed, contributing to increased strength by extending the interfacial area of the filler and matrix.

Conversely, alignment might raise their modulus and tensile strength, causing the composite material to display anisotropy. Due to the connection between filler and polymer, external tension exerted on composites may be transferred to the nanofiller, allowing the latter to tolerate more pressure. The purpose of nanofiller has thus always been to enhance their interaction and dispersion within the polymer matrix.

Table 8.7 lists several techniques that earlier researchers employed to create nanocomposite materials based on nanoclay, either with a single or hybrid filler. The procedure involves dry blending, electrospinning, melt mixing, melt extrusion, in-situ polymerization, hot pressing, and solution casting.

Table 8.7 Method of preparing clay/nanocarbon nanocomposite.

Polymer	Nanofiller	Method	References
Polyethylene (PE)	Modified MMT	Melt-mixing	Merinska et al. (2012)
Low-Density Polyethylene (LDPE)	MWCNT	Hot pressing	Gorrasi et al. (2007)
Polypropylene (PP)	MMT	Melt-Extrusion	Duleba et al. (2014)
Polypropylene (PP)	SWCNT	Shear-mixing	Manchado et al. (2005)
Polypropylene (PP)	MWCNT	Melt fiber spinning	Jose et al. (2007)
Polystyrene (PS)	MWCNTs	Solution casting	Qian et al. (2000)
Poly (methyl methacrylate) (PMMA)	Oxidized MWCNT	In situ bulk polymerization	Jia et al. (1999)
Poly (vinyl alcohol) (PVA)	Hydoxy-modified SWCNT	Solution casting	Liu et al. (2005)
Polyimide (PI)	SWCNT	Melt extrusion	Siochi et al. (2004)
Polylactide	Nanoclay (3 wt.%)	Melt mixing	Pluta et al. (2007)
Polymer	**Hybrid Nanofiller**	**Method**	**References**
Low-Density Polyethylene (LDPE)	MWCNTs/CB	Melt-mixing	Paszkiewicz et al. (2020)
Polypropylene (PP)	MWCNTs/Clay	Dilution batch	Prashantha et al. (2014)
High-density polyethylene (HDPE)	MWCNTs/ modified MMT	Dry blending	Ali Mohsin et al. (2014)

8.8 Nanocomposites characterization technique

Understanding the physical and chemical characteristics of PNCs requires experience in using characterization techniques for nanocomposites. Several different characterization techniques are often used in studying polymer nanocomposites. In general, transmission electron microscopy (TEM), scanning electron microscopy (SEM), and X-ray diffraction (XRD) are the most efficient techniques (TEM). XRD examination may identify clay alterations by polymer exfoliation or intercalation into clay galleries (Kanda et al., 2018). Due to its ease of use and accessibility, it is the easiest way to see how the clay layers possess the gap. The examination may show a peak for clays and organoclays to be stable with layered structures. The clay structure's platelet, or d-spacing, conforms to the peak. When d-spacing increases, the analytical peak will migrate to lower diffraction angles. According to Sharma et al. (2012), an increase in the d-spacing value from 18.26854 to 38.05891 showed that the polymer might intercalate into the space between the layers of platelets and created an intercalated structure (Sharma et al., 2012). In the meanwhile, the exfoliation structure is indicated by the lack of an intensified peak. According to Chow's research for OMMT in 2007, the characterization peak has completely vanished in epoxy/glass/OMMT. According to this finding, silicate platelets in the epoxy matrix were exfoliated (Chow, 2007).

SEM and TEM are the best techniques to obtain magnified solutions of nanoparticles dispersed in the polymer matrix. TEM enables direct observation of the exfoliation condition of clay, whether it is intercalated or exfoliated. In contrast to magnified scanning, which is accomplished by focusing the electrical beam on the specimen, TEM creates electronic interference by passing an electrical beam through an ultrathin specimen. While Fourier transforms infrared (FTIR), thermogravimetric analysis (TGA), thermomechanical analysis, differential scanning calorimeter (DSC), dynamic modulus analysis, and rheometer are commonly used methods for thermal characterization and studying the cure behavior of PNCs.

Often employed for qualitative and quantitative examination of their nanofiller and nanocomposites is Fourier transform infrared (FTIR) spectroscopy. FTIR will describe the nanofiller in qualitative evaluations, including a metal oxide, carbonaceous material, nanoclay, the synergy effect, and polymer nanocomposites. Whereas in quantitative analysis, FTIR will change the band of spectra to look at how the characteristics of the nanocomposite film are affected by the nanofiller. Also, this method may offer information on the composition of functional and structural groupings (Jaleh & Fakhri, 2016). When a sample is heated, TGA measures the change in sample mass and determines if it is chemical or physical (Kanda, 2018). For investigating phenomena that occur during the thermal scan of nanofiller and PNC, such as crystallization, glass transition, cure kinetics, and melting, DSCs were often utilized (Corcione & Frigione, 2012). Dynamic mechanical analysis, however, focuses on describing the viscoelastic characteristics of polymers (Kanda et al., 2018) as nitrogen gas is an inert gas and may be used in BET research to measure pore size and surface area and calculate material-specific surface area (Brunauer et al., 1938).

8.9 Methodology

8.9.1 Materials

The raw material for this research is pine sawdust (biomass to produce nanocarbon), obtained from the Russian Federation (Fig. 8.7) and was air-dried before storage for subsequent use. Modified MMT K10 was obtained from Sigma-Aldrich. Polylactic acid (4043D grade) powder with 1.24 g/cm^3 density and 145°C–160°C melting point. Other chemical includes acetic acid glacial 100% (Merk KgaA) and Chloroform (Merk KgaA).

Figure 8.7 Sawdust of pine obtained from Vyatka State University.

8.9.2 Design of experiment with response surface methodology

A collection of analytical techniques called response surface methodology (RSM) examines the connections between controlled experimental conditions and computed responses that rely on one or more parameters (Box & Wilson, 1951; Gao et al., 2007). For the manufacture of graphene oxide PNCs, Perez et al. (2017) used the RSM approach to optimize the concentrations of graphene oxide (GO), glutaraldehyde (GLA), and polyethyleneimine (PEI) (Perez et al., 2017). Yalçinkaya et al. (2010) used RSM to investigate the effects of organoclay concentration and polymerization speed on creating PS-MMT nanocomposites (Yalçinkaya et al., 2010).

The hybrid filler bionanocomposite was developed in this experiment using the RSM technique, which also helped to discover the best conditions for mixture composition and process parameter optimization. The input variables are varied throughout a series of test runs to detect changes in the output response. To examine the initial design and carry out the design of the experiment, the statistical program "Design Expert ® software version 11." will be used (DOE). This software offers comparison testing, screening, characterization, optimization, resilient parameter design, mixture designs, and combination designs. Moreover, it offers test matrices that are constructed using analysis of variance (ANOVA) for screening up to 50 components. Also, it aids in determining how each aspect affects the intended outcome and highlights any possible data errors. Various material compositions are anticipated to be produced to create the nanocomposite.

8.9.3 Biomass preparation

The Panasonic MX-AC400 Mixer Grinder grounds the pine sawdust into even smaller pieces. After the grid procedure, the sample was sieved through a 900 μm sieve to generate particles with the same micrometer size and it was then kept in a cold, dry location for later use.

8.9.4 Pine sawdust chemical activation

A 0.05 M stock solution was made from 100% pure (glacial) acetic acid. The solution was then diluted till the pH was between 4 and 5. The diluted acid's ultimate pH was 4.5 shown in Fig. 8.8A. According to published literature, the pine sawdust was impregnated with an acetic acid solution (1:1) at a ratio of 1/5 (w/v) (Jiao et al., 2017). The mixture was

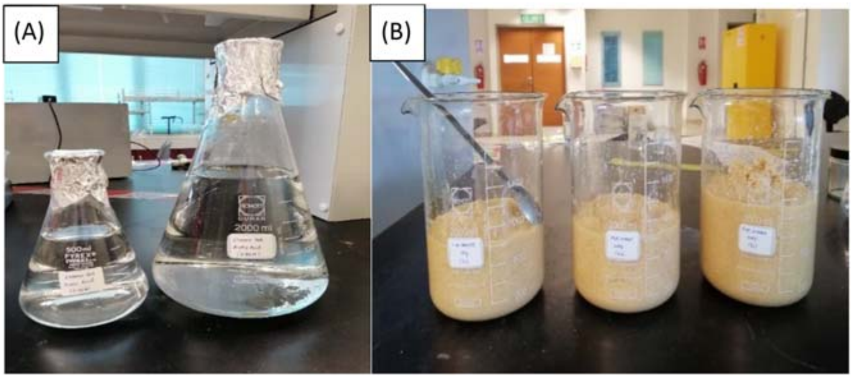

Figure 8.8 ***(A) Acetic acid with pH4.5, and (B) chemical activation process.*** Acetic acid and its chemical activation.

slowly stirred for 1 and a half hours (Fig. 8.8B). Following activation, the mixture was rinsed with distilled water until the wastewater became neutral, then dried for 48 hours at a temperature between 33°C and 45°C before carbonization. The sample was regularly removed and mixed to ensure equal heating. Moreover, the changeable hotspots throughout the drying process are eliminated.

8.9.5 Pine sawdust carbonization

The carbonization process was performed in an LT furnace at the Civil Geotechnical lab, UNIMAS. The dried mixture of precursor and the activating agent were then transferred into a ceramic bowl and wrapped using aluminum foil and a layer of clay before the carbonization process to prevent sample oxidation. Subsequently, placed into the LT furnace for the carbonization process. About 500 g of raw pine sawdust and 650 g of activated pine sawdust were inserted into the furnace. During the carbonization step, the temperature ramped from room temperature to 200°C to 400°C with a heating rate of 10°C/minute. At 400°C, the carbonization temperature was held (soaking) for 1 hour. The furnace was cooled at 6.16°C/minute until it reached room temperature. The sample was left overnight and removed from the furnace in the morning. Fig. 8.9A and B depict LT Furnace and the graph of time settings for the carbonization process. As illustrated in Fig. 8.10, when the carbonization process was finished, the biochar was collected and sieved through a 200 μm sieve to decrease its size further and aid in the ball milling procedure.

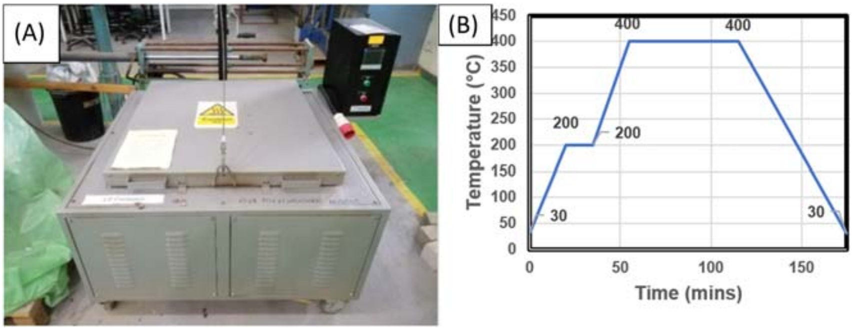

Figure 8.9 ***(A) LT Furnace, and (B) time setting for LT furnace.*** Furnace and the time setting used for the biocarbon process.

Figure 8.10 Biocarbon obtained after process.

8.9.6 Ball milling process

Fig. 8.11A depicts the ball milling device to create nanoscale biochar. The generated biochar is pulverized in a grinder for around 5 minutes at a speed range from 18,000 to 20,000 rpm to aid the ball milling process according to the Planetary ball mill requirements. 20 stainless steel balls weighing 0.5 g each are used to compress the biochar to a size of around 55% in two cylindrical containers. The biochar was ground for 30 hours,

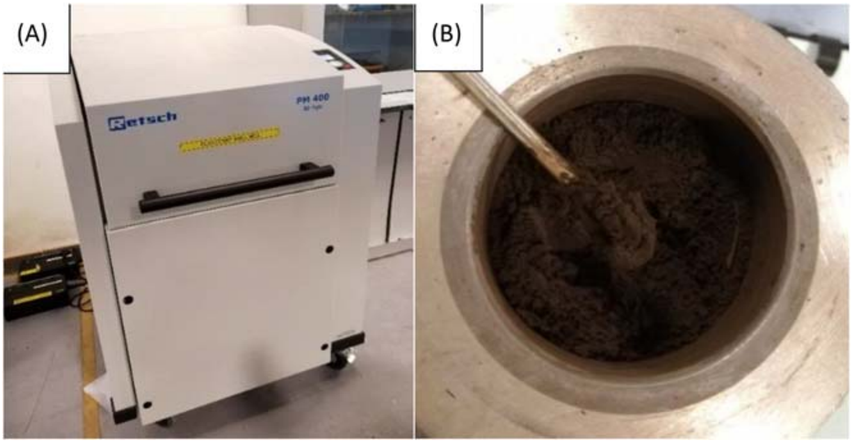

Figure 8.11 (A) Retsch PM400 ball milling machine, and (B) fine biochar.

and samples were frequently taken for testing. After being ball milled, the fine biochar is shown in Fig. 8.11B.

8.9.7 Preparation of bio-nanocomposite by solution casting method

According to Table 8.8, the nanocarbon/MMT/PLA combination was uniformly blended. The combination of biochar, MMT, and PLA was dissolved in chloroform at 55°C on a hot plate machine. The mixture was continuously agitated with a magnetic stirrer until the PLA powder dissolved and the liquid thickened. The mixture was then transferred to a glass Petri dish and left to cool overnight at room temperature. The film is then removed for analysis.

Fig. 8.12 depicts the created bio-nanocomposite film with increasing nanocarbon loading at 0.25, 0.50, 0.75, and 1 wt.%. The fixed MMT weight percentage was 1 wt.%.

8.9.8 Characterization of nanocarbon/clay bio-nanocomposite

Characterizing a nanocarbon/MMT/PLA bio-nanocomposite involves conducting analytical research on its morphological, chemical, and physical characteristics. PSD, FTIR spectroscopy, SEM, and BET measurements were all used in the characterization (BET). The real test is performed many times for each sample, and the most representative findings are chosen.

Table 8.8 Composition of polylactic acid-based bio-nanocomposite.

PLA (wt.%)	RC/AC (wt.%)	MMT (wt.%)
100	0	0
98.75	0.25	1
98.5	0.50	1
98.25	0.75	1
98	1	1

Figure 8.12 ***Pure polylactic acid (PLA) and nanocarbon/montmorillonite (MMT)/PLA bio-nanocomposite film.*** Bio-nanocomposite film made from PLA and nanocarbon/MMT/PLA.

8.9.8.1 Particle size distribution

The laser particle size analyzer (CILAS 1090) measures the particle size of activated and unactivated biochar in liquid mode at intervals between 0.04 and 500 μm. PSDs of the two biochar types are compared before and after ball milling (ABM).

8.9.8.2 Bunauer–Emmett–Teller surface area analysis

The study of BET surface area of biochar samples with N_2 adsorption uses a Quantachrome Autosorb iQ (Quantachrome Instruments, Boynton Beach, FL, USA) under (Standard Test Method for Carbon Black—Total & External Surface Area by Nitrogen Adsorption, 2014) standard. The analysis is done for 12 hours at a degassing temperature of 250°C.

8.9.8.3 Scanning electron microscopy (SEM-EDX)

Using Hitachi's TM4000 Plus tabletop SEM, biochar and bio-nanocomposite SEM micrographs were taken (Tokyo, Japan). The samples were mounted to the aluminum stubs using double-sided adhesive tape. The SEM's field emission gun was used in BSE and conventional vacuum modes to take images of composite and biochar at magnifications of 60–1500 ×. The test was carried out under the (Standard Guide for Preparation of Plastics & Polymeric Specimens for Microstructural Examination, 2021) standard. Before X-ray net counts were collected, SEM-EDX analysis was utilized to ascertain the film's elemental composition and distribution in a randomly chosen location.

8.9.8.4 Fourier transform infrared spectroscopy

By locating the existing functional groups in activated/nonactivated biochar and bio-nanocomposite, nanocomposites with IR spectrum bands in the range 4000−4000/cm were analyzed using a Shimadzu IRAffinity-1 FTIR spectrophotometer. The examination of the qualitative and quantitative components of the FTIR spectrum was performed under ASTM E1252-98 (2021) ("Standard Practice for General Techniques for Obtaining Infrared Spectra for Qualitative Analysis," n.d.) and ASTM E168-16 (2023) ("Standard Practices for General Techniques of Infrared Quantitative Analysis," n.d.) standards. Combining 1 mg of raw biochar and 200 mg of IR-grade KBr powder and pressing the mixture into a pellet using a hydraulic press, the raw and activated biochar are ready for FTIR analysis for carbon analysis.

8.10 Results and discussions

8.10.1 Particle size distribution

In the PSD study, the range of size distribution for raw pine sawdust biochar (non-AC Pine) before ball milling (BBM) ranges from 210 to 13 μm, with 90% of the biochar being 208 μm and a mean diameter of 90 μm. In contrast, the size of the biochar particles in acetic acid-activated pine sawdust (AC Pine) BBM ranged from 117 to 13 μm, with 90% of the particles being tiny (116.11 μm) and having an average mean diameter of 56.41 μm.

The raw pine sawdust biochar PSD in a water suspension with ultrasonic dispersion is shown in Fig. 8.13. The distribution of raw pine sawdust biochar by a laser analyzer reveals a broad range of particle sizes from 1.15 to 14.50 μm, with 90% of the biochar being 13.55 μm and a mean diameter of 7.07 μm. In contrast, the size of the particles in activated pine sawdust biochar spans from 0.35 to 22 μm, with 90% of the particles being less than 21.66 μm and having an average mean diameter of 9.78 μm.

The particle size is observed to grow rather than decrease after 30 hours of ball milling (ABM 30 hours). It may sometimes occur as a result of

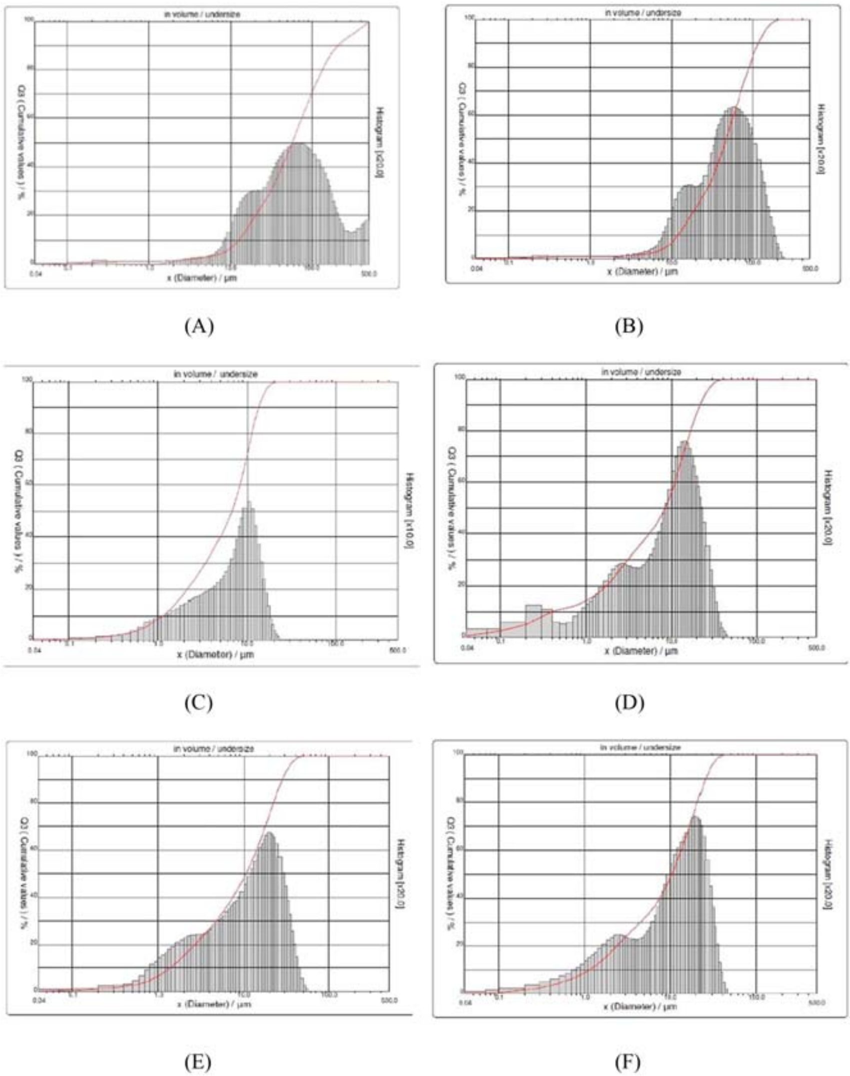

Figure 8.13 Particle site distribution of (A) non-AC Pine before ball milling (BBM), (B) AC Pine BBM, (C) non-AC Pine BBM 6 h, (D) AC Pine ABM 6 h, (E) non-AC Pine ABM 30 h, and (F) AC Pine ABM 30 h.

particle agglomeration, and larger particle sizes are also seen (Cetin et al., 2004). Agglomeration occurs when attractive forces are greater than repulsive forces, and the finer the particle, the stronger these forces are (Mishra & Ramaprabhu, 2012). A group of loosely linked particles, an aggregate, or

Table 8.9 Effect of ball milling time on particle size.

Duration	BBM 0 h		ABM 6 h		ABM 30 h	
Type	**Non-AC Pine**	**AC Pine**	**Non-AC Pine**	**AC Pine**	**Non-AC Pine**	**AC Pine**
Ultrasounds (s)	100	100	100	100	100	100
Diameter at 10% (μm)	12.62	12.08	1.15	0.39	1.38	1.15
Diameter at 50% (μm)	57.23	46.88	6.76	8.32	10.66	10.42
Diameter at 90% (μm)	208.60	116.11	13.55	21.66	28.40	25.61
Mean diameter (μm)	90.42	56.41	7.07	9.78	12.98	11.98

a combination of two, with a resultant exterior surface area comparable to the total of the surfaces of the individual components, is identified as an agglomeration process (ISO/TS, 2008). Van der Waals force and physical entanglement are two examples of weak forces that keep the aggregate together (Henry et al., 2013). Table 8.9 summarizes the impact of ball milling time on particle size; it demonstrates that when the time of ball milling is increased, the size of the particles is decreased from micrometer to nanoscale, increasing the specific surface area.

8.10.2 Bunauer–Emmett–Teller analysis for biocarbon

According to Li et al. (2013) and Zhao et al. (2017), the pyrolysis process of biomass may also gradually breakdown organic molecules like cellulose and lignin, increasing the surface area and volume of pores (Li et al., 2013; Zhao et al., 2017). Certain amorphous carbon structures can also emerge because of the degradation of cellulose (Zhao et al., 2017). Biochar made from pine sawdust has a huge surface area and a highly porous structure after pyrolysis; ball milling may further improve the surface area. Earlier investigations have shown that the biochar grains might be broken into ultrafine particles during ball-milling (Peterson et al., 2012). Table 8.10 BET data shows that non-AC and AC have more surface area ABM.

BET surface area for the non-AC was 1.41 m^2/g at the outset, compared to 0.24 m^2/g for the AC. According to Lyu et al. (2019), the common unmilled biochar generated at low temperatures, had a very low surface area of 0–2m^2/g, and the surface area rose to 8.3–10.8 m^2/g ABM (Lyu et al., 2019). According to research by Qiu et al. (2009), nonactivated carbon (biochar) had a BET surface area marginally greater than activated carbon, at 1057 m^2/g and 970 m^2/g, respectively (Qiu et al., 2009).

Table 8.10 BET results of non-ac carbon and activated carbon.

	Specific surface (m^2/g)	Average pore size (Å)	Total pore volume (cc/g)
Before ball milling (BBM)			
Non-AC Pine BBM	1.405	19.73 nm	1.386e-02
AC Pine BBM	0.237	54.47 nm	6.146e-03
After ball milling (ABM)			
Non-AC Pine ABM	5.331	11.13 nm	2.969e-02
AC Pine ABM	9.368	6.73 nm	3.154e-02

Nevertheless, due to the average pore diameter of biochar (5.2 nm) being bigger than that of activated carbon (0.32 mL/g), the micropore volume of biochar is lower (0.24 mL/g) than that of activated carbon (3.3 nm). According to Shaaban et al. (2013), the release of more volatile materials from biomass causes the temperature of pyrolysis to have a substantial influence on the growth of the surface area and pores. It also explains how some volatile stuff may still be trapped within the nonactivated carbon's (biochar) limited surface area.

The BET surface area of non-AC and AC rose to 5.33 and 9.37 m^2/g, respectively, after the ball milling procedure. As a result, compared to the sample BBM, milling increased the surface area of non-AC and AC by a factor of 4 and 40 times, respectively. Because of its larger porosity from acid impregnation and a tendency for its structure to be weak due to ball milling's mechanical effect, the AC is discovered to have the highest increase factor. Nevertheless, owing to the ball milling conditions, such as the ball-to-sample ratio, milling speed (rpm), duration, and milling medium, the final surface area of biochar and the pore volume of both products do not reach the same or equivalent results (Peterson et al., 2012).

The increased surface area of non-AC and AC are demonstrated by multipoint, and isotherm BET, plots, provided in, Figs. 8.14–8.16. Except for activated biochar BBM, all samples indicate that relative pressure (P/P_0) is precisely proportional to STP volume (cc/g). P/P_0 is known as the relative pressure, the ratio of adsorbate pressure to saturation pressure. As seen in Fig. 8.14, carbon always has a bigger volume after 30 hours of ball milling than it had previously. The adsorption and desorption isotherms of all biochar are shown in Figs. 8.15 and 8.16. The graph provides details on each sample's adsorption and desorption capacities. The results also show that the adsorption and desorption of

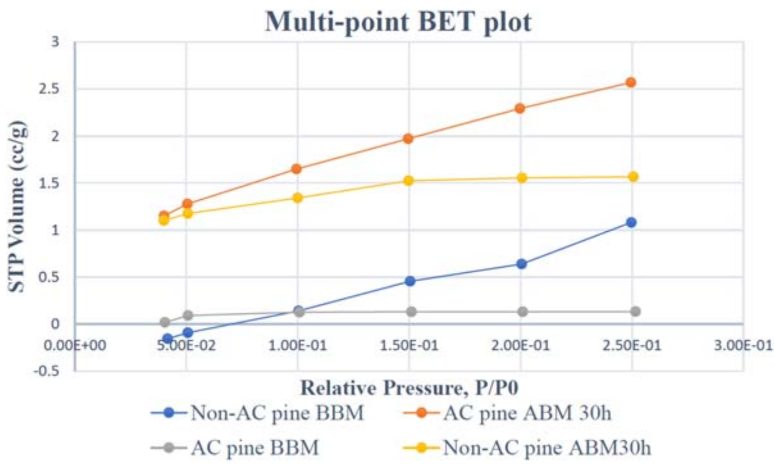

Figure 8.14 Multi-point, Brunauer—Emmett—Teller, plot, of all, biochar, samples.

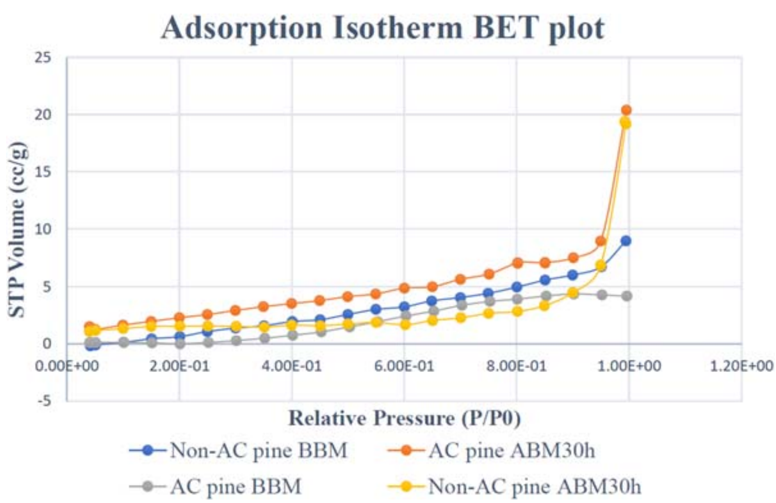

Figure 8.15 Adsorption isotherm Brunauer—Emmett—Teller plot of all biochar samples.

biochar increase when the ball milling duration is increased. More N_2 gas may be absorbed with a larger surface area and pore capacity. In conclusion, the ball milling method has enhanced the surface area of both nonactivated (biochar) and activated carbon and their adsorption and desorption capacities.

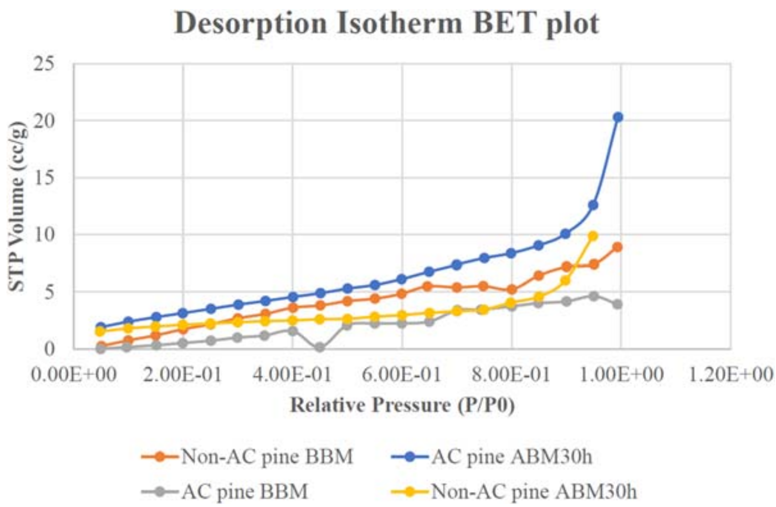

Figure 8.16 Desorption isotherm Brunauer—Emmett—Teller plot for all biochar samples.

8.10.3 Scanning electron microscopy-energy dispersive X-ray analysis

8.10.3.1 Scanning electron microscopy-energy dispersive X-ray analysis for biochar

Scanning electron microscopy analysis

The SEM analysis showed that the pine sawdust biochar gradually reduced in size after a lengthy ball milling procedure. Fig. 8.17 displays the SEM images of the unactivated (non-AC Pine) and acetic acid-activated (AC Pine) pine sawdust biochars BBM. Fig. 8.18 depicts the changes in particle size following ball milling for 6 hours (ABM 6 hours), and Fig. 8.19 depicts the changes following ball milling for 30 hours (ABM 30 hours).

Fig. 8.17 shows how the SEM results revealed the morphology of the starting material for raw pine biochar and activated pine biochar. They have a dense fibrous structure organized orderly with the characteristic of pores found on the surface and some longitudinal fracture along the surface, probably due to dehydration and volatilization of pine sawdust in a high-temperature furnace. As seen in the red circle, it was discovered that the AC Pine had a rougher surface and more micropores than the non-AC Pine. The results demonstrate that the char's uneven and roughed-up structure gives it great potential for adsorbate retention. After being ball milled for 6 hours, Fig. 8.18 demonstrates that both biochar particles exhibit microsize range particles, with some nanosized particles also observed in a

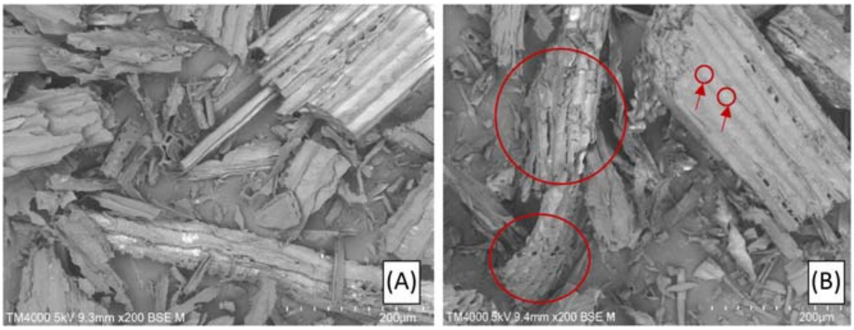

Figure 8.17 SEM images with 200× magnification at 5 kV voltage for pine sawdust-derived biochar before ball milling (BBM): (A) non-AC Pine BBM and (b) AC Pine BBM.

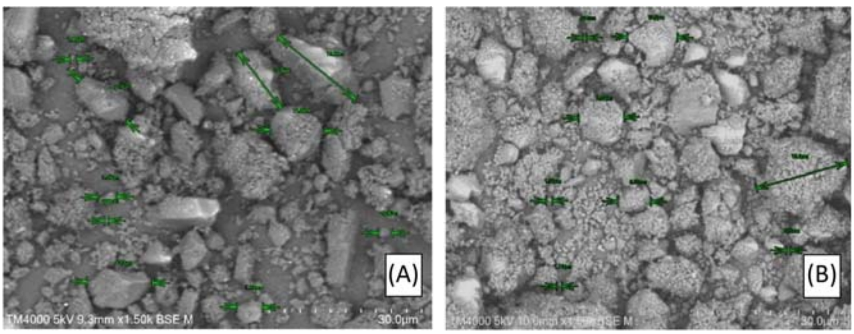

Figure 8.18 SEM images with 1500× magnification at 5 kV voltage for pine sawdust derived biochar after 6 h of milling: (A) non-AC Pine ABM 6 h and (b) AC Pine ABM 6 h.

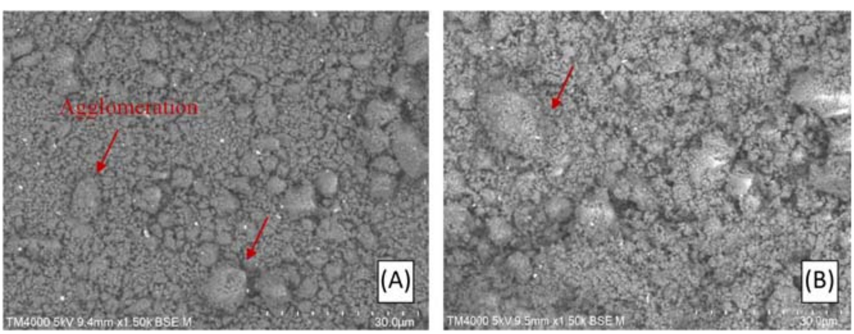

Figure 8.19 SEM images with 1500× magnification at 5 kV for pine sawdust derived biochar after 30 h of milling: (A) non-AC Pine ABM 30 h and (b) AC Pine ABM 30 h.

tiny proportion. According to Fig. 8.19, which shows ABM 30 hours, the irregular granular-like carbon particles are shown to become nanosized in about 1 nm (1000 nm) and exhibit the feature of agglomeration. The highest limit of nanoparticles indicated by the House of Lords Science Committee, according to Klaessig et al. (2011), is 1000 nm, consistent with the most recent research findings (Klaessig et al., 2011).

Energy dispersive X-ray analysis

Table 8.11 shows the element composition of biochar made from non-AC pine BBM, after 6 hours of milling (ABM 6 h), and after 30 hours of milling (ABM 30 h). The graphs associated with the data in Table 8.11 are shown in Figs. 8.20–8.22. According to Table 8.11, the elements in the sample include iodine, silicon, scandium, oxygen, carbon, and silicon.

The EDX element composition of activated pine sawdust is shown in Table 8.12, and the spectrum graphs are shown in Figs. 8.23–8.25 in connection to the data from Table 8.12. According to Table 8.12,

Table 8.11 Energy dispersive X-ray element composition of non-AC pine derived biochar before ball milling and after ball milling.

Element	Atm no.	Mass [%]	Atom [%]	Abs. error [%] -1 sigma	Rel. error [%] -1 sigma
0 h milling (BBM)					
I	53	95.28	66.64	19.67	20.64
C	6	4.16	30.72	0.48	11.55
O	8	0.43	2.36	0.080	18.81
Sc	21	0.14	0.28	0.053	37.23
6 h milling (ABM 6 h)					
C	6	74.89	83.93	8.22	10.97
O	8	15.61	13.13	2.01	12.88
S2c	21	8.99	2.69	1.64	18.29
Si	14	0.52	0.25	0.06	11.31
30 h milling (ABM 30 h)					
C	6	73.19	83.46	8.30	11.34
O	8	14.96	12.81	2.09	13.99
Sc	21	11.19	3.41	2.23	19.97
Si	14	0.66	0.32	0.07	10.91
Cs	55	0	0	0	10

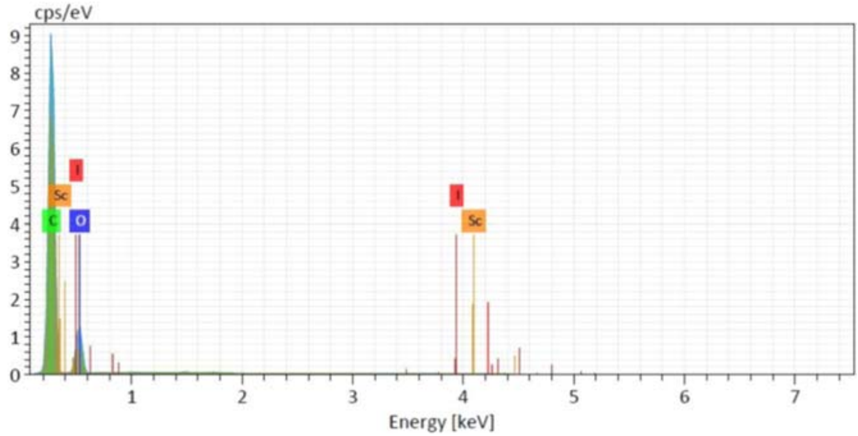

Figure 8.20 Energy dispersive X-ray spectrum graph of non-AC before ball milling.

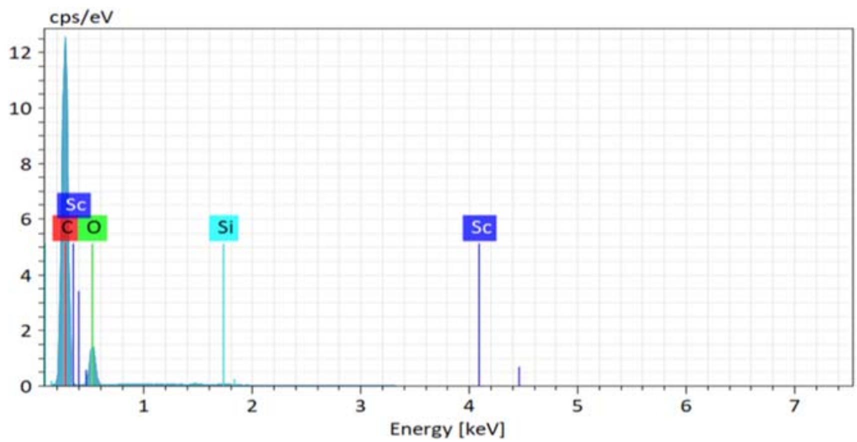

Figure 8.21 Energy dispersive X-ray spectrum graph for non-AC after ball milling 6 h.

the elements that exist in the sample are iodine, carbon, oxygen, scandium, silicon, and silver.

According to the EDX results for each biochar, it is seen that C and O are the main elements. The findings show that the major skeleton of the biochar sample is composed of carbon with oxygen and oxygen functional groups like −COOH and −OH as well as oxygen metal minerals like phosphate, sulfate, and carbonate (Liang et al., 2016). Raw pine sawdust has more carbon and oxygen than Tables 8.11 and 8.12 indicate.

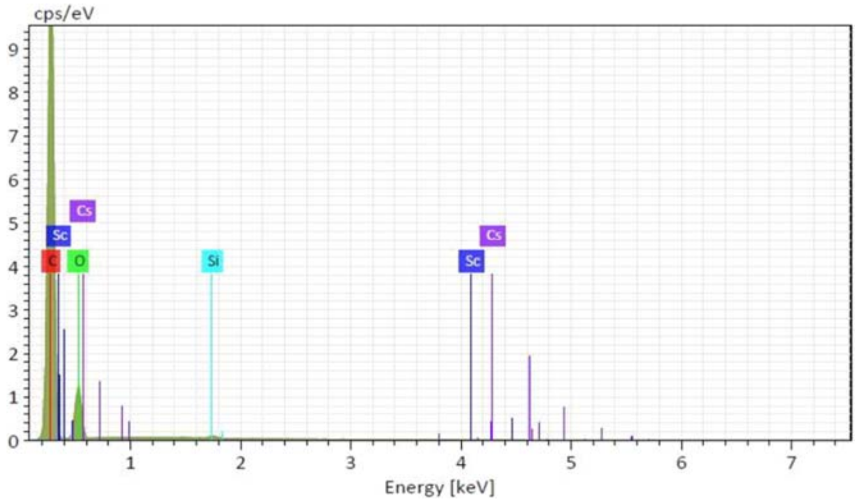

Figure 8.22 Energy dispersive X-ray spectrum graph of non-AC after ball milling30 h.

Table 8.12 Energy dispersive X-ray element composition of AC pine-derived biochar before ball milling and after ball milling.

Element	Atm. No.	Mass [%]	Atom [%]	Abs. error [%] -1 sigma	Rel. error [%] -1 sigma
0 h milling					
I	53	96.69	74.52	18.15	18.77
C	6	2.84	23.10	0.34	11.84
O	8	0.340	2.08	0.068	20.07
Sc	21	0.11	0.25	0.046	40.97
Si	14	0.011	0.039	0.001	8.81
Ag	47	0.011	0.01	0.0017	15.43
6 h milling					
C	6	73.84	83.25	8.11	10.98
O	8	16.27	13.77	2.09	12.85
Sc	21	9.89	2.98	1.77	17.92
30 h milling					
C	6	72.94	83.06	8.00	10.98
O	8	15.60	13.34	2.00	12.87
Sc	21	10.85	3.30	1.89	17.40
Si	14	0.61	0.30	0.06	10.32

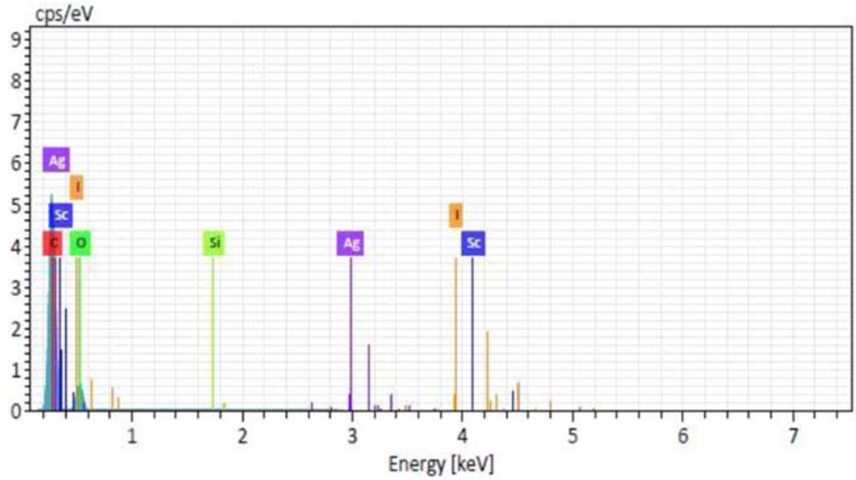

Figure 8.23 Energy dispersive X-ray spectrum graph of AC before ball milling.

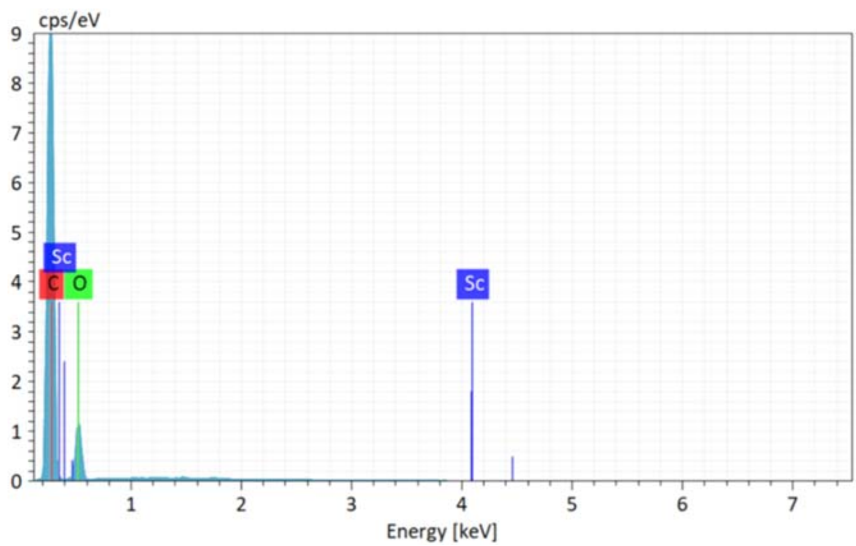

Figure 8.24 Energy dispersive X-ray spectrum graph of AC after ball milling 6 h.

However, there is a minor quantity of another ingredient in the mix. The carbon contents of RC Pine and AC pine have been recorded as 74%–75%. One study stated that fixed carbon presence in pine shaving was correlated with the pyrolysis temperature of biomass. As the temperature increased from 100°C to 700°C, the C% increased from 50.60% to 92.30%.

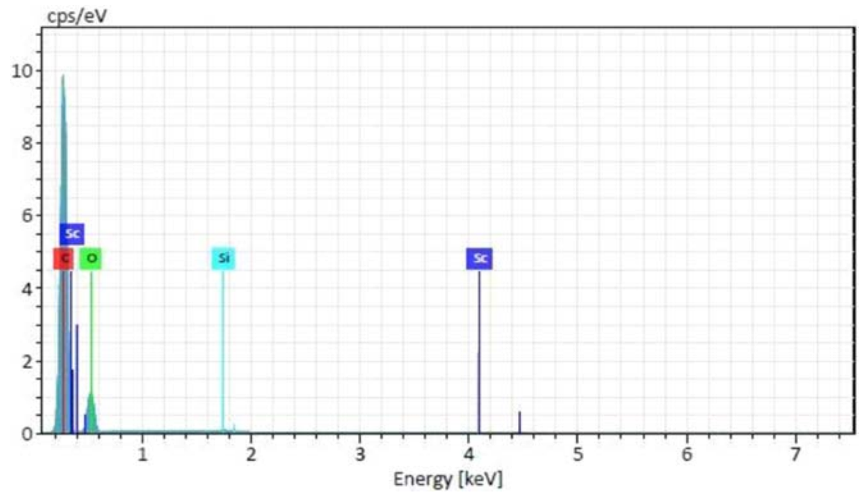

Figure 8.25 Energy dispersive X-ray spectrum graph of AC after ball milling 30 h.

At a temperature of 400°C, the elementary composition of pine shaving comprises C (74.10%), H (4.95%), O (20.90%), and N (1.14%), with a surface area of 28.7 m^2/g (Ahmad et al., 2014). The changes in the mass percentage of elemental components are due to milling conditions, such as time and the ratio of ball to biochar. The biochar produced had the smallest particle size of 274 nm and a 93% mass percentage of carbon. Carbon elements present in the highest percentage, and the reduced particle size, increased the carbon mass percentage, as indicated by their EDX results. The varied elemental compositions could be associated with the consistency of the EDX machine to detect and characterize elements present in the sample.

8.10.3.2 Scanning electron microscopy-energy dispersive X-ray analysis for Bio-nanocomposite

Scanning electron microscopy analysis

As shown in Fig. 8.26, empty matrix materials often have fractured cross-sectional surfaces that are relatively smooth due to the lack of large-scale plastic deformation. This PLA fracture pattern also explains why the film-drying fracture occurred since pure PLA polymer is innately brittle (Yuniarto et al., 2017). Several gaps have been noticed due to the moisture absorption of samples during the manufacturing process (Cheung et al., 2008). To improve the features of PLA film, which include brittleness, poor thermal stability, and low water vapor

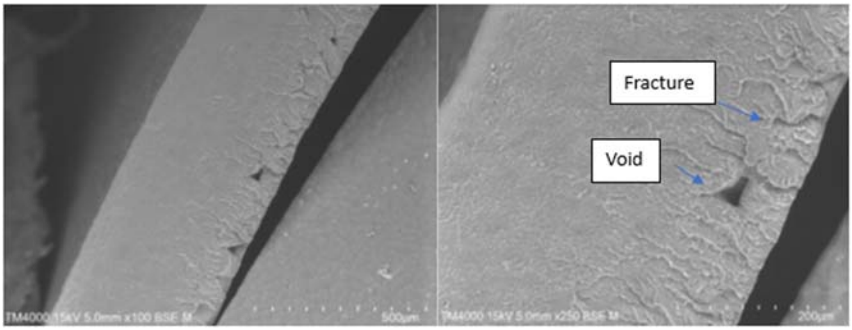

Figure 8.26 Scaning electron microscopy morphology of pure polylactic acid with 100× (*left*) and 250× (*right*) magnification at 15 kV.

and oxygen barrier (Garlotta, 2001), nanofiller such as nanoparticles and nanofibers may be added to PLA film (Baheti et al., 2014; George & Siddaramaiah, 2012). Images of the fracture cross-sectional surface of nonactivated nanocarbon/MMT/PLA with increasing carbon loading at 0.25, 0.50, 0.75, and 1 wt.% are shown in Fig. 8.27A–D.

The surface topology of clean PLA becomes rough with the addition of the nanocarbon/MMT filler, resulting in uneven filler distribution within the matrix. The inclusion of filler impacted the composites' homogeneity, resulting in a heterogeneous structure containing visible biochar particles. This investigation set the MMT concentration at 1 wt.% since greater MMT concentrations caused premature material failure before the shearing process could begin (Jiang et al., 2007). The MMT K10 is employed in these investigations, which has been thermally and acid-treated to produce highly porous materials with a large surface area and nanopores. Thermal processing causes MMT's crystal structure to be substantially broken, and MMT K10 also loses its swelling properties (Maiti et al., 2016). It is known that a persistent net negative charge may arise in K10 when the cations undergo isomorphic substitution (Tombácz & Szekeres, 2006). It makes chemically modified MMT less hydrophilic. The characteristics of clays shift from hydrophilic to hydrophobic when organo-minerals from biochar, including K^+ ions, are added. MMT may attach to biochar's flaky structure, porous morphology, and embedded lattices of carbonaceous material (Ashiq et al., 2019). By exerting high stiffness and suppressing the chain of PLA, MMT particles will boost the tensile strength and Young Modulus of the nanocomposite, creating no deformation (Yang et al., 2007).

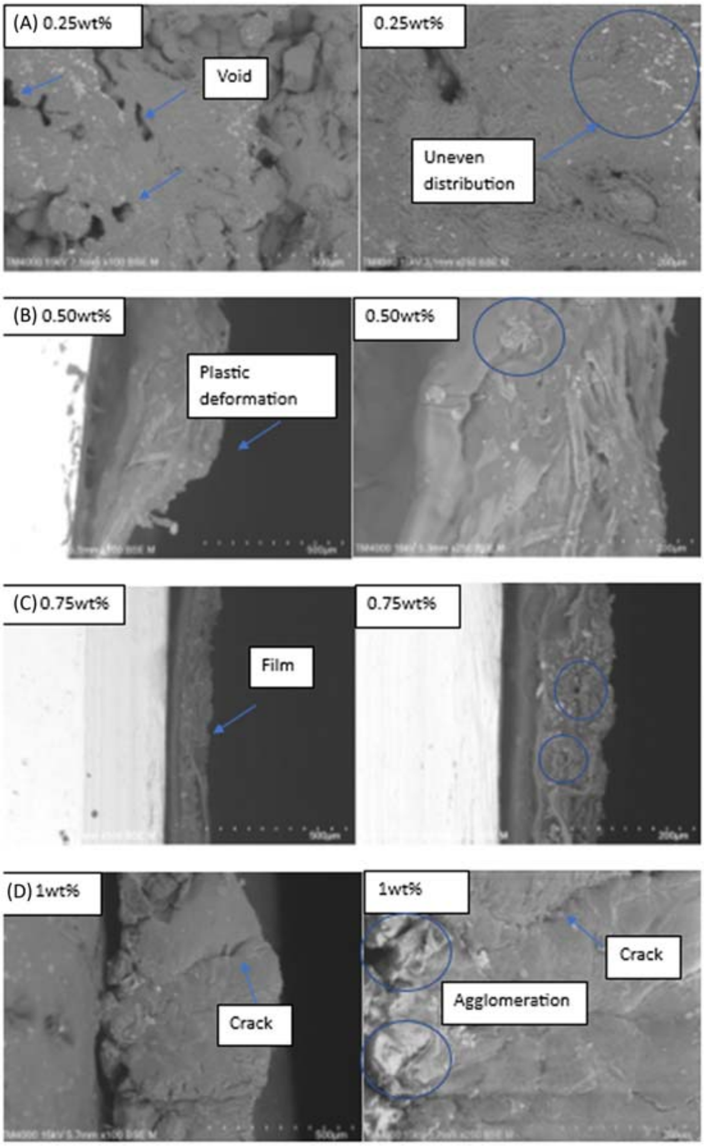

Figure 8.27 Scaning electron microscopy morphology of bio-nanocomposite film: (A) 0.25 wt.% non-AC/montmorillonite (MMT)/polylactic acid (PLA), (B) 0.50 wt.% non-AC/MMT/PLA, (C) 0.75 wt.% non-AC/MMT/PLA, and (D) 1 wt.% non-AC/MMT/PLA.

This improvement resulted, from MMT dispersion, platelet alignment within PLA, silicate interlayer augmentation, and polymer matrix incorporation of MMT (He et al., 2011; Yang et al., 2007).

Modest loading of 0.25 wt.% RC may cause plastic deformation and the creation of air spaces. It is discovered that filler dispersion in the PLA matrix might affect matrix characteristics. Due to insufficient biochar filler dispersion, the PLA matrix exhibits poor interfacial contact and particle debonding at low carbon loading. MMT powder and nanocarbon with smaller particle sizes may better disperse in the PLA matrix. The tiny, white bits are nanofillers incorporated into the PLA matrix (Gond & Gupta, 2021), though it is challenging to identify the nanocarbon in a hybrid nanocomposite. This is because MMT may be attached to nanocarbon or even coated by MMT platelets. Since less nanofiller is employed and there is less filler-matrix interaction, it is evident that the distribution is unequal at 0.25 wt.%. Yet, an equal distribution is seen after increasing the nanofiller loading.

Nevertheless, more interaction between PLA and biochar was seen when RC Pine loading increased steadily to 0.50 and 0.75 wt.%. There is less void because PLA and biochar are compatible since they are both hydrophobic (Kothapalli et al., 2005; Nitayaphat et al., 2009). They can efficiently transmit pressure because as filler loading increases, interparticle distance decreases, and sample resistance to indentation due to applied force increases (Devendra & Rangaswamy, 2012; Phutane et al., 2013). The increased connection between the PLA and biochar particles results in less debonding when stress is applied, which raises the composite's flexural characteristics. The red circle shows the existence of certain microvoids inside the PLA matrix, and plastic deformation is less visible owing to enhanced interfacial contact between the filler and PLA matrix.

The surface of the composite has a smoother appearance with some surface fracture and agglomeration characteristics at 1 wt.% filler loading of biochar in PLA matrix. Due to the usage of hybrid filler, at high filler loading contents, the interaction between the fillers is more favorable than between the filler and matrix, leading to filler agglomeration (Arjmandi et al., 2014, 2016). The composites' effective cross-sectional area would decrease as microfracture developed. It was suggested that biochar was under stress, which encouraged the development of cracks when the filler was loaded and resulted in flexural strength that was less robust than pure PLA. Images of the fracture cross-sectional surface of activated nanocarbon/MMT/PLA with increasing carbon loading at 0.25, 0.50, 0.75, and 1 wt.% were shown in Fig. 8.28A–D.

As noted in the BET study, activated carbon has a greater surface area and pore volume. Activated biochar and MMT were used to create a

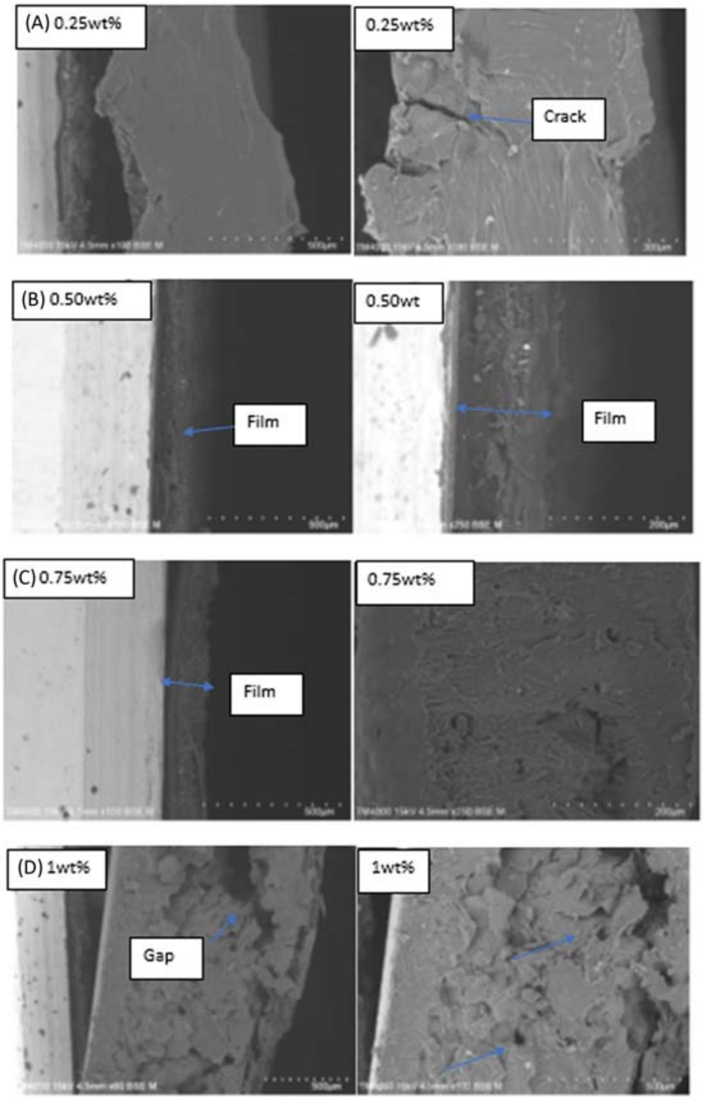

Figure 8.28 Scaning electron microscopy morphology of bio-nanocomposite film: (A) 0.25 wt.% AC/montmorillonite (MMT)/polylactic acid (PLA), (B) 0.50 wt.% AC/MMT/PLA, (C) 0.75 wt.% AC/MMT/PLA, and (D) 1 wt.% AC/MMT/PLA.

bio-nanocomposite that had improved interfacial interaction. Intense carbonization temperatures and chemical activation created activated carbon with a high surface area and porous structure. PLA solution might flow into the activated carbon structure when the mold was cooled, creating a physical/mechanical interlocking structure. Compared to the interfacial structure made of fiber and polymer, this biochar and polymer interlocking structure could transmit stress more efficiently and had superior flexural characteristics (Das et al., 2016). The PLA-based composite is shown in Fig. 8.28A to have a smoother surface at 0.25 wt.% AC loading. However, film fracturing was seen when the magnification of the observed region's micrograph was raised. The matrix began to improve when the hybrid filler interacted with the PLA matrix to avoid plastic deformation with further increments of AC loading to 0.50 and 0.75 wt.%. The benefits of using biochar as a filler were evident in the SEM micrographs of the biochar-reinforced composite.

Nevertheless, when activated biochar raised the filler loading to 1 wt.%, a substantial gap was generated, leaving a huge air space inside the PLA matrix. Major deformation and surface roughness were observed. Due to the filler and PLA's weak interfacial adhesion, the heterogeneous matrix began to break and spread to the bottom portion region. It was anticipated that the outer layer would seem to be peeling off if an external force exacerbated the split.

Energy dispersive X-ray analysis

Tables 8.13–8.15 indicate the elemental composition of pure PLA, non-AC/MMT/PLA bio-nanocomposite, and AC/MMT/PLA bio-nanocomposite, while Figs. 8.29–8.31 show the corresponding EDX spectra.

C, O_2, and Cl are the three elements in pure PLA film. This outcome is akin to some literature (Gond & Gupta, 2021). Table 8.13 provides information on pure PLA's mass and atom percentages, while Fig. 8.29 displays the EDX spectrum. Studies proved that the primary elements present in PLA are carbon (C) and oxygen (O). Biocarbon nanocomposite concentration decreases, and its other element composition increases due to the addition of nanocarbon and MMT filler.

As shown in Tables 8.14 and 8.15, bio-nanocomposite has the highest percentage of C (54%–55%), with O_2 coming in second (32%–40%) and other elements like Cl, Ni, Cl, P, Na, and K standing out. Na and K are present in lesser amounts. High amounts of carbon fraction and other

Table 8.13 Energy dispersive X-ray element composition of pure polylactic acid.

Element	Atm no.	Mass [%]	Atom [%]	Abs. error [%] (1 sigma)	Rel. error [%] (1 sigma)
C	6	54.02	61.49	6.15	11.38
O	8	44.31	37.87	5.20	11.74
Cl	17	1.66	0.64	0.08	5.01

Table 8.14 Energy dispersive X-ray element composition of non-AC/montmorillonite/polylactic acid bio-nanocomposite.

Element	Atm no.	Mass [%]	Atom [%]	Abs. error [%] (1 sigma)	Rel. error [%] (1 sigma)
C	6	55.65	64.45	7.70	13.84
O	8	39.16	34.05	5.99	15.31
Ni	28	3.59	0.85	0.23	6.40
Cl	17	1.05	0.41	0.08	7.92
P	15	0.54	0.24	0.06	11.80

Table 8.15 Energy dispersive X-ray element composition of AC/montmorillonite/polylactic acid bio-nanocomposite.

Element	Atm no.	Mass [%]	Atom [%]	Abs. error [%] 1 sigma	Rel. error [%] 1 sigma
C	6	53.99	65.99	4.75	18.76
O	8	31.68	29.07	3.26	21.95
Ni	28	7.82	1.96	0.26	7.16
Cl	17	2.76	1.15	0.12	9.26
P	15	2.23	1.06	0.11	10.90
Na	11	0.77	0.49	0.10	29.29
K	19	0.73	0.27	0.06	19.93

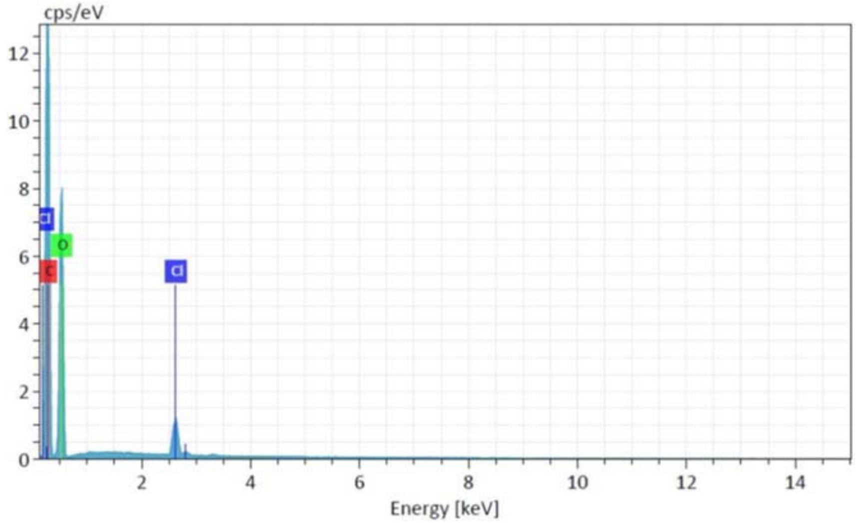

Figure 8.29 Energy dispersive X-ray spectrum graph for pure polylactic acid.

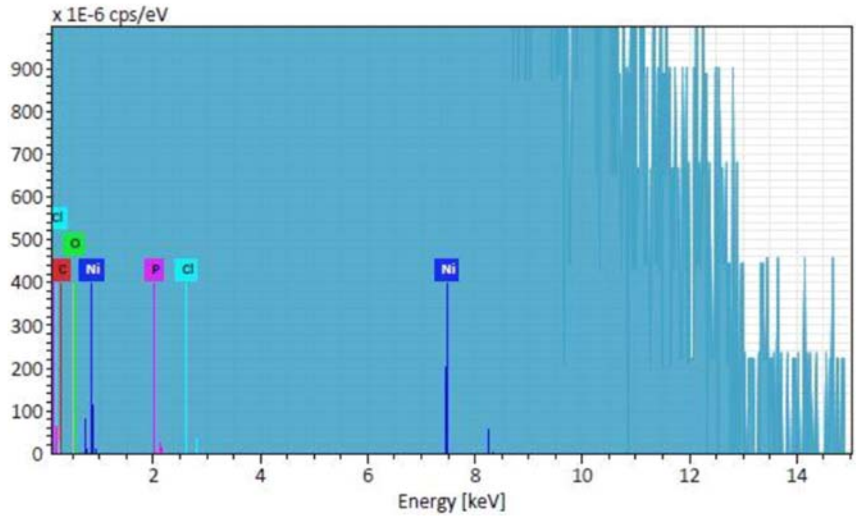

Figure 8.30 Energy dispersive X-ray spectrum graph for non-AC/montmorillonite/polylactic acid bio-nanocomposite.

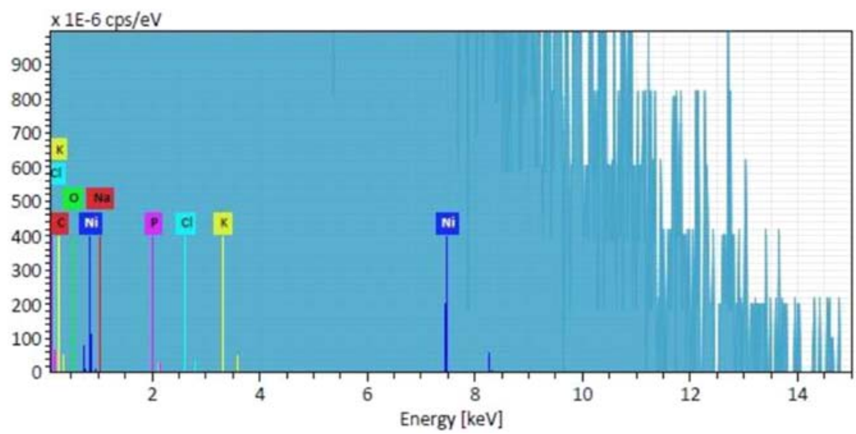

Figure 8.31 Energy dispersive X-ray spectrum graph for AC/montmorillonite/polylactic acid bio-nanocomposite.

minerals, such as alkaline earth metals (Ca, Mg, etc.) or alkali metals (K, Na, etc.), are often found in biochar in the form of carbonates, phosphates, or oxides. Al concentration is minimal (unable to be identified), whereas Na and K are present in minuscule amounts, according to EDX examination. It indicates that during acid treatment, certain ions are leached off (Borah & Das, 2018).

8.10.4 Fourier transform infrared analysis

8.10.4.1 Fourier transform infrared analysis for biochar

The FTIR spectra of non-AC Pine BBM, non-AC Pine ABM, AC Pine BBM, and AC Pine ABM, produced under identical carbonization conditions, are shown in Fig. 8.32A and B.

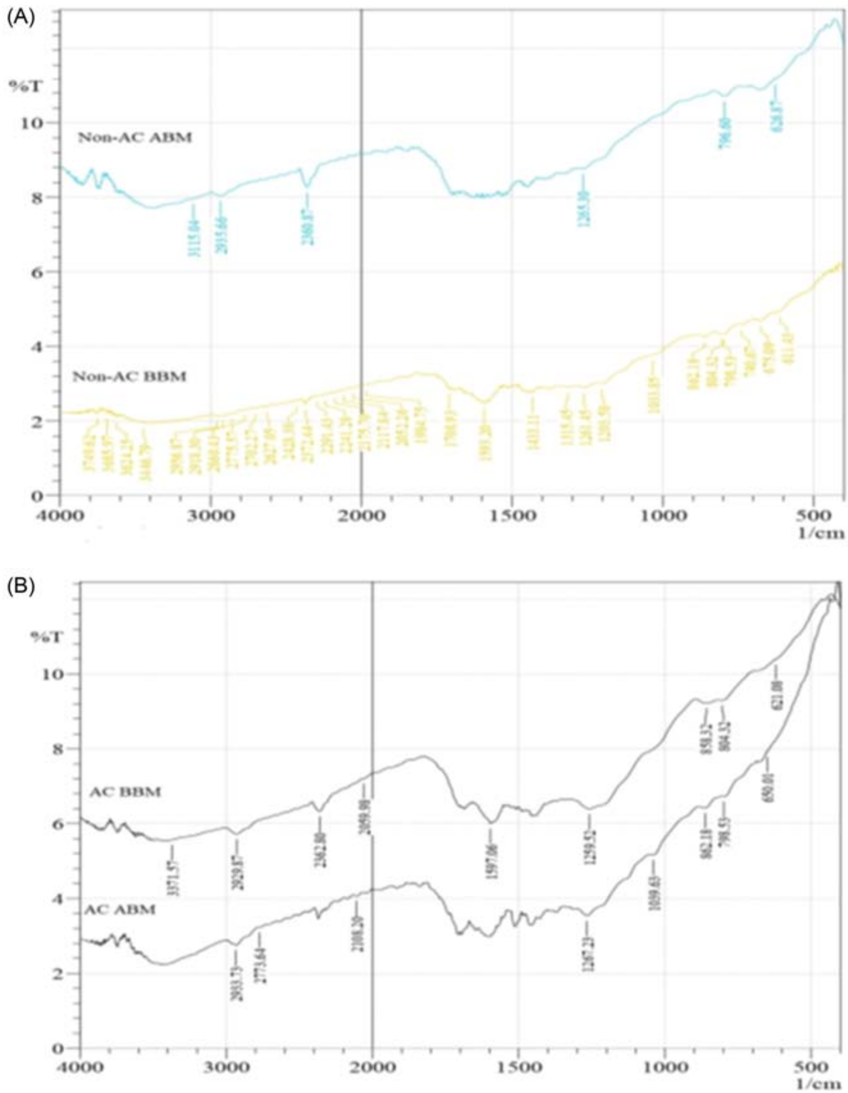

Figure 8.32 Fourier transform infrared spectra of biochar: (A) non-AC before ball milling (BBM) and after ball milling (ABM), and (B) AC BBM and ABM.

Generally, the two spectra in Fig. 8.32A and B do not significantly vary; this indicates that the chars have a similar structure, a large carbon matrix with some oxygenate functional groups, and an absence of a major aliphatic structure. The peak indicated the presence of water, phenols, and alcohol at 3100–3800/cm, which was attributable to the –OH vibration (Sajjadi et al., 2019). The peak confirmed alkenes and carboxylic acid at 2929–2935/cm, attributed to CH_2 and CH_3 asymmetric and symmetric stretching vibrations. Carbonyl C = O stretching is correlated with a wavelength of around 1700/cm.

The interaction of cellulose and lignin during heating causes the peak to develop (Worasuwannarak et al., 2007). Conjugated ketones, quinones, and aromatic C = C and C = O stretching are blamed for the peak intensity of 1590–1600/cm, which suggests that phenolic and carboxylic chemicals are present in lignin (Uchimiya et al., 2011). The symmetric C = O in cellulose, hemicellulose, and lignin cause peaks in 1033–1270/cm. Compared to acid-activated biochar, the peak was much lower for raw biochar, which explained why cellulose, hemicellulose, and lignin disruption occurred following acid treatment (Palniandy et al., 2019). At 1022–1043/cm, a wide band that may exhibit the characteristic of C–O–C asymmetric stretch was produced (Sajjadi et al., 2019). The presence of mono and polycyclic substituted aromatic groups was verified by the adsorption band 862–611/cm associated with C–H bending vibrations (Qian et al., 2000; Qian et al., 2013; Qian et al., 2016).

Compared to raw biochar, the peak of acid-treated biochar was approximately 3600–3800/cm for OH– stretching, 2800–3000/cm for C–H stretching to become sharp, and a new peak around 1500–1600/cm showed the existence of C = C/C = O stretching. This is because the acidic surface functional groups, which may take the forms of lactone, quinone, hydroxyl, carbonyl, and carboxyl, are enhanced (Nizamuddin et al., 2015; Yin et al., 2007). The higher peak is likely due to the hydroxyl and carboxyl groups since these functional groups are similar to those of acetic acids, such as –COOH and –OH. In addition, it is discovered that raw and activated biochar exhibit a notable increase in O–H stretching and aromatic C–H bending following ball milling. According to one research, ball milling of carbonaceous materials might introduce functional groups that include oxygen, such as carboxyl and hydroxyl groups (Munkhbayar et al., 2013). Hence, the high apex was seen.

8.10.4.2 Fourier transform infrared analysis of bio-nanocomposites

Figs. 8.33 and 8.34 show the FTIR spectra of pure PLA and PLA-MMT blends, respectively, with various loadings of nonactivated nanocarbon at 0.25, 0.50, 0.75, and 1 wt.%. Fig. 8.35 shows the FTIR spectra of activated nanocarbon.

FTIR analysis was compared to determine the composite's presence and nature of interfacial interactions. Fig. 8.33 depiction of PLA demonstrates the typical stretching frequencies for the material: OH stretching at 3741.90/cm, C = O ester carbonyl groups at 1749.44/cm, and the C−O stretching band at 1184.29 and 1083.99/cm. Although bending vibration was seen at 1361.74/cm, the asymmetric and symmetric stretching bands of C−H from CH^3 groups of the side chains were seen at 2997.38/cm. The C−H stretching group was responsible for the main chain of PLA at 2946/cm, and their bending vibration emerged at 1384 and 1358/cm (Li & Sun, 2010). PLA had large peaks at 1750 and 1180/cm related to its C = O and C−O−C stretching, respectively (Mofokeng et al., 2012). These peaks can be seen in the spectra of all bio-nanocomposite materials. It is because each composite contains around 98 wt.% t of the substance. The variation in PLA peak intensities in each composite point to a modification in the molecular arrangement in polymer chains (Mohanty et al., 2012). The C−C single bond's stretching vibration was measured at

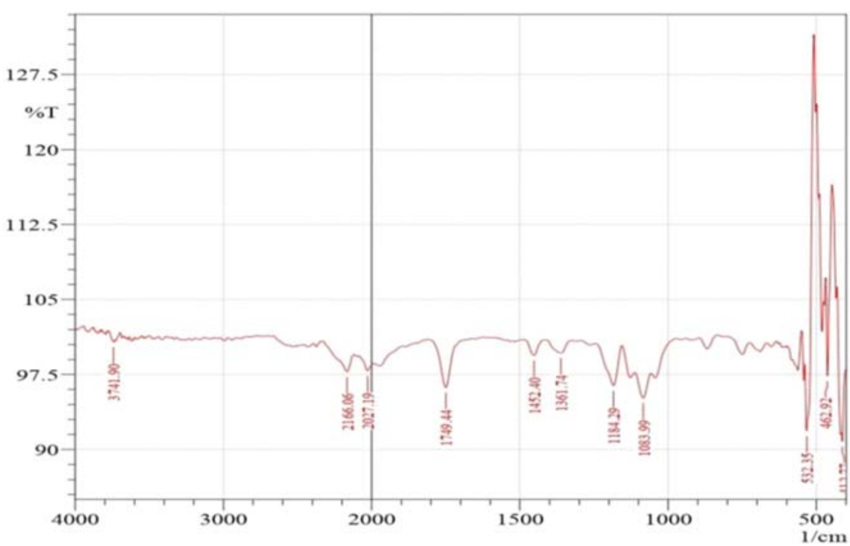

Figure 8.33 Fourier transform infrared spectra of pure polylactic acid.

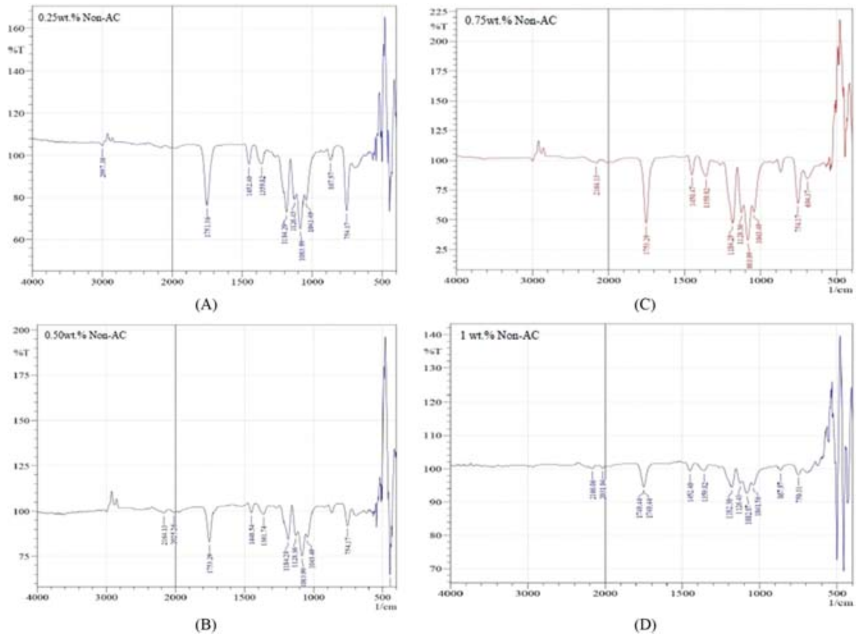

Figure 8.34 Fourier transform infrared spectra of non-AC/montmorillonite/polylactic acid bio-nanocomposite with different non-AC filler loading at (A) 0.25 wt.% non-AC, (B) 0.50 wt.% non-AC, (C) 0.75 wt.% non-AC, and (D) 1 wt.% non-AC.

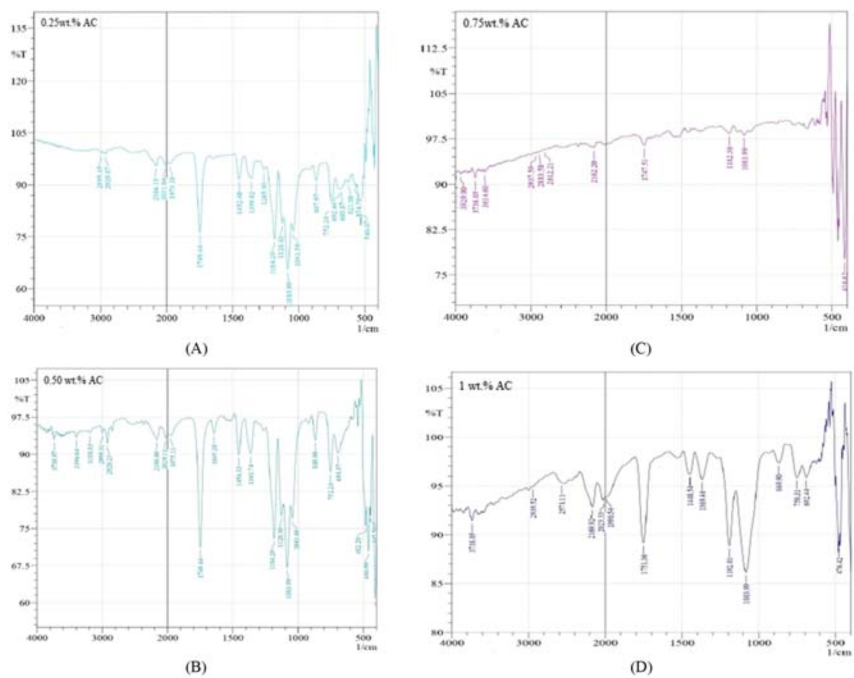

Figure 8.35 Fourier transform infrared spectra of AC/montmorillonite/polylactic acid bio-nanocomposite with different AC filler loading at (A) 0.25 wt.% AC, (B) 0.50 wt.% AC, (C) 0.75 wt.% AC, and (D) 1 wt.% AC.

868–920/cm (Arjmandi et al., 2014). The absorption peak of pure PLA is reduced when hybrid fillers are added to the PLA matrix.

According to Sari and Kaynak (2016), chemical interactions such as hydrogen bonds or dipolar interactions between the reinforcement material and polymer matrix have produced variations in the IR spectra of the polymer matrix material (Sari & Kaynak, 2016). In general, band shifting and widening are the most common IR spectral alterations that may be seen.

Fig. 8.34 shows that with the addition of MMT filler, the PLA peak intensity of the –OH hydroxyl group at 3741.90/cm became broader or vanished, and the C–O group at 1083.99/cm migrated to a lower intensity at 1082.07/cm. While C-O remains the same (1083.99/cm), the addition of MMT nanofiller causes the intensity peak for –OH to shift to (3738.05/cm), as seen in Fig. 8.35A, and a presence of tiny new peak at 540.07 and 621.08/cm, which confirmed the presence of MMT due to Al–O and Si–O stretching.

According to Molinaro et al. (2013), characteristic IR bands of the silicate layers, such as Al–O stretching around 520/cm and Si–O bonding at 627/cm, might occur when MMT was grafted to the PLA matrix (Molinaro et al., 2013). The polar contacts between the PLA's hydroxyl group and the Si–O groups of the MMT filler were responsible to cause the lowered peak to explain the strong connection between PLA and MMT filler (Chen et al., 2011; Liu et al., 2013). As mentioned in the literature review, the MMT structure exhibits highly polarized sites evenly distributed across the structure, demonstrating the concentration of electron densities at surfaces and interlayer gaps. As a result, there is little difficulty in the polar contact between MMT and the PLA matrix.

A smaller number of surface functional groups are present in biochar after pyrolysis compared to the original precursor, and the biochar's hydrophobicity is caused by its low H_2 and O_2 concentration (Batista et al., 2018). By employing biochar as a natural filler, the issue of dispersion inside hydrophobic polymers like PLA will be overcome. The peak intensity of OH stretching decreased, as filler was added to the PLA matrix, indicating that adding more nanocarbon to the composite may have weakened the polar functional groups, particularly the hydroxyl group (Zhang & Li, 2009; Zhang et al., 2019; Zhang et al., 2020)

As carbon loading increases in the polymer matrix from 0.25 to 1 wt.% in Fig. 8.36, there is also an increase in the intensity of the –C = O bands at 1749.44/cm to a higher intensity at 1753.29/cm, except for 1 wt.%, while in Fig. 8.37 the peak intensity of the –C = O also increases

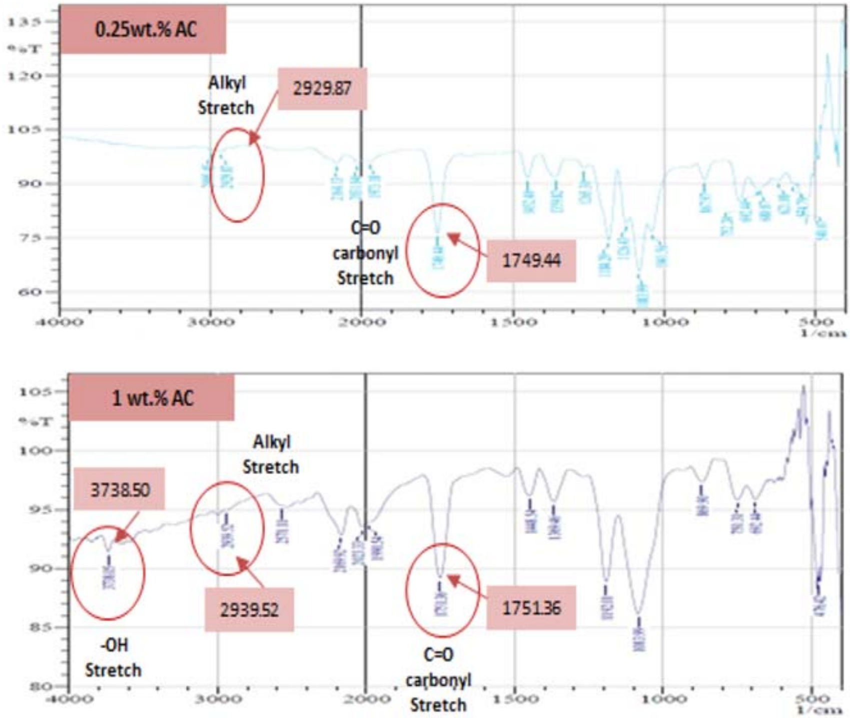

Figure 8.36 Effect of addition of carbon loading from 0.25 to 1 wt.%.

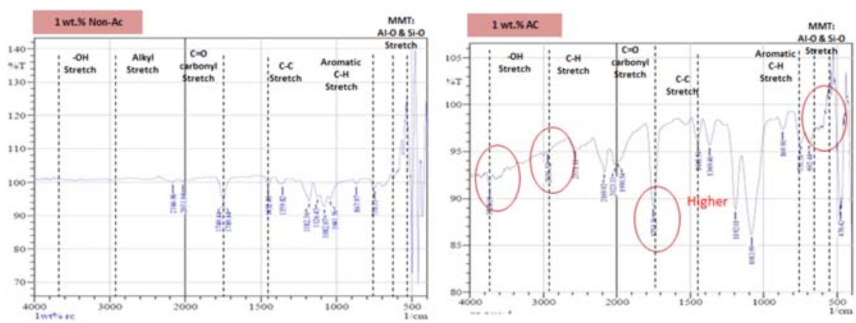

Figure 8.37 Comparison of non-AC and AC-based polylactic acid/montmorillonite bio-nanocomposite.

from 1749.44 to 1751.36/cm, which is related to an increase in the number of free carboxylic groups. Also, it was discovered that the alkyl group in Fig. 8.37 increased from 2929.87 to 2939.52/cm due to adding alkyl groups to the polymer matrix, such as the -CH group of biochar and the

CH_3 group of acetic acid. With one carboxylic acid per molecule, acetic acid is a weak acid. It's interesting to note that the carbonyl peak of the bio-nanocomposite with activated carbon filler is more intense than the one with nonactivated nanocarbon. This clarifies the existence of other carboxylic groups in composites made with activated carbon. By strengthening the hydrogen link between the PLA matrix and the carbon filler, the hydrophobic characteristics of PLA may be improved.

The strong and most well-resolved peak in the FTIR spectra of bio-nanocomposite with PLA occurs at a wavelength of around 1750/cm. It does not exhibit positional change among various composites. Nevertheless, the chemical bonding between PLA molecules and biochar after compounding resulted in a stronger peak of $C=O$ carbonyl stretching vibration at 1750/cm and −OH hydroxyl bending at 1359−1369/cm. Given that both biochar and PLA are hydrophobic and have strong surface compatibility, this explains why there are physical interlocks between the two phases of each material (Qian et al., 2000, 2013, 2016). Yet, the bonds between them are kept together by the hydrogen contact and relatively weak Van der Waal's force (Qian et al., 2016). C−H on the benzene ring forms the out-of-plane vibration absorption peak at 750−754/cm (Qian et al., 2016). As a result, there are chemical and physical linkages present at the interface of biochar and PLA. Fig. 8.36 demonstrates the impact of adding carbon to the polymer matrix with concentrations ranging from 0.25 to 1 wt.%, and Fig. 8.37 compares PLA/MMT bio-nanocomposites made with non-AC and AC. Activated carbon has many functional groups, so the intensity peak of bio-nanocomposite using AC filler is sharper than non-AC filler.

8.11 Conclusion

A bio-composite made of nanocarbon, MMT, and PLA was effectively created using the solution-casting approach. Between the carbon and the PLA matrix, nanocarbon serves as fiber reinforcement, while MMT serves as reinforcement. By exerting high stiffness and preventing PLA chain deformation, MMT filler is utilized to enhance the mechanical characteristics of the PLA matrix at the low loading of 1 wt.%. Ball milling for 30 hours at 380 rpm may reduce particle size from μm to nm, and the tiniest size of nanocarbon obtained in this work is around 1 μm

(1000 nm). Moreover, BET research reveals that compared to non-AC, AC has a larger surface area and pore volume. According to SEM micrographs, the PLA-based composite exhibits the greatest interfacial contact and strength when employing 0.75 wt.% of AC filler and 1 wt.% of non-AC filler. It was discovered that filler dispersion in the PLA matrix might affect matrix characteristics. Weak interfacial contact with low carbon loading is seen as a result of insufficient filler dispersion in the PLA matrix. Agglomeration began when additional carbon (non-AC and AC) loading was added to the polymer matrix. Biochar's high-stress levels also encourage fracture development and deteriorate its mechanical qualities. When compounded in a polymer matrix, AC may provide improved interaction due to its increased functional group and porous structure. The FTIR results show the excellent interaction between the hybrid filler and matrix. The presence of MMT filler was verified by causing a decrease in the $-OH$ peak and a new peak of $Si-O$ and $Al-O$. Due to establishing a chemical link between the PLA molecule and the biochar, the carbon loading from 0.25 to 1 wt.% will increase the Carbonyl $C=O$ peak and $-OH$ bending. This research study thus demonstrates the benefits of utilizing hybrid fillers. Their synergy effect was also discovered to boost the morphological characteristics, physical bonding, and chemical interaction, leading to increased mechanical performance in bio-nanocomposite. MMT bio-nanocomposite could be used successfully as a filler material to enhance the strength of the composites.

8.12 Future works and recommendations

The dispersion and intercalation of filler and PLA matrix affect the matrix's properties. It is recommended that in situ polymerization could be used in place of the solution casting approach in future research. In order to produce a stable solution using the solution casting process, an acceptable minimum solid content and viscosity should be generated. When filler and polymer matrix interact strongly during in-situ polymerization, stress transmission is resolved, and filler is quickly distributed uniformly throughout the polymer matrix. Moreover, it offers excellent miscibility for polymer matrixes with large filler loadings. This technique also encourages the likelihood that the reinforcement surfaces are clean, which makes it possible to produce a stronger matrix dispersion bond. To further examine their performance in physical bonding and chemical interaction, other weight percentages of nanocarbon and MMT filler that are more than 1 wt.% should be employed in future studies. Tensile strength and Young Modulus tests may be performed to describe the mechanical characteristics of bio-nanocomposites. Mechanical properties can also be optimized by determining the right amount of MMT and nanocarbon filler to put in the composite to get the best strength and modulus possible. The effectiveness of the bio-color composite's removal may also be tested in water treatment applications using varied filler contents.

References

Abbas, A. F., & Ahmed, M. J. (2016). Mesoporous activated carbon from date stones (*Phoenix dactylifera* L.) by one-step microwave assisted K2CO3 pyrolysis. *Journal of Water Process Engineering*, *9*, 201–207. Available from https://doi.org/10.1016/j.jwpe.2016.01.004, http://www.journals.elsevier.com/journal-of-water-process-engineering/.

Adamu, M., Rahman, M. R., Hamdan, S., Bakri, M. K. B., & Yusof, F. A. B. M. (2020). Impact of polyvinyl alcohol/acrylonitrile on bamboo nanocomposite and optimization of mechanical performance by response surface methodology. *Construction and Building Materials*, *258*. Available from https://doi.org/10.1016/j.conbuildmat.2020.119693, https://www.journals.elsevier.com/construction-and-building-materials.

Adamu, M., Rahman, M. R., & Hamdan, S. (2019). Formulation optimization and characterization of bamboo/polyvinyl alcohol/clay nanocomposite by response surface methodology. *Composites Part B: Engineering*, *176*, 107297. Available from https://doi.org/10.1016/j.compositesb.2019.107297.

Agronomy Fact Sheet Series (Fact Sheet 22) (2008). http://www.ccs.cornell.edu.

Aguilar, H., Yazdani-Pedram, M., Toro, P., Quijada, R., & López-Manchado, M. Á. (2014). Synergic effect of two inorganic fillers on the mechanical and thermal properties of hybrid polypropylene composites. *Journal of the Chilean Chemical Society*, *59*(2), 2468–2473. Available from https://doi.org/10.4067/S0717-97072014000200015, http://www.scielo.cl/pdf/jcchems/v59n2/art15.pdf.

Ahmad, M., Rajapaksha, A. U., Lim, J. E., Zhang, M., Bolan, N., Mohan, D., Vithanage, M., Lee, S. S., & Ok, Y. S. (2014). Biochar as a sorbent for contaminant management in soil and water: A review. *Chemosphere*, *99*, 19–33. Available from https://doi.org/10.1016/j.chemosphere.2013.10.071, http://www.elsevier.com/locate/chemosphere.

Akpan, E. I., Shen, X., Wetzel, B., & Friedrich, K. (2019). *Design and synthesis of polymer nanocomposites* (pp. 47–83). Elsevier BV. Available from https://doi.org/10.1016/b978-0-12-814064-2.00002-0.

Al-Essa, K. (2018). Activation of Jordanian bentonite by hydrochloric acid and its potential for olive mill wastewater enhanced treatment. *Journal of Chemistry*. Available from https://doi.org/10.1155/2018/8385692.

Alhinai, M., Azad, A. K., Bakar, M. S. A., & Phusunti, N. (2018). Characterisation and thermochemical conversion of rice husk for biochar production. *International Journal of Renewable Energy Research*, *8*(3), 1648–1656. Available from http://www.ijrer.org.

Ali Mohsin, M. E., Arsad, A., Fouad, H., Jawaid, M., & Alothman. O.Y. (2014). Enhanced mechanical and thermal properties of CNT/HDPE nanocomposite using MMT as secondary filler. In *AIP conference proceedings*. 1599:206-209. <http://scitation.aip.org/content/aip/proceeding/aipcp. https://doi.org/10.1063/1.4876814>.

Amari, A., Gannouni, H., Khan, M., Almesfer, M., Elkhaleefa, A., & Gannouni, A. (2018). Effect of structure and chemical activation on the adsorption properties of green clay minerals for the removal of cationic dye. *Applied Sciences*, *8*(11), 2302. Available from https://doi.org/10.3390/app8112302.

Annu, A., Bhattacharya, B., Singh, P. K., Shukla, P. K., & Rhee, H. W. (2017). Carbon nanotube using spray pyrolysis: Recent scenario. *Journal of Alloys and Compounds*, *691*, 970−982. Available from https://doi.org/10.1016/j.jallcom.2016.08.246.

Antal, M. J., & Grønli, M. (2003). The art, science, and technology of charcoal production. *Industrial and Engineering Chemistry Research*, *42*(8), 1619−1640. Available from https://doi.org/10.1021/ie0207919, http://pubs.acs.org/journal/iecred.

Ao, W., Fu, J., Mao, X., Kang, Q., Ran, C., Liu, Y., Zhang, H., Gao, Z., Li, J., Liu, G., & Dai, J. (2018). Microwave assisted preparation of activated carbon from biomass: A review. *Renewable and Sustainable Energy Reviews*, *92*, 958−979. Available from https://doi.org/10.1016/j.rser.2018.04.051, https://www.journals.elsevier.com/renewable-and-sustainable-energy-reviews.

Arjmandi, R., Hassan, A., Haafiz, M. K. M., Zakaria, Z., & Inuwa, I. M. (2014). Pencirian komposit polilaktik asid/selulosa mikrohablur/ hibrid montmorilonit. *Malaysian Journal of Analytical Sciences*, *18*(3), 642−650. Available from http://www.ukm.my/mjas/v18_n3/Reza%20Arjmandi_18_3_18.pdf.

Arjmandi, R., Hassan, A., Mohamad Haafiz, M. K., & Zakaria, Z. (2016). *Effects of micro- and nano-cellulose on tensile and morphological properties of montmorillonite nanoclay reinforced polylactic acid nanocomposites*. *Engineering materials* (pp. 103−125). Malaysia: Springer Science and Business Media B.V. Available from http://springer.com/series/4288, https://doi.org/10.1007/978-981-10-0950-1_5.

Ashiq, A., Sarkar, B., Adassooriya, N., Walpita, J., Rajapaksha, A. U., Ok, Y. S., & Vithanage, M. (2019). Sorption process of municipal solid waste biochar-montmorillonite composite for ciprofloxacin removal in aqueous media. *Chemosphere*, *236*. Available from https://doi.org/10.1016/j.chemosphere.2019.124384, http://www.elsevier.com/locate/chemosphere.

ASTM E1252-98 (2021). Practice for general techniques for obtaining infrared spectra for qualitative analysis. ASTM International Standard. https://doi.org/10.1520/E1252-98R21.

ASTM E168-16 (2023). ASTM international standard practices for general techniques of infrared quantitative analysis. https://doi.org/10.1520/E0168-16.

Avella, M., La Rota, G., Martuscelli, E., Raimo, M., Sadocco, P., Elegir, G., & Riva, R. (2000). *Journal of Materials Science*, *35*(4), 829−836. Available from https://doi.org/10.1023/A:1004773603516.

Baheti, V., Mishra, R., Militky, J., & Behera, B. K. (2014). Influence of noncellulosic contents on nano scale refinement of waste jute fibers for reinforcement in polylactic acid films. *Fibers and Polymers*, *15*(7), 1500−1506. Available from https://doi.org/10.1007/s12221-014-1500-5, http://link.springer.com/journal/volumesAndIssues/12221.

Bakri, M. K. B., Jayamani, E., Hamdan, S., Rahman, M. R., & Kakar, A. (2018). Potential of *Borneo acacia* wood in fully biodegradable bio-composites' commercial production and application. *Polymer Bulletin*, *75*(11), 5333−5354. Available from https://doi.org/10.1007/s00289-018-2299-9, https://rd.springer.com/journal/289.

Bakri, M. K. B., & Rahman, M. R. (2021). *Fundamentals and recent advances in nanocomposites based on polymers and nanocellulose*. *Cellulose-based composite carbon nanofibers* (pp. 159−174). Malaysia: Elsevier. Available from https://www.sciencedirect.com/book/9780323857710, https://doi.org/10.1016/B978-0-323-85771-0.00009-9.

Balat, M. (2007). Influence of coal as an energy source on environmental pollution. *Energy Sources, Part A: Recovery, Utilization and Environmental Effects*, *29*(7), 581−589. Available from https://doi.org/10.1080/15567030701225260.

Bartholmal, M., & Schartel, B. (2004). Layered silicate polymer nanocomposites: New approach or illusion for fire retardacy? Investigations of the potentials and the tasks using a model system. *Polymers for Advanced Technologies*, *15*(7), 355–364. Available from https://doi.org/10.1002/pat.483.

Batista, E. M. C. C., Shultz, J., Matos, T. T. S., Fornari, M. R., Ferreira, T. M., Szpoganicz, B., De Freitas, R. A., & Mangrich, A. S. (2018). Effect of surface and porosity of biochar on water holding capacity aiming indirectly at preservation of the Amazon biome. *Scientific Reports*, *8*(1). Available from https://doi.org/10.1038/s41598-018-28794-z, http://www.nature.com/srep/index.html.

Bhattacharya, M. (2016). Polymer nanocomposites—A comparison between carbon nanotubes, graphene, and clay as nanofillers. *Materials*, *9*(4), 262. Available from https://doi.org/10.3390/ma9040262.

Bitinis, N., Hernandez, M., Verdejo, R., Kenny, J. M., & Lopez-Manchado, M. A. (2011). Recent advances in clay/polymer nanocomposites. *Advanced Materials*, *23*(44), 5229–5236. Available from https://doi.org/10.1002/adma.201101948.

Borah, S. J., & Das, D. K. (2018). Modified montmorillonite: An active heterogeneous catalyst for the synthesis of benzimidazoles. *Journal of Chemical and Pharmaceutical Research*, *10*(7), 118–123.

Box, G. E. P., & Wilson, K. B. (1951). On the experimental attainment of optimum conditions. *Journal of the Royal Statistical Society: Series B (Methodological)*, *13*(1), 1–38. Available from https://doi.org/10.1111/j.2517-6161.1951.tb00067.x.

Brunauer, S., Emmett, P. H., & Teller, E. (1938). Adsorption of gases in multimolecular layers. *Journal of the American Chemical Society*, *60*(2), 309–319. Available from https://doi.org/10.1021/ja01269a023.

Cetin, E., Moghtaderi, B., Gupta, R., & Wall, T. F. (2004). Influence of pyrolysis conditions on the structure and gasification reactivity of biomass chars. *Fuel*, *83*(16), 2139–2150. Available from https://doi.org/10.1016/j.fuel.2004.05.008.

Cheah, S., Jablonski, W. S., Olstad, J. L., Carpenter, D. L., Barthelemy, K. D., Robichaud, D. J., Andrews, J. C., Black, S. K., Oddo, M. D., & Westover, T. L. (2016). Effects of thermal pretreatment and catalyst on biomass gasification efficiency and syngas composition. *Green Chemistry*, *18*(23), 6291–6304. Available from https://doi.org/10.1039/c6gc01661h, http://pubs.rsc.org/en/journals/journal/gc.

Chen, N., Feng, H., Guo, J., Luo, H., & Qiu, J. (2011). Biodegradable poly(lactic acid)/TDI-montmorillonite nanocomposites: Preparation and characterization. *Advanced Materials Research*, *221*, 211–215. Available from https://doi.org/10.4028/http://www.scientific.net/AMR.221.211.

Cheung, H. Y., Lau, K. T., Tao, X. M., & Hui, D. (2008). A potential material for tissue engineering: Silkworm silk/PLA biocomposite. *Composites Part B: Engineering*, *39*(6), 1026–1033. Available from https://doi.org/10.1016/j.compositesb.2007.11.009.

Choudalakis, G., & Gotsis, A. D. (2009). Permeability of polymer/clay nanocomposites: A review. *European Polymer Journal*, *45*(4), 967–984. Available from https://doi.org/10.1016/j.eurpolymj.2009.01.027.

Chowdhury, Z. Z., Hamid, S. B. A., Das, R., Hasan, M. R., Zain, S. M., Khalid, K., & Uddin, M. N. (2013). Preparation of carbonaceous adsorbents from lignocellulosic biomass and their use in removal of contaminants from aqueous solution. *BioResources*, *8*(4). Available from https://doi.org/10.15376/biores.8.4.6523-6555, http://www.ncsu.edu/bioresources/BioRes_08/BioRes_08_4_6523_Review_Chowdhury_ADHZKN_Ligno_Biomass_C_Liquid_Sorption_4292.pdf.

Chow, W. S. (2007). Water absorption of epoxy/glass fiber/organo-montmorillonite nanocomposites. *Express Polymer Letters*, *1*(2), 104–108. Available from https://doi.org/10.3144/expresspolymlett.2007.18Malaysia, http://www.expresspolymlett.com/letolt.php?file = EPL-0000081&mi = c.

Chowdhury, Z. Z., Karim, M. Z., Ashraf, M. A., & Khalid, K. (2016). Influence of carbonization temperature on physicochemical properties of biochar derived from slow pyrolysis of durian wood (*Durio zibethinus*) sawdust. *BioResources*, *11*(2). Available from https://doi.org/10.15376/biores.11.2.3356-3372.

Corcione, C. E., & Frigione, M. (2012). Characterization of nanocomposites by thermal analysis. *Materials*, *5*(12), 2960−2980. Available from https://doi.org/10.3390/ma5122960Italy, http://www.mdpi.com/1996-1944/5/12/2960/pdf.

Costache, M. C., Heidecker, M. J., Manias, E., Camino, G., Frache, A., Beyer, G., Gupta, R. K., & Wilkie, C. A. (2007). The influence of carbon nanotubes, organically modified montmorillonites and layered double hydroxides on the thermal degradation and fire retardancy of polyethylene, ethylene-vinyl acetate copolymer and polystyrene. *Polymer*, *48*(22), 6532−6545. Available from https://doi.org/10.1016/j.polymer.2007.08.059, http://www.journals.elsevier.com/polymer/.

Creamer, A. E., Gao, B., & Zhang, M. (2014). Carbon dioxide capture using biochar produced from sugarcane bagasse and hickory wood. *Chemical Engineering Journal*, *249*, 174−179. Available from https://doi.org/10.1016/j.cej.2014.03.105, http://www.elsevier.com/inca/publications/store/6/0/1/2/7/3/index.htt.

Daful, A. G., & Chandraratne, M. R. (2018). *Biochar production from biomass waste-derived material. Reference module in materials science and materials engineering* (pp. 11249−11258). Elsevier.

Dantas de Oliveira, A., & Augusto Gonçalves Beatrice, C. (2019). *Polymer nanocomposites with different types of nanofiller*. IntechOpen. Available from https://doi.org/10.5772/intechopen.81329.

Das, O., Sarmah, A. K., Zujovic, Z., & Bhattacharyya, D. (2016). Characterisation of waste derived biochar added biocomposites: Chemical and thermal modifications. *Science of the Total Environment*, *550*, 133−142. Available from https://doi.org/10.1016/j.scitotenv.2016.01.062, http://www.elsevier.com/locate/scitotenv.

Deng, H., Li, G., Yang, H., Tang, J., & Tang, J. (2010). Preparation of activated carbons from cotton stalk by microwave assisted KOH and K2CO3 activation. *Chemical Engineering Journal*, *163*(3), 373−381. Available from https://doi.org/10.1016/j.cej.2010.08.019.

Deroiné, M., César, G., Le Duigou, A., Davies, P., & Bruzaud, S. (2015). Natural degradation and biodegradation of poly(3-hydroxybutyrate-co-3-hydroxyvalerate) in liquid and solid marine environments. *Journal of Polymers and the Environment*, *23*(4), 493−505. Available from https://doi.org/10.1007/s10924-015-0736-5, http://www.kluweronline.com/issn/1566-2543/.

Devendra, K., & Rangaswamy, T. (2012). Determination of mechanical properties of Al2O3, Mg (OH)2 and SiC filled E-glass/epoxy composites. *International Journal of Engineering Research Applications*, *2*(5), 2028−2033.

Ding, J., Xue, G., Dai, Q., & Cheng, R. (1993). Glass transition temperature of polystyrene microparticles. *Polymer*, *34*(15), 3325−3327. Available from https://doi.org/10.1016/0032-3861(93)90412-4.

Drobny, J. G. (2014). *Additives* (pp. 17−32). Elsevier BV. Available from https://doi.org/10.1016/b978-0-323-22136-8.00003-x.

Duleba, B., Greškovič, F., Spišák, E., & Dulebová, L. (2014). *Preparation and characterization of polypropylene/MMT nanocomposites*, . *Advanced Materials Research* (893, pp. 132−135). Slovakia: Trans Tech Publications. Available from https://doi.org/10.4028/http://www.scientific.net/AMR.893.132.

Fischer, H. (2003). Polymer nanocomposites: From fundamental research to specific applications. *Materials Science and Engineering C*, *23*(6-8), 763−772. Available from https://doi.org/10.1016/j.msec.2003.09.148.

FHWA (2003). Estimating Clay Content. US Department of Transportation, Federal Highway Program.

Foo, M. E., & Gopinath, S. C. B. (2017). Feasibility of graphene in biomedical applications. *Biomedicine and Pharmacotherapy*, *94*, 354–361. Available from https://doi.org/10.1016/j.biopha.2017.07.122, http://www.elsevier.com/locate/biomedpharm.

Fu, X., & Qutubuddin, S. (2000). Synthesis of polystyrene–clay nanocomposites. *Materials Letters*, *42*(1-2), 12–15. Available from https://doi.org/10.1016/s0167-577x(99)00151-2.

Gallo, F., Fossi, C., Weber, R., Santillo, D., Sousa, J., Ingram, I., Nadal, A., & Romano, D. (2018). Marine litter plastics and microplastics and their toxic chemicals components: the need for urgent preventive measures. *Environmental Sciences Europe*, *30*(1). Available from https://doi.org/10.1186/s12302-018-0139-z, http://www.springer.com/environment/journal/12302.

Gao, Y. L., Ju, X. R., Qiu, W. F., & Jiang, H. H. (2007). Investigation of the effects of food constituents on Bacillus subtilis reduction during high pressure and moderate temperature. *Food Control*, *18*(10), 1250–1257. Available from https://doi.org/10.1016/j.foodcont.2006.08.007.

Garlotta, D. (2001). A literature review of poly(lactic acid). *Journal of Polymers and the Environment*, *9*(2), 63–84.

George, J., & Siddaramaiah. (2012). High performance edible nanocomposite films containing bacterial cellulose nanocrystals. *Carbohydrate Polymers*, *87*(3), 2031–2037. Available from https://doi.org/10.1016/j.carbpol.2011.10.019.

Giannelis, E. P. (1996). Polymer layered silicate nanocomposites. *Advanced Materials*, *8*(1), 29–35. Available from https://doi.org/10.1002/adma.19960080104, http://www3.interscience.wiley.com/journal/119030556/issue.

Gill, Y. Q., Irfan, M. S., Khan, F. U. H., Saeed, F., Ehsan, H., & Shakoor, A. (2019). Carbon black/nickel hybrid filler reinforced conductive polypropylene composites. *Materials Research Express*, *6*(8). Available from https://doi.org/10.1088/2053-1591/ab1a5d, https://iopscience.iop.org/article/10.1088/2053-1591/ab1a5d/pdf.

Gironi, F., & Piemonte, V. (2011). Bioplastics and petroleum-based plastics: Strengths and weaknesses. *Energy Sources, Part A: Recovery, Utilization and Environmental Effects*, *33*(21), 1949–1959. Available from https://doi.org/10.1080/15567030903436830.

Gond, R. K., & Gupta, M. K. (2021). Preparation of PLA based biodegradable nanofibre films and their characterization. *Indian Journal of Fibre and Textile Research*, *46*(1), 9–14. Available from http://nopr.niscair.res.in/bitstream/123456789/56440/1/IJFTR%2046(1)%209-14.pdf.

Gorrasi, G., Sarno, M., Di Bartolomeo, A., Sannino, D., Ciambelli, P., & Vittoria, V. (2007). Incorporation of carbon nanotubes into polyethylene by high energy ball milling: Morphology and physical properties. *Journal of Polymer Science, Part B: Polymer Physics*, *45*(5), 597–606. Available from https://doi.org/10.1002/polb.21070.

Gulrez, S. K. H., Abdel-Ghany, A. M., Al-Helal, I. M., Al-Zaharani, S. M., & Alsadon, A. A. (2013a). Evaluation of PE films having NIR-reflective additives for greenhouse applications in arid regions. *Advances in Materials Science and Engineering*, *2013*, 1–8. Available from https://doi.org/10.1155/2013/575081.

Gulrez, S. K. H., Mohsin., Shaikh, H., Anis, A., Pulose, A. M., Yadav, M. K., Qua, E. H. P., & Al-Zahrani, S. M. (2013b). *Polymer Composites*, *35*.

Gul, S., Kausar, A., Muhammad, B., & Jabeen, S. (2015). Research progress on properties and applications of polymer/clay nanocomposite. *Polymer-Plastics Technology and Engineering*, *55*(7), 684–703. Available from https://doi.org/10.1080/03602559.2015.1098699.

Guo, F., Aryana, S., Han, Y., & Jiao, Y. (2018). A review of the synthesis and applications of polymer–nanoclay composites. *Applied Sciences*, *8*(9), 1696. Available from https://doi.org/10.3390/app8091696.

Gupta, S., & Kua, H. W. (2017). Factors determining the potential of biochar as a carbon capturing and sequestering construction material: Critical review. *Journal of Materials in Civil Engineering*, *29*(9). Available from https://doi.org/10.1061/(asce)mt.1943-5533.0001924.

Hamdan, S., Rahman, Saleh, A., & Islam, M.S. (n.d.). Influence of N, N-dimethylacetamid on the thermal and mechanical properties of polymer-filled wood. *Zainal Abidin Talib.*, *5*(4)0.2611–2624.

Harding, K., Dennis, J., Vonblottnitz, H., & Harrison, S. (2007). Environmental analysis of plastic production processes: Comparing petroleum-based polypropylene and polyethylene with biologically-based poly-β-hydroxybutyric acid using life cycle analysis. *Journal of Biotechnology*, *130*(1), 57–66. Available from https://doi.org/10.1016/j.jbiotec.2007.02.012.

Henry, F., Marchal, P., Bouillard, J., Vignes, A., Dufaud, O., & Perrin, L. (2013). Italian Association of Chemical Engineering - AIDIC France: The effect of agglomeration on the emission of particles from nanopowders flow. *Chemical Engineering Transactions*, *31*, 811–816. Available from https://doi.org/10.3303/CET1331136, http://www.aidic.it/cet/13/31/136.pdf.

He, Y., Guo, K., Chen, J., Niu, M., Wang, W., & Li, X. (2011). Preparation and characterization of Poly(lactic acid)/montmorillonite nanocomposites via a masterbatching method. *Advanced Materials Research*, *335-336*, 1493–1498. Available from https://doi.org/10.4028/http://www.scientific.net/AMR.335-336.1493.

Imran, M., Revol-Junelles, A. M., Martyn, A., Tehrany, E. A., Jacquot, M., Linder, M., & Desorby, S. (2010). Active food packaging evolution: Transformation from micro- to nanotechnology. *Critical Reviews in Food Science and Nutrition*, *50*, 799–821. Available from https://doi.org/10.1080/10408398.2010.503694.

Introduction to Plastics and Elastomers. (2012). Elsevier BV, xxi-xxxiv, Available from https://doi.org/10.1016/b978-1-4557-7896-6.00059-5.

Irshidat, M. R., & Al-Saleh, M. H. (2018). Thermal performance and fire resistance of nanoclay modified cementitious materials. *Construction and Building Materials*, *159*, 213–219. Available from https://doi.org/10.1016/j.conbuildmat.2017.10.127.

Islam, Hamdan, Rahman, M. R., Jusoh, Ahmed, A. S., & Idrus, M. (n.d.). Dynamic Young's modulus, morphological, and thermal stability of 5 tropical light hardwoods modified by benzene diazonium salt treatment. *BioResources, 6* (1)737–750.

ISO/TS (2008). Nanotechnologies — Terminology and definitions for nano-objects — Nanoparticle, nanofibre and nanoplate.

Jaafar, M. (2017). *Development of hybrid fillers/polymer nanocomposites for electronic applications. Hybrid nanomaterials: advances in energy, environment and polymer nanocomposites* (pp. 349–369). Malaysia: Wiley. Available from https://onlinelibrary.wiley.com/doi/book/10.1002/9781119160380, https://doi.org/10.1002/9781119160380.ch7.

Jaleh, B., & Fakhri, P. (2016). *Infrared and Fourier transform infrared spectroscopy for nanofillers and their nanocomposites*. *Spectroscopy of polymer nanocomposites* (pp. 112–129). Iran: Elsevier Inc. Available from http://www.sciencedirect.com/science/book/9780323401838, https://doi.org/10.1016/B978-0-323-40183-8.00005-7.

James, A. A., Rahman, M. R., Huda, D., Aqlan, F. M., Matin, M. M., Bakri, M. K. B., Kuok, K. K., & Rahman, M. M. (2022). Synthesis and characterization of novel nano-carbon mixture from Dabai (*Canarium odontophyllum*) nutshell. *BioResources*, *17* (3), 4452–4469. Available from https://doi.org/10.15376/biores.17.3.4452-4469, https://bioresources.cnr.ncsu.edu/wp-content/uploads/2022/06/BioRes_17_3_4452_James_RHUBK_Synth_Charac_Novel_Nano_Mix_Dabai_Nutshell_19715.pdf.

Jayamani, E., Heng, S. K., & Bin Bakri, M. K. (2017). Dielectric properties of pineapple leaf fiber reinforced epoxy based composites. *Key Engineering Materials*, *730*, 42–47. Available from https://doi.org/10.4028/http://www.scientific.net/KEM.730.42, https://www.scientific.net/KEM.

Jayamani, E., Tan, H. L., Benhur, D. A., & Bakri, M. K. B. (2019). *Environmental impact analysis of wood and natural fiber bio-composites*. *Engineering Materials* (pp. 153–170).

Malaysia: Springer Science and Business Media B.V. Available from http://springer.com/series/4288, https://doi.org/10.1007/978-3-030-29627-8_7.

Jeon, I., & Nam, K. (2019). Change in the site density and surface acidity of clay minerals by acid or alkali spills and its effect on pH buffering capacity. *Scientific Reports*, *9*(1). Available from https://doi.org/10.1038/s41598-019-46175-y, http://www.nature.com/srep/index.html.

Jiang, L., Zhang, J., & Wolcott, M. P. (2007). Comparison of polylactide/nano-sized calcium carbonate and polylactide/montmorillonite composites: Reinforcing effects and toughening mechanisms. *Polymer*, *48*(26), 7632−7644. Available from https://doi.org/10.1016/j.polymer.2007.11.001, http://www.journals.elsevier.com/polymer/.

Jia, Z., Wang, Z., Xu, C., Liang, J., Wei, B., Wu, D., & Zhu, S. (1999). Study on poly (methyl methacrylate)/carbon nanotube composites. *Materials Science and Engineering A*, *271*(1-2), 395−400. Available from https://doi.org/10.1016/s0921-5093(99)00263-4, http://www.elsevier.com.

Jiao, Y., Han, D., Lu, Y., Rong, Y., Fang, L., Liu, Y., & Han, R. (2017). Characterization of pine-sawdust pyrolytic char activated by phosphoric acid through microwave irradiation and adsorption property toward CDNB in batch mode. *Desalination and Water Treatment*, *77*, 247−255.

Jose, M. V., Dean, D., Tyner, J., Price, G., & Nyairo, E. (2007). Polypropylene/carbon nanotube nanocomposite fibers: Process-morphology- property relationships. *Journal of Applied Polymer Science*, *103*(6), 3844−3850. Available from https://doi.org/10.1002/app.25475.

Kanda, M., Puggal, S., Dhall, N., & Sharma, A. (2018). Recent developments in the fabrication, characterization, and properties enhancement of polymer nanocomposites: A critical review. *Materials Today: Proceedings*, *14*(5), 28243−28252. Available from https://doi.org/10.1016/j.matpr.2018.10.069, https://www.sciencedirect.com/journal/materials-today-proceedings.

Kashiwagi, T., Du, F., Douglas, J. F., Winey, K. I., Harris, R. H., & Shields, J. R. (2005). Nanoparticle networks reduce the flammability of polymer nanocomposites. *Nature Materials*, *4*(12), 928−933. Available from https://doi.org/10.1038/nmat1502.

Keddie, J. L., Jones, R. A. L., & Cory, R. A. (1994). Interface and surface effects on the glass-transition temperature in thin polymer films. *Faraday Discussions*, *98*, 219. Available from https://doi.org/10.1039/fd9949800219.

Khairulzaim, A. A. B. M., Rahman, M. R., Roslan, L., Bakri, M. K. B., Khan, A., & Matin, M. M. (2021). Analysis of char prepared by pyrolysis of Dabai (*Canarium odontophyllum*) nutshells as a potential precursor of biocarbon used for wastewater treatment. *BioResources*, *16*(3), 5036−5046. Available from https://doi.org/10.15376/biores.16.3.5036-5046, http://www.ncsu.edu/bioresources/Back_Issues.htm.

Khelfa, A., Rodrigues, F. A., Koubaa, M., & Vorobiev, E. (2020). Microwave-assisted pyrolysis of pine wood sawdust mixed with activated carbon for bio-oil and bio-char production. *Processes*, *8*(11), 1437. Available from https://doi.org/10.3390/pr8111437.

Khui, P. L. N., Rahman, M. R., & Bakri, M. K. B. (2023). A review on the extraction of cellulose and nanocellulose as a filler through solid waste management. *Journal of Thermoplastic Composite Materials*, *36*(3), 1306−1327. Available from https://doi.org/10.1177/08927057211020800, https://journals.sagepub.com/home/JTC.

Khui, P. L. N., Rahman, M. R., & Bakri, M. K. B. (2021). *Cellulose reinforcement in bioplastic composites. Fundamentals and recent advances in nanocomposites based on polymers and nanocellulose* (pp. 143−158). Malaysia: Elsevier. Available from https://www.sciencedirect.com/book/9780323857710, https://doi.org/10.1016/B978-0-323-85771-0.00016-6.

Kim, H., Abdala, A. A., & MacOsko, C. W. (2010). Graphene/polymer nanocomposites. *Macromolecules*, *43*(16), 6515−6530. Available from https://doi.org/10.1021/ma100572e.

Klaessig, F., Marrapese, M., & Abe, S. (2011). *Current perspectives in nanotechnology terminology and nomenclature* (pp. 21−52). Springer Science and Business Media LLC. Available from https://doi.org/10.1007/978-1-4419-7853-0_2.

Kojima, Y., Usuki, A., Kawasumi, M., Okada, A., Fukushima, Y., Kurauchi, T., & Kamigaito, O. (1993). Mechanical properties of nylon 6-clay hybrid. *Journal of Materials Research*, *8*(5), 1185−1189. Available from https://doi.org/10.1557/JMR.1993.1185.

Kordás, K., Tóth, G., Moilanen, P., Kumpumäki, M., Vähäkangas, J., Uusimäki, A., Vajtai, R., & Ajayan, P. M. (2007). Chip cooling with integrated carbon nanotube microfin architectures. *Applied Physics Letters*, *90*(12), 123105. Available from https://doi.org/10.1063/1.2714281.

Kothapalli, C. R., Shaw, M. T., & Wei, M. (2005). Biodegradable HA-PLA 3-D porous scaffolds: Effect of nano-sized filler content on scaffold properties. *Acta Biomaterialia*, *1*(6), 653−662. Available from https://doi.org/10.1016/j.actbio.2005.06.005, http://www.journals.elsevier.com/acta-biomaterialia.

Lee, T., Zubir, Z. A., Jamil, F. M., Matsumoto, A., & Yeoh, F. Y. (2014). Combustion and pyrolysis of activated carbon fibre from oil palm empty fruit bunch fibre assisted through chemical activation with acid treatment. *Journal of Analytical and Applied Pyrolysis*, *110*(1), 408−418. Available from https://doi.org/10.1016/j.jaap.2014.10.010.

Lehmann, J., Gaunt, J., & Rondon, M. (2006). Bio-char sequestration in terrestrial ecosystems - A review. *Mitigation and Adaptation Strategies for Global Change*, *11*(2), 403−427. Available from https://doi.org/10.1007/s11027-005-9006-5.

Lehmann, J., & Joseph, S. (2012). *Biochar for environmental management: An introduction. Biochar for Environmental Management: Science and Technology* (pp. 1−12). United States: Taylor and Francis. Available from http://www.taylorandfrancis.com/books/details/9781849770552/, https://doi.org/10.4324/9781849770552.

Liang, H., Chen, L., Liu, G., & Zheng, H. (2016). Surface morphology properties of biochars produced from different feedstocks. In *Proceedings of the 2016 international conference on civil*. https://doi.org/10.2991/iccte-16.2016.210.

Liew, F. K., Hamdan, S., Rahman, M. R., Mahmood, M. R., & Lai, J. C. H. (2018). The effects of nanoclay and tin(IV) oxide nanopowder on morphological, thermo-mechanical properties of hexamethylene diisocyanate treated jute/bamboo/polyethylene hybrid composites. *Journal of Vinyl and Additive Technology*, *24*(4), 358−366. Available from https://doi.org/10.1002/vnl.21600, http://onlinelibrary.wiley.com/journal/10.1002/(ISSN)1548-0585.

Liew, F. K., Hamdan, S., Rahman, M. R., Rusop, M., & Khan, A. (2020). Thermomechanical properties of jute/bamboo/polyethylene hybrid composites: The combined effects of silane coupling agent and copolymer. *Polymer Composites*, *41*(11), 4830−4841. Available from https://doi.org/10.1002/pc.25755, http://onlinelibrary.wiley.com/journal/10.1002/(ISSN)1548-0569.

Liu, L., Barber, A. H., Nuriel, S., & Wagner, H. D. (2005). Mechanical properties of functionalized single-walled carbon-nanotube/ poly(vinyl alcohol) nanocomposites. *Advanced Functional Materials*, *15*(6), 975−980. Available from https://doi.org/10.1002/adfm.200400525.

Liu, L., Niu, Z., & Chen, J. (2018). Flexible supercapacitors based on carbon nanotubes. *Chinese Chemical Letters*, *29*(4), 571−581. Available from https://doi.org/10.1016/j.cclet.2018.01.013, http://www.elsevier.com/wps/find/journaldescription.cws_home/997/description#description.

Liu, M., Zhang, Y., & Zhou, C. (2013). Nanocomposites of halloysite and polylactide. *Applied Clay Science*, *75-76*, 52−59. Available from https://doi.org/10.1016/j.clay.2013.02.019.

Li, X., Shen, Q., Zhang, D., Mei, X., Ran, W., Xu, Y., Yu, G., & Motta, A. (2013). Functional groups determine biochar properties (pH and EC) as studied by two-dimensional 13C NMR correlation spectroscopy. *PLoS One*, *8*(6), e65949. Available from https://doi.org/10.1371/journal.pone.0065949.

Li, Y., & Sun, X. S. (2010). Preparation and characterization of polymer-Inorganic nanocomposites by in situ melt polycondensation of l -Lactic acid and surface-hydroxylated MgO. *Biomacromolecules*, *11*(7), 1847–1855. Available from https://doi.org/10.1021/bm100320q.

Lyu, H., Yu, Z., Gao, B., He, F., Huang, J., Tang, J., & Shen, B. (2019). Ball-milled biochar for alternative carbon electrode. *Environmental Science and Pollution Research*, *26* (14), 14693–14702. Available from https://doi.org/10.1007/s11356-019-04899-4.

Maiti, S., Pramanik, A., Chattopadhyay, S., De, G., & Mahanty, S. (2016). Electrochemical energy storage in montmorillonite K10 clay based composite as supercapacitor using ionic liquid electrolyte. *Journal of Colloid and Interface Science*, *464*, 73–82. Available from https://doi.org/10.1016/j.jcis.2015.11.010, http://www.elsevier.com/inca/publications/store/6/2/2/8/6/1/index.htt.

Mallakpour, S., & Naghdi, M. (2018). Polymer/SiO_2 nanocomposites: Production and applications. *Progress in Materials Science*, *97*, 409–447. Available from https://doi.org/10.1016/j.pmatsci.2018.04.002.

Manchado, M. A. L., Valentini, L., Biagiotti, J., & Kenny, J. M. (2005). Thermal and mechanical properties of single-walled carbon nanotubes-polypropylene composites prepared by melt processing. *Carbon*, *43*(7), 1499–1505. Available from https://doi.org/10.1016/j.carbon.2005.01.031.

Manias, E., Touny, A., Wu, L., Strawhecker, K., Lu, B., & Chung, T. C. (2001). Polypropylene/montmorillonite nanocomposites. Review of the synthetic routes and materials properties. *Chemistry of Materials*, *13*(10), 3516–3523. Available from https://doi.org/10.1021/cm0110627.

Merinska, D., Kubisova, H., Kalendova, A., Svoboda, P., & Hromadkova, J. (2012). Processing and properties of polyethylene/montmorillonite nanocomposites. *Journal of Thermoplastic Composite Materials*, *25*(1), 115–131. Available from https://doi.org/10.1177/0892705711404939.

Messersmith, P. B., & Giannelis, E. P. (1995). Synthesis and barrier properties of poly (ε-caprolactone)-layered silicate nanocomposites. *Journal of Polymer Science Part A: Polymer Chemistry*, *33*(7), 1047–1057. Available from https://doi.org/10.1002/pola.1995.080330707.

Mishra, A. K., & Ramaprabhu, S. (2012). Palladium nanoparticles decorated graphite nanoplatelets for room temperature carbon dioxide adsorption. *Chemical Engineering Journal*, *187*, 10–15. Available from https://doi.org/10.1016/j.cej.2011.01.024.

Mofokeng, J. P., Luyt, A. S., Tábi, T., & Kovács, J. (2012). Comparison of injection moulded, natural fibre-reinforced composites with PP and PLA as matrices. *Journal of Thermoplastic Composite Materials*, *25*(8), 927–948. Available from https://doi.org/10.1177/0892705711423291.

Mohanty, D. S., Biswal, S. K., Palve, P. Y., & Nayak, P. (2012). Synthesis and characterization of polylactic acid/cloisite 30B (MMT) nanocomposite for controlled release of anticancer drug curcumin. *International; Journal of Pharmaceutical Research and Applied Sciences*, *4*(1), 63–70.

Mohan, D., Sarswat, A., Ok, Y. S., & Pittman, C. U. (2014). Organic and inorganic contaminants removal from water with biochar, a renewable, low cost and sustainable adsorbent - A critical review. *Bioresource Technology*, *160*, 191–202. Available from https://doi.org/10.1016/j.biortech.2014.01.120, http://www.elsevier.com/locate/biortech.

Mohd Din, A. T., Hameed, B. H., & Ahmad, A. L. (2009). Batch adsorption of phenol onto physiochemical-activated coconut shell. *Journal of Hazardous Materials*, *161*(2-3), 1522−1529. Available from https://doi.org/10.1016/j.jhazmat.2008.05.009.

Molinaro, S., Cruz Romero, M., Boaro, M., Sensidoni, A., Lagazio, C., Morris, M., & Kerry, J. (2013). Effect of nanoclay-type and PLA optical purity on the characteristics of PLA-based nanocomposite films. *Journal of Food Engineering*, *117*(1), 113−123. Available from https://doi.org/10.1016/j.jfoodeng.2013.01.021.

Monica Veca, L., Meziani, M. J., Wang, W., Wang, X., Lu, F., Zhang, P., Lin, Y., Fee, R., Connell, J. W., & Sun, Y. P. (2009). Carbon nanosheets for polymeric nanocomposites with high thermal conductivity. *Advanced Materials*, *21*(20), 2088−2092. Available from https://doi.org/10.1002/adma.200802317, http://www3.interscience.wiley.com/cgi-bin/fulltext/122221224/PDFSTART.

Moniruzzaman, M., & Winey, K. I. (2006). Polymer nanocomposites containing carbon nanotubes. *Macromolecules*, *39*(16), 5194−5205. Available from https://doi.org/10.1021/ma060733p.

Morgan, A. B. (2006). Flame retarded polymer layered silicate nanocomposites: A review of commercial and open literature systems. *Polymers for Advanced Technologies*, *17*(4), 206−217. Available from https://doi.org/10.1002/pat.685.

Muniyasamy, S., Ofosu, O., John, M. J., & Anandjiwala, R. D. (2016). Mineralization of poly(lactic acid) (PLA), poly(3-hydroxybutyrate-co-valerate) (PHBV) and PLA/PHBV blend in compost and soil environments. *Journal of Renewable Materials*, *4*(2), 133−145. Available from https://doi.org/10.7569/JRM.2016.634104, http://www.techscience.com/JRM/index.html.

Munkhbayar, B., Nine, M. J., Jeoun, J., Bat-Erdene, M., Chung, H., & Jeong, H. (2013). Influence of dry and wet ball milling on dispersion characteristics of the multi-walled carbon nanotubes in aqueous solution with and without surfactant. *Powder Technology*, *234*, 132−140. Available from https://doi.org/10.1016/j.powtec.2012.09.045.

Müller, K., Bugnicourt, E., Latorre, M., Jorda, M., Echegoyen Sanz, Y., Lagaron, J., Miesbauer, O., Bianchin, A., Hankin, S., Bölz, U., Pérez, G., Jesdinszki, M., Lindner, M., Scheuerer, Z., Castelló, S., & Schmid, M. (2017). Review on the processing and properties of polymer nanocomposites and nanocoatings and their applications in the packaging, automotive and solar energy fields. *Nanomaterials*, *7*(4), 74. Available from https://doi.org/10.3390/nano7040074.

Naz, A., Kausar, A., Siddiq, M., & Choudhary, M. A. (2015). Comparative review on structure, properties, fabrication techniques, and relevance of polymer nanocomposites reinforced with carbon nanotube and graphite fillers. *Polymer-Plastics Technology and Engineering*, *55*(2), 171−198. Available from https://doi.org/10.1080/03602559.2015.1055504.

Ndé, H. S., Tamfuh, P. A., Clet, G., Vieillard, J., Mbognou, M. T., & Woumfo, E. D. (2019). Comparison of HCl and H2SO4 for the acid activation of a cameroonian smectite soil clay: palm oil discolouration and landfill leachate treatment. *Heliyon*, *5*(12), e02926. Available from https://doi.org/10.1016/j.heliyon.2019.e02926.

Nitayaphat, W., Jiratumnukul, N., Charuchinda, S., & Kittinaovarat, S. (2009). Mechanical properties of chitosan/bamboo charcoal composite films made with normal and surface oxidized charcoal. *Carbohydrate Polymers*, *78*(3), 444−448. Available from https://doi.org/10.1016/j.carbpol.2009.04.027.

Nizamuddin, S., Jayakumar, N. S., Sahu, J. N., Ganesan, P., Bhutto, A. W., & Mubarak, N. M. (2015). Hydrothermal carbonization of oil palm shell. *Korean Journal of Chemical Engineering*, *32*(9), 1789−1797. Available from https://doi.org/10.1007/s11814-014-0376-9, http://www.springerlink.com/content/120599/.

Nyuk Khui, P. L., Rahman, M. R., Hamdan, S., Bakri, M. K. B., Jayamani, E., & Kakar, A. (2019). *Effect of nano-enhancement on acacia wood bio-composites*. *Engineering materials* (pp. 187–205). Malaysia: Springer Science and Business Media B.V. Available from http://springer.com/series/4288, https://doi.org/10.1007/978-3-030-29627-8_9.

Odetoye, T. E., Abu Bakar, M. S., & Titiloye, J. O. (2019). Pyrolysis and characterization of Jatropha curcas shell and seed coat. *Nigerian Journal of Technological Development*, *16*(2), 71. Available from https://doi.org/10.4314/njtd.v16i2.4.

Odetoye, T. E., Afolabi, T. J., Abu Bakar, M. S., & Titiloye, J. O. (2018). Thermochemical characterization of Nigerian Jatropha curcas fruit and seed residues for biofuel production. *Energy, Ecology and Environment*, *3*(6), 330–337. Available from https://doi.org/10.1007/s40974-018-0104-0, https://link.springer.com/journal/40974.

Özbay, G., Özçifçi, A., Kökten, E. S., Toker, H., & Baysal, E. (2015). Bio-char production from pyrolysis of furniture products waste. In *Research for furniture industry: Proceedings of the 27th international conference*. Turkey.

Palniandy, L. K., Yoon, L. W., Wong, W. Y., Yong, S. T., & Pang, M. M. (2019). Application of Biochar derived from different types of biomass and treatment methods as a fuel source for direct carbon fuel cells. *Energies*, *12*(13). Available from https://doi.org/10.3390/en12132477, https://www.mdpi.com/1996-1073/12/13.

Paszkiewicz, S., Szymczyk, A., Zubkiewicz, A., Subocz, J., Stanik, R., & Szczepaniak, J. (2020). Enhanced functional properties of low-density polyethylene nanocomposites containing hybrid fillers of multi-walled carbon nanotubes and nano carbon black. *Polymers*, *12*(6), 1356. Available from https://doi.org/10.3390/polym12061356.

Paul, D. R., & Robeson, L. M. (2008). Polymer nanotechnology: Nanocomposites. *Polymer*, *49*(15), 3187–3204. Available from https://doi.org/10.1016/j.polymer.2008.04.017, http://www.journals.elsevier.com/polymer/.

Perez, J. V. D., Nadres, E. T., Nguyen, H. N., Dalida, M. L. P., & Rodrigues, D. F. (2017). Response surface methodology as a powerful tool to optimize the synthesis of polymer-based graphene oxide nanocomposites for simultaneous removal of cationic and anionic heavy metal contaminants. *RSC Advances*, *7*(30), 18480–18490. Available from https://doi.org/10.1039/c7ra00750g, http://pubs.rsc.org/en/journals/journalissues.

Peterson, S. C., Jackson, M. A., Kim, S., & Palmquist, D. E. (2012). Increasing biochar surface area: Optimization of ball milling parameters. *Powder Technology*, *228*, 115–120. Available from https://doi.org/10.1016/j.powtec.2012.05.005.

Phutane, P., Jatti, V. K. S., Sekhar, R., & Singh, T. P. (2013). Synthesis and characterization of SiC reinforced HE-30 al alloy particulate MMCs. *International Journal of Engineering and Technology*, *5*(3), 2866–2870. Available from http://www.enggjournals.com/ijet/docs/IJET13-05-03-313.pdf.

Pluta, M., Jeszka, J. K., & Boiteux, G. (2007). Polylactide/montmorillonite nanocomposites: Structure, dielectric, viscoelastic and thermal properties. *European Polymer Journal*, *43*(7), 2819–2835. Available from https://doi.org/10.1016/j.eurpolymj.2007.04.009.

Prashantha, K., Soulestin, J., Lacrampe, M. F., & Krawczak, P. (2014). Processing and characterization of polypropylene filled with multiwalled carbon nanotube and clay hybrid nanocomposites. *International Journal of Polymer Analysis and Characterization*, *19*(4), 363–371. Available from https://doi.org/10.1080/1023666X.2014.902715, http://www.tandf.co.uk/journals/titles/1023666x.html.

Qian, D., Dickey, E. C., Andrews, R., & Rantell, T. (2000). Load transfer and deformation mechanisms in carbon nanotube-polystyrene composites. *Applied Physics Letters*, *76*(20), 2868–2870. Available from https://doi.org/10.1063/1.126500, http://scitation.aip.org/content/aip/journal/apl.

Qian, K., Kumar, A., Patil, K., Bellmer, D., Wang, D., Yuan, W., & Huhnke, R. L. (2013). Effects of biomass feedstocks and gasification conditions on the physiochemical properties of char. *Energies*, *6*(8), 3972–3986. Available from https://doi.org/10.3390/en6083972, http://www.mdpi.com/1996-1073/6/8/3972/pdf.

Qian, S., Sheng, K., Yao, W., & Yu, H. (2016). Poly(lactic acid) biocomposites reinforced with ultrafine bamboo-char: Morphology, mechanical, thermal, and water absorption properties. *Journal of Applied Polymer Science*, *133*(20). Available from https://doi.org/10.1002/app.43425.

Qiu, Y., Zheng, Z., Zhou, Z., & Sheng, G. D. (2009). Effectiveness and mechanisms of dye adsorption on a straw-based biochar. *Bioresource Technology*, *100*(21), 5348−5351. Available from https://doi.org/10.1016/j.biortech.2009.05.054.

Qi, X. Y., Yan, D., Jiang, Z., Cao, Y. K., Yu, Z. Z., Yavari, F., & Koratkar, N. (2011). Enhanced electrical conductivity in polystyrene nanocomposites at ultra-low graphene content. *ACS Applied Materials and Interfaces*, *3*(8), 3130−3133. Available from https://doi.org/10.1021/am200628c.

Radenahmad, N., Azad, A. T., Saghir, M., Taweekun, J., Bakar, M. S. A., Reza, M. S., & Azad, A. K. (2020). A review on biomass derived syngas for SOFC based combined heat and power application. *Renewable and Sustainable Energy Reviews*, *119*. Available from https://doi.org/10.1016/j.rser.2019.109560, https://www.journals.elsevier.com/renewable-and-sustainable-energy-reviews.

Rahman, M. R., & Bakri, M. K. B. (2021). *Educational and awareness of bamboo nanocomposites towards sustainable environment*. *Engineering materials* (pp. 193−205). Malaysia: Springer Science and Business Media B.V. Available from http://springer.com/series/4288, https://doi.org/10.1007/978-3-030-68090-9_10.

Rahman, M. R., Hamdan, S., Ahmed, A. S., Islam, M. S., Talib, Z. A., Wan Abdullah, W. F., & Che Mat, M. S. (2011). Thermogravimetric analysis and dynamic Young's modulus measurement of N,N-dimethylacetamide-impregnated wood polymer composites. *Journal of Vinyl and Additive Technology*, *17*(3), 177−183. Available from https://doi.org/10.1002/vnl.20275.

Rahman, M. R., Hui, J. L. C., Hamdan, S., Ahmed, A. S., Baini, R., & Saleh, S. F. (2013). Combined styrene/MMA/nanoclay cross-linker effect on wood-polymer composites (WPCs). *BioResources*, *8*(2), 4227−4237. Available from http://www.ncsu.edu/bioresources/Back_Issues.htm.

Rahman, M. R., Hamdan, S., & Bakri, M. K. B. (2021). *Polylactic acid activated bamboo carbon nanocomposites*. *Engineering materials* (pp. 63−82). Malaysia: Springer Science and Business Media B.V. Available from http://springer.com/series/4288, https://doi.org/10.1007/978-3-030-68090-9_4.

Rahman, M. R., Khui, P. L. N., & Bakri, M. K. B. (2021b). *Bamboo nanocomposites future development and applications*. *Engineering materials* (pp. 183−191). Malaysia: Springer Science and Business Media B.V. Available from http://springer.com/series/4288, https://doi.org/10.1007/978-3-030-68090-9_9.

Rahman, M. R., Othman, A. K. B., Yurkin, Y., Burkov, A., Shestakova, U., Bakri, M. K. B., Alfaifi, S. Y., Madkhali, O., Aljabri, M. D., & Rahman, M. M. (2023). Rheological and mechanical study of micro-nano sized biocarbon-PLA biodegradable biocomposites. *BioResources*, *18*(3), 4492−4509. Available from https://doi.org/10.15376/biores.18.3.4492-4509, https://bioresources.cnr.ncsu.edu/wp-content/uploads/2023/05/BioRes_18_3_4492_Rahman_YBSBAMAR_Rheolog_Mechanical_Biocarbon_PLA_Composite_22606.pdf.

Rashidi, N. A., & Yusup, S. (2017). A review on recent technological advancement in the activated carbon production from oil palm wastes. *Chemical Engineering Journal*, *314*, 277−290. Available from https://doi.org/10.1016/j.cej.2016.11.059, http://www.elsevier.com/inca/publications/store/6/0/1/2/7/3/index.htt.

Ray, S. S., Yamada, K., Okamoto, M., & Ueda, K. (2002). Polylactide-layered silicate nanocomposite: A novel biodegradable material. *Nano Letters*, *2*(10), 1093−1096. Available from https://doi.org/10.1021/nl0202152.

Reza, M. S., Yun, C. S., Afroze, S., Radenahmad, N., Bakar, M. S. A., Saidur, R., Taweekun, J., & Azad, A. K. (2020). Preparation of activated carbon from biomass and its' applications in water and gas purification: A review. *Arab Journal of Basic and Applied Sciences*, *27*(1), 208–238. Available from https://doi.org/10.1080/25765299.2020.1766799, https://www.tandfonline.com/loi/tabs20.

Saba, N., Jawaid, M., Fouad, H., & Alothman, O. (2019). Nanocarbon: preparation, properties, and applications. *Nanocarbon and its Composites*, 327–354. Available from https://doi.org/10.1016/b978-0-08-102509-3.00009-2.

Sajjadi, B., Chen, W. Y., & Egiebor, N. O. (2019). A comprehensive review on physical activation of biochar for energy and environmental applications. *Reviews in Chemical Engineering*, *35*(6), 735–776. Available from https://doi.org/10.1515/revce-2017-0113, http://www.reference-global.com/loi/revce.

Sakhiya, A. K., Anand, A., & Kaushal, P. (2020). Production, activation, and applications of biochar in recent times. *Biochar*, *2*(3), 253–285. Available from https://doi.org/10.1007/s42773-020-00047-1, http://springer.com/journal/42773.

Samir, A., Ashour, F. H., Hakim, A. A. A., & Bassyouni, M. (2022). Recent advances in biodegradable polymers for sustainable applications. *NPJ Materials Degradation*, *6*(1). Available from https://doi.org/10.1038/s41529-022-00277-7, http://nature.com/npjmatdeg/.

Sam, S. T., Nuradibah, M. A., Chin, K. M., & Hani, N. (2015). *Current application and challenges on packaging industry based on natural polymer blending. Natural polymers: Industry techniques and applications* (pp. 163–184). Malaysia: Springer International Publishing. Available from http://doi.org/10.1007/978-3-319-26414-1, https://doi.org/10.1007/978-3-319-26414-1_6.

Sari, B., & Kaynak, C. (2016). Effects of montmorillonite content and maleic anhydride compatibilization on the mechanical behavior of polylactide nanocomposites. *International Polymer Processing*, *31*(4), 454–462. Available from https://doi.org/10.3139/217.3226, http://www.hanser-elibrary.com/doi/pdf/10.3139/217.3226.

Sasaki, T., Shimizu, A., Mourey, T. H., Thurau, C. T., & Ediger, M. D. (2003). Glass transition of small polystyrene spheres in aqueous suspensions. *The Journal of Chemical Physics*, *119*(16), 8730–8735. Available from https://doi.org/10.1063/1.1613257.

Schmidt, D., Shah, D., & Giannelis, E. P. (2002). New advances in polymer/layered silicate nanocomposites. *Current Opinion in Solid State and Materials Science*, *6*(3), 205–212. Available from https://doi.org/10.1016/S1359-0286(02)00049-9.

Schütz, M. R., Kalo, H., Lunkenbein, T., Breu, J., & Wilkie, C. A. (2011). Intumescent-like behavior of polystyrene synthetic clay nanocomposites. *Polymer*, *52*(15), 3288–3294. Available from https://doi.org/10.1016/j.polymer.2011.05.030, http://www.journals.elsevier.com/polymer/.

Sen, M. (2020). *Nanocomposite materials*. IntechOpen. Available from https://doi.org/10.5772/intechopen.93047.

Shaaban, A., Se, S. M., Mitan, N. M. M., & Dimin, M. F. (2013). Characterization of biochar derived from rubber wood sawdust through slow pyrolysis on surface porosities and functional groups. *Procedia Engineering*, *68*, 365–371. Available from https://doi.org/10.1016/j.proeng.2013.12.193, http://www.sciencedirect.com/science/journal/18777058.

Shankar, S., & Rhim, J.-W. (2018). *Bionanocomposite Films for Food Packaging Applications*. Elsevier BV. Available from https://doi.org/10.1016/b978-0-08-100596-5.21875-1.

Sharma, B., Mahajan, S., Chhibber, R., & Mehta, R. (2012). Glass fiber reinforced polymer-clay nanocomposites: Processing, structure and hygrothermal effects on mechanical properties. *Procedia Chemistry*, *4*, 39–46. Available from https://doi.org/10.1016/j.proche.2012.06.006.

Shen, Y. (2015). Chars as carbonaceous adsorbents/catalysts for tar elimination during biomass pyrolysis or gasification. *Renewable and Sustainable Energy Reviews*, *43*, 281–295. Available from https://doi.org/10.1016/j.rser.2014.11.061, https://www.journals.elsevier.com/renewable-and-sustainable-energy-reviews.

Shin, S. Y. A., Simon, L. C., Soares, J. B. P., & Scholz, G. (2003). Polyethylene-clay hybrid nanocomposites: In situ polymerization using bifunctional organic modifiers. *Polymer*, *44*(18), 5317–5321. Available from https://doi.org/10.1016/S0032-3861(03)00564-0, http://www.journals.elsevier.com/polymer/.

Shrivastava, A. (2018). Introduction to Plastics Engineering. (pp. 1–246). United States: Elsevier. Available from https://www.sciencedirect.com/book/9780323395007, https://doi.org/10.1016/C2014-0-03688-X.

Shtein, M., Nadiv, R., Buzaglo, M., & Regev, O. (2015). Graphene-based hybrid composites for efficient thermal management of electronic devices. *ACS Applied Materials and Interfaces*, 7(42), 23725–23730. Available from https://doi.org/10.1021/acsami.5b07866, http://pubs.acs.org/journal/aamick.

Singh, R., Singh, P., Singh, H., & Raghubanshi, A. S. (2019). Impact of sole and combined application of biochar, organic and chemical fertilizers on wheat crop yield and water productivity in a dry tropical agro-ecosystem. *Biochar*, *1*(2), 229–235. Available from https://doi.org/10.1007/s42773-019-00013-6, http://springer.com/journal/42773.

Siochi, E. J., Working, D. C., Park, C., Lillehei, P. T., Rouse, J. H., Topping, C. C., Bhattacharyya, A. R., & Kumar, S. (2004). Melt processing of SWCNT-polyimide nanocomposite fibers. *Composites Part B: Engineering*, *35*(5), 439–446. Available from https://doi.org/10.1016/j.compositesb.2003.09.007.

Sorrentino, A., Gorrasi, G., & Vittoria, V. (2007). Potential perspectives of bio-nanocomposites for food packaging applications. *Trends in Food Science and Technology*, *18*(2), 84–95. Available from https://doi.org/10.1016/j.tifs.2006.09.004.

Standard guide for preparation of plastics and polymeric specimens for microstructural examination. ASTM. (2021). Available from https://doi.org/10.1520/E2015-04R21.

Standard test method for carbon black—Total and external surface area by nitrogen adsorption. ASTM International. (2014). ASTM International 6556-14. Available from https://doi.org/10.1520/D6556-21.

Steurer, P., Wissert, R., Thomann, R., & Mülhaupt, R. (2009). Functionalized graphenes and thermoplastic nanocomposites based upon expanded graphite oxide. *Macromolecular Rapid Communications*, *30*(4-5), 316–327. Available from https://doi.org/10.1002/marc.200800754Germany, http://www3.interscience.wiley.com/cgi-bin/fulltext/121628054/PDFSTART.

Tate, R. S., Fryer, D. S., Pasqualini, S., Montague, M. F., de Pablo, J. J., & Nealey, P. F. (2001). Extraordinary elevation of the glass transition temperature of thin polymer films grafted to silicon oxide substrates. *The Journal of Chemical Physics*, *115*(21), 9982–9990. Available from https://doi.org/10.1063/1.1415497.

Thostenson, E. T., Ren, Z., & Chou, T. W. (2001). Advances in the science and technology of carbon nanotubes and their composites: A review. *Composites Science and Technology*, *61*(13), 1899–1912. Available from https://doi.org/10.1016/S0266-3538(01)00094-X, http://www.journals.elsevier.com/composites-science-and-technology/.

Tombácz, E., & Szekeres, M. (2006). Surface charge heterogeneity of kaolinite in aqueous suspension in comparison with montmorillonite. *Applied Clay Science*, *34*(1-4), 105–124. Available from https://doi.org/10.1016/j.clay.2006.05.009.

Tomczyk, A., Sokołowska, Z., & Boguta, P. (2020). Biochar physicochemical properties: Pyrolysis temperature and feedstock kind effects. *Reviews in Environmental Science and Biotechnology*, *19*(1), 191–215. Available from https://doi.org/10.1007/s11157-020-09523-3, http://www.kluweronline.com/issn/1569-1705.

Uchimiya, M., Wartelle, L. H., Klasson, K. T., Fortier, C. A., & Lima, I. M. (2011). Influence of pyrolysis temperature on biochar property and function as a heavy metal sorbent in soil. *Journal of Agricultural and Food Chemistry*, *59*(6), 2501–2510. Available from https://doi.org/10.1021/jf104206c.

Veksha, A., McLaughlin, H., Layzell, D. B., & Hill, J. M. (2014). Pyrolysis of wood to biochar: Increasing yield while maintaining microporosity. *Bioresource Technology*, *153*, 173–179. Available from https://doi.org/10.1016/j.biortech.2013.11.082, http://www.elsevier.com/locate/biortech.

Vengatesan, M. R. (2016). Nanoparticle and nanofiber based polymer nanocomposites: An overview. *Spherical and Fibrous Filler Composites*.

Vert, M., Doi, Y., Hellwich, K. H., Hess, M., Hodge, P., Kubisa, P., Rinaudo, M., & Schué, F. (2012). Terminology for biorelated polymers and applications (IUPAC recommendations 2012). *Pure and Applied Chemistry*, *84*(2), 377–410. Available from https://doi.org/10.1351/PAC-REC-10-12-04, http://www.iupac.org/publications/pac/84/2/0335/pdf/.

Wang, D., Li, B., Yang, H., Zhao, C., Yao, D., & Chen, H. (2019). Influence of biochar on the steam reforming of biomass volatiles: Effects of activation temperature and atmosphere. *Energy and Fuels*, *33*(3), 2328–2334. Available from https://doi.org/10.1021/acs.energyfuels.8b04412, http://pubs.acs.org/journal/enfuem.

Wang, S., Tambraparni, M., Qiu, J., Tipton, J., & Dean, D. (2009). Thermal expansion of graphene composites. *Macromolecules*, *42*(14), 5251–5255. Available from https://doi.org/10.1021/ma900631c, http://pubs.acs.org/doi/pdfplus/10.1021/ma900631c.

What Is Hot - Multi-client study (2023). World plastics supply 2005-2015. <http://www.pardos-marketing.com/hot01.htm>.

Worasuwannarak, N., Sonobe, T., & Tanthapanichakoon, W. (2007). Pyrolysis behaviors of rice straw, rice husk, and corncob by TG-MS technique. *Journal of Analytical and Applied Pyrolysis*, *78*(2), 265–271. Available from https://doi.org/10.1016/j.jaap.2006.08.002.

Xie, L., Xu, F., Qiu, F., Lu, H., & Yang, Y. (2007). Single-walled carbon nanotubes functionalized with high bonding density of polymer layers and enhanced mechanical properties of composites. *Macromolecules*, *40*(9), 3296–3305. Available from https://doi.org/10.1021/ma062103t.

Xu, R., Manias, E., Snyder, A. J., & Runt, J. (2001). Macromolecules.

Yalçinkaya, S. E., Yildiz, N., Ak, M. S., & Çalimli, A. (2010). Preparation of polystyrene/montmorillonite nanocomposites: Optimization by response surface methodology (RSM). *Turkish Journal of Chemistry*, *34*(4), 581–592. Available from https://doi.org/10.3906/kim-0908-235, http://journals.tubitak.gov.tr/chem/issues/kim-10-34-4/kim-34-4-10-0908-235.pdf.

Yang, K. K., Wang, X. L., & Wang, Y. Z. (2007). Progress in nanocomposite of biodegradable polymer. *Journal of Industrial and Engineering Chemistry*, *13*(4), 485–500.

Yasmin, A., Luo, J. J., & Daniel, I. M. (2006). Processing of expanded graphite reinforced polymer nanocomposites. *Composites Science and Technology*, *66*(9), 1182–1189. Available from https://doi.org/10.1016/j.compscitech.2005.10.014, http://www.journals.elsevier.com/composites-science-and-technology/.

Yin, C. Y., Aroua, M. K., & Daud, W. M. A. W. (2007). Review of modifications of activated carbon for enhancing contaminant uptakes from aqueous solutions. *Separation and Purification Technology*, *52*(3), 403–415. Available from https://doi.org/10.1016/j.seppur.2006.06.009.

Yuniarto, K., Welt, B. A., Irawan, H., & Candra. (2017). Morphological, thermal and oxygen barrier properties plasticized film polylactic acid. *Journal of Applied Packaging Research*, *9*.

Yun, C. M., Rahman, M. R., Huda, D., Kuok, K. K., Sze, A. C. P., Lin, D. C. X., & Bakri, M. K. B. (2022a). *Plastic waste as fine aggregate for sand filler replacement in concrete* *engineering materials* (pp. 149–168). Malaysia: Springer Science and Business Media Deutschland GmbH. Available from http://springer.com/series/4288, https://doi.org/10.1007/978-3-030-98812-8_9.

Yun, C. M., Rahman, M. R., Huda, D., Kuok, K. K., Sze, A. C. P., Seng, J. K., & Bakri, M. K. B. (2022b). *Sawdust as sand filler replacement in concrete*. *Engineering materials* (pp. 133–148). Malaysia: Springer Science and Business Media Deutschland GmbH. Available from http://springer.com/series/4288, https://doi.org/10.1007/978-3-030-98812-8_8.

Yun, C. M., Rahman, M. R., Kuok, K. K., Sze, A. C. P., Kung-Jiek, J. T., & Bakri, M. K. B. (2022c). *Uncrushed cockleshell as coarse aggregate filler replacement in concrete*. *Engineering materials* (pp. 63–80). Malaysia: Springer Science and Business Media Deutschland GmbH. Available from http://springer.com/series/4288, https://doi.org/10.1007/978-3-030-98812-8_4.

Yun, C. M., Rahman, M. R., Kuok, K. K., Sze, A. C. P., Zhiing, K. J. K., & Bakri, M. K. B. (2022d). *Glass waste as fine aggregate filler replacement in concrete addition of superplasticizer*. *Engineering materials* (pp. 45–61). Malaysia: Springer Science and Business Media Deutschland GmbH. Available from http://springer.com/series/4288, https://doi.org/10.1007/978-3-030-98812-8_3.

Yusoh, K., Kumaran, S. V., & Ismail. F. S. (2018). Surface modification of nanoclay for the synthesis of polycaprolactone (PCL) - Clay nanocomposite. In *MATEC web of conferences* (p. 150). EDP Sciences Malaysia. <http://www.matec-conferences.org/. https://doi.org/10.1051/matecconf/201815002005>.

Zeng, Q. H., Yu, A. B., Lu, G. Q., & Paul, D. R. (2005). Clay-based polymer nanocomposites: Research and commercial development. *Journal of Nanoscience and Nanotechnology*, *5*(10), 1574–1592. Available from https://doi.org/10.1166/jnn.2005.411.

Zhang, Q., Lei, H., Cai, H., Han, X., Lin, X., Qian, M., Zhao, Y., Huo, E., Villota, E. M., & Mateo, W. (2020). Improvement on the properties of microcrystalline cellulose/polylactic acid composites by using activated biochar. *Journal of Cleaner Production*, *252*, 119898. Available from https://doi.org/10.1016/j.jclepro.2019.119898.

Zhang, M., & Li, J. (2009). Carbon nanotube in different shapes. *Materials Today*, *12*(6), 12–18. Available from https://doi.org/10.1016/S1369-7021(09)70176-2.

Zhang, H., Zhou, J., Muhammad, Y., Tang, R., Liu, K., Zhu, Y., & Tong, Z. (2019). Citric acid modified bentonite for congo red adsorption. *Frontiers in Materials*, *6*. Available from https://doi.org/10.3389/fmats.2019.00005, https://www.frontiersin.org/articles/10.3389/fmats.2019.00005/pdf.

Zhao, S. X., Ta, N., & Wang, X. D. (2017). Effect of temperature on the structural and physicochemical properties of biochar with apple tree branches as feedstock material. *Energies*, *10*(9). Available from https://doi.org/10.3390/en10091293, http://www.mdpi.com/1996-1073/10/9/1293.

Zhao, S., Yan, W., Shi, M., Wang, Z., Wang, J., & Wang, S. (2015). Improving permeability and antifouling performance of polyethersulfone ultrafiltration membrane by incorporation of ZnO-DMF dispersion containing nano-ZnO and polyvinylpyrrolidone. *Journal of Membrane Science*, *478*, 105–116. Available from https://doi.org/10.1016/j.memsci.2014.12.050, http://www.elsevier.com/locate/memsci.

WOODHEAD PUBLISHING IN MATERIALS

The book covers the latest research findings on nanocarbon polymer biocomposites, their properties and manufacturing, as well as the possible ways to reduce waste and improve their sustainability.

Nanocarbon polymer biocomposites have gained increased attention from both researchers and manufacturers due to the significant improvement in their physico-mechanical, thermal, and barrier properties when compared to conventional materials. Their dimensions, biodegradable character, cost-effectiveness, and sustainability are among the main drivers for increasing demand. However, it is difficult to achieve uniform dispersion between the carbon filler and matrix as it easily forms agglomerations. Production of nanocarbon polymer biocomposites with high mechanical and thermal properties is also limited, but there has been rapid progress in processing possibilities to produce nanocomposites based on various biodegradable fillers. Advanced Nanocarbon Polymer Biocomposites collects all these novel scientific findings in one place. It discusses in detail their physical, chemical, and electrical properties and presents the latest research findings on nanocarbon polymer biocomposites with filler loadings and their improvement on compatibility. The book will be of great interest for those researchers who are concerned with the production and use of nanocarbon polymer biocomposites as a new innovative advanced material.

Key Features

- Emphasizes on nanoscale fillers and their improvement on compatibility
- Evaluates the impact of polymer production through life cycle analysis of both single and hybrid polymers and nanocomposites
- Puts a strong focus on sustainability and green chemistry perspectives

About the Editors

Md Rezaur Rahman is a senior lecturer (assistant professor) in the Department of Chemical Engineering and Energy Sustainability, Faculty of Engineering, University Malaysia Sarawak, Malaysia. He is also a visiting research fellow at the Faculty of Engineering, Tokushima University, Japan since 2012. He previously worked as a teaching assistant at the Faculty of Engineering, Bangladesh University of Engineering and Technology and as a research project leader supported by the Ministry of Higher Education, Malaysia. He was appointed as an external supervisor for the Faculty of Engineering, Swinburne University of Technology, Australia in 2015. He received his PhD degree from the University Malaysia Sarawak, Malaysia. He has more than 12 years of experience in teaching, research, and working with industry. His areas of research include conducting polymers; silica/clay dispersed elastomeric polymer nanocomposites; hybrid filler–loaded polymer composites; advanced materials: graphene/nanoclay/fire retardants; nanocellulose (cellulose nanocrystals and nanofibrillar) and cellulose-reinforced/filled polymer composites; chemical modification and treatment of lignocellulosic fibers including jute, coir, sisal, kenaf, hemp, and solid wood; nanocomposites and nanocellulose fibers; and polymer blends. He has published 7 books and 20 book chapters and more than 100 International journal papers.

Muhammad Khusairy Bin Bakri obtained his Doctor of Philosophy, PhD (2018), Master of Engineering (by Research), MEng (2016), and Bachelor of Engineering (Mechanical Engineer), BEng (2014) from Swinburne University of Technology, Australia. Currently, he is working with UNIMAS as a research fellow with priority on materials science, polymer composites, biomaterials, and education. He is working under the supervision of Dr. Md Rezaur Rahman at the Faculty of Engineering, University Malaysia Sarawak. Previously, he joined as a higher degree researcher/teaching assistant from 2014 to 2018. During that time, he taught subjects such as computer-aided design, materials and process, materials and manufacturing, and thermodynamics. He also assists his supervisors in monitoring undergraduate final-year projects. He has published more than 60 publications, both local and international (journal, book chapters, and conference papers). He is also one of the main contributors for the book on "Silica and Clay Dispersed Polymer Nanocomposites," published by Elsevier.

ISBN 978-0-443-13981-9

9 780443 139819

ELSEVIER

WP
WOODHEAD PUBLISHING
An imprint of Elsevier
elsevier.com/books-and-journals